Wireless Body Area Networks: Enabling Robust Coexistence and Interference Management

Jie Dong

Australian National University

A thesis submitted for the degree of

Doctor of Philosophy

The Australian National University

– 11 September 2015

September 2015

– 11 September 2015

Except where otherwise indicated, this thesis is my own original work.

Jie Dong

11 September 2015

This thesis is dedicated to my Parents, Mr. Liming Dong and Ms Minwen Tan, and also my partner Ms. Rui Feng.

– 11 September 2015

– 11 September 2015

Acknowledgments

It has been a wonderful journey for me since my PhD program started in 2011. There have been many pleasures and obstacles during this journey, and I have received valued helps from various people during the past three and half years.

Firstly, I would like to express my sincere gratitude to my primary supervisor Dr. David Smith. It has been a great time working with him. David has provided me consistent supports since I met him in 2010 during my summer research internship at National ICT Australia (NICTA). It was David's encouragements helped me overcome frustrations and disappointments. Without his kindness, patience and intelligent mentoring, I wouldn't be able to achieve all the results and complete this dissertation.

Then, I am also very grateful to my co-supervisor Dr. Leif Hanlen for his time and efforts devoted to this work. Leif shared his valuable experiences and provided helpful suggestions, which helped substantially in my work and also to my future career. Adding on this, I would also like to thank Leif and the HPI team at NICTA for giving me the opportunity to process the BAN channel measurements and put them onto the OpenNICTA database. My thanks also go to Prof. Thushara Abhayapala from Australian National University (ANU), his support means a lot to me. I am also grateful to NICTA and ANU for providing me scholarships and various supports during the past few years, particularly thanks to Prof. Aruna Sensviratne, Ms. Prashanthi Jay, Mr. Steve Marlor and Ms Elspeth Davies.

I would like to extend my thanks to Dr. Akram Alomainy, Mr. Ke Yang and all other people at the Queen Mary University of London for hosting me graciously on an academic visiting. I also owe my gratitude to Dr. Yu Ge and her team at Institute for Infocomm Research (I2R), Singapore to support me for the two-month internship there. During that time, it was also my honour to become friends with Mr. Kengyong Tan, Mr. Pokang Chen, Mr. Cihang Zhou, Mr. Ni Wei and Ms. Shan Zhao, who gave me a lot assistances in both my work and life in Singapore.

I also want to acknowledge Mr. Raja Venkateswar from QBE Insurance Australia and his recognition on the value of my work gave me much confidence and encouragement. The precious feedback he provided for the presentation I gave at the NASSCOM competition helped me in better refining my thesis.

My thanks also go to my dear colleagues at NICTA and ANU, including but not limited to Dr. Eddie Li, Ms. Nicole Sawyer, Mr. Frank Su, Mr. Jan-Christoph Kuester, Dr. Vasanta Chaganti for their valued help. In addition, I also enjoyed the time when Mr. Hjalmar Wennerström from Uppsala University came to Canberra for his internship. His effort in editing this thesis is very much appreciated.

My other acknowledge should go to my best friends, Lu Xu and Chennan Yu for their encouragements. Also thanks to my lovely housemates, Zhengyu Tai, Jin Qian, Yilu Zhang, Wenzhe Chen, Xing Fu, Sijie He and Rui Wang who have brought a lot joys to my life in Canberra, especially towards the final stage of the PhD.

At last, I would like to express my sincerest thanks to my partner Rachel for her continuous support during my PhD, as well as all other time since I met her back in 2008. It is Rachel's understanding and tolerance that make our long-distance relationship work and also makes this dissertation submitted. At last, most importantly, I would like to thank my parents, Mr. Liming Dong and Ms. Minwen Tan for shaping me into the individual I am now. I was once knocked out by the result of the university entrance examination in China. They helped me cheer up, and encouraged me to explore the world. The characteristics, skills and knowledge which they helped my developed since I was born lead to all my achievements so far. I miss them!

– 11 September 2015

Abstract

The global trends for dramatic population growth and an ageing society are likely to increase the strain on scarce medical resources in the coming decades. The next generation of personal area networks, Wireless Body Area Networks (BANs), provide a promising solution to this problem with advantages of, e.g. high flexibility, low cost, location independence, real-time monitoring etc. Hence the use of BAN is becoming pervasive. However, the increasing number of active BAN units is a challenge as significant co-channel radio interference is generated, which often causes severe performance degradation and harms system reliability. Because of the difficulty of global coordination amongst multiple, coexisting and uncoordinated, BANs, due to significant dynamics, effective interference management schemes are urgently needed to enable reliable coexistence.

Here the main theme is the investigation of the feasibility and efficiency of a few co-channel interference mitigation schemes for BANs. The schemes we study in this thesis are based on the following: 1) cooperative communications with relays; 2) transmit power control; and 3) a cross layer design that integrates 1) and 2). Two types of power control methods are investigated: a) the first is a light-weight prediction-based power control method, which adaptively adjusts transmit power, at the sensors and relays, with respect to channel condition variations; b) the second method employs game theory and models the coexistence as a non-cooperative game. These techniques have been studied for other conventional wireless networks in the literature. However, there is very-limited work for radio interference mitigation for BANs.

Another main contribution of the thesis is, instead of using channel models as presented in the literature, many open-access empirical body-centric channel measurements are used for the investigation of interference mitigation schemes proposed. These measurements contain subjects performing different "everyday" activities over many hundreds of hours in various environments. The use of the measurements in

our study further enhances this by capturing factors that can significantly influence the on-body and inter-body channels. These factors include variations in body shapes and sizes of different subjects, subjects' local and spatial movement, body orientation and the effect of the surrounding environment.

The performance, of the proposed schemes, is compared with traditional single-hop star-topology BANs for the same coexisting scenarios and BANs employing other conventional power control methods commonly used in the literature. We analyse their effectiveness with respect to first- and second-order statistics, particularly outage probability, level crossing rate, and average outage/non-outage duration, of the received packets' Signal to Interference and Noise Ratio (SINR) at the hub of a BAN. The power consumption of using the proposed schemes is also compared with other schemes. Finally, it is shown that employing relays and the proposed power control schemes can greatly enhance a BAN's ability to mitigate co-channel radio interference. The use of a non-cooperative power control game enforces BANs to minimise the interference they create in the coexisting environment while maintaining reliability requirements. Importantly, there is fast convergence to a socially optimum outcome, which is the outcome where the overall performance-of-interest of the coexisting BANs is maximised.

Overall, there is significant impetus to using the schemes proposed here in future, practical, BAN implementations, as elucidated in this dissertation.

List of Publication

Awards

A1. Dong, J.; Smith, D.; Hanlen, L.; and Sawyer, N., "Socially Optimal Power Control for Wireless Body Area Networks", selected as a national finalist in NASSCOM Student IT Innovation Awards 2015, commendation from judges was received. http://www.nicta.com.au/publications/research-publications/?pid=8756

Journal Articles

J1. Dong, J.; Smith, D.; and Hanlen, L., "Socially Optimal Coexistence of Wireless Body Area Networks Enabled by a Non-Cooperative Game", accepted as major revision in *ACM Transactions on Sensor Networks*, revision to be submitted on May 30th, 2015.

J2. Dong, J.; and Smith, D., "Cooperative Receive Diversity for Coded GFSK Body-area Communications". In *Electronics letter*, vol. 47, no. 19, 2011, pp. 1098-1100.

J3. Dong, J.; and Smith, D., "Enhancing Wireless Body Area Networks Coexistence: Cooperative Communications by Opportunistic Relaying with Power Control", submitted to *IEEE Transactions on Communications* on May 22nd, 2015.

J4. Dong, J.; Ge, Y.; Smith, D.; and Hanlen, L., "Tow-hop Relay-assisted Cooperative Communication in Wireless Body Area Networks: an Empirical Study", to be submitted to *ACM Transactions on Sensor Networks* on Jun 15th, 2015.

Conference Papers

C1. Dong, J.; and Smith, D., "Cooperative body-area-communications: Enhancing Coexistence without Coordination Between Networks". In *Personal Indoor and*

Mobile Radio Communications (PIMRC), IEEE 23rd International Symposium on. IEEE. Sydney, Australia 2012, pp. 2269-2274.

C2. Dong, J.; and Smith, D., "Opportunistic Relaying in Wireless Body Area Networks: Coexistence Performance". In *Communications (ICC), IEEE International Conference on*. IEEE. Budapest, Hungry, 2013, pp. 5613-5618.

C3. Dong, J.; and Smith, D., "Joint Relay Selection and Transmission Power Control for Wireless Body Area Networks Coexistence". In *Communications (ICC), IEEE International Conference on*. IEEE. Sydney, Australia, 2014, pp. 5676-5681.

Measurement Data Sets

D1. Smith, D.; Hanlen, L.; Rodda, D.; Gilbert, B.; Dong, J.; and Chaganti, V., "Body Area Network Radio Channel Measurement Ste". [Online] <http://opennicta.com/datasets>. 2012

Contents

List of Figures

List of Tables

Glossary

BAN Wireless Body Area Network. xiii–xv, xvii–xix, xxiii–xxv, 1–7, 11–17, 19–31, 33–45, 47, 50–62, 65, 67–72, 75–77, 79–83, 85–104, 106–112, 114–124

BER Bit Error Rate. 21, 25, 33, 47, 49, 51, 118

CFP Contention Free Period. 36

CSMA/CA Carrier Sense Multiple Access with Collision Avoidance. 22, 36

γ Signal to interference and noise ratio. 39, 84

GFSK Gaussian Frequency Shift Keying. 51, 118

GTS Guaranteed Time Slot. 36, 54, 69

h Average channel gain across the length of a received packet. Throughout the thesis, different superscripts and subscripts are used and are explained in the context.. 40, 57, 83, 84

HBC Human Body Communication. 14

LCR Level Crossing Rate. 62, 65, 66, 68, 73, 77, 119, 120

M Total number of BANs coexisting in close proximity (including both active and idle BANs. 100

m Number of coexisting BANs that are transmitting concurrently. 36, 37, 59, 100

MAC Medium Access Control. 53

MIMO Multiple-input Multiple-output. 23

MRC Maximal Ratio Combining. 39, 49, 51–55

NB Narrow Band. 16, 17, 20, 23, 24, 35

N_c Number of orthogonal channels used in the inter-BAN TDMA scheme. 99

p Average transmit power across a packet-of-interest; In Chapter 6, p_i represents the transmit power of the ith BAN, and p_{-i} is the collection of transmit powers except ith BAN; When it is denoted as P, it represents constants, e.g. P_i^{min} and P_i^{max} are the minimum and maximum transmit power of a sensor in BAN i. 83, 84, 103

PDR Packet Delivery Ratio. 2, 7, 95–97, 101, 103, 105, 107, 108, 110–116, 120, 121

PER Packet Error Rate. 3, 23, 35

PLR Packet Loss Rate. 21, 22

QoS Quality of Service. 24, 30

RSSI Received Signal Strength Indicator. 18, 19, 40, 41, 60

S Set of all coexisting BANs, including active and idle BANs;. 100

S_{active} Set of all BANs transmitting concurrently. 100, 103

SC Selection Combining. 39, 43, 49, 51–55

S_{idle} Set of all idle BANs. 100

SINR Signal to Interference and Noise Ratio. x, xv, xviii, xix, 6, 33, 34, 39, 42–46, 52, 56–58, 61, 62, 65, 77, 79, 81, 83, 84, 88, 89, 91, 92, 94–97, 100–105, 108, 111, 112, 115, 118–121

SNR Signal to Noise Ratio. 25, 33, 40

T_{beacon} Time between two consecutive beacons sent by the same BAN. 100

T_d Time length of superframe, from the transmission of the beacon by the hub till all associated sensors complete transmission. 36, 37, 59

TDMA Time Division Multiple Access. xviii, xxiv, 6, 33, 36, 37, 43, 53, 55, 58, 59, 85, 86, 99, 117, 118

T_{idle} Time length of the idle period between two consecutive superframes from the same BAN. 37, 59

$U(\cdot)$ Utility function of the proposed non-cooperative power control game. 103

UWB Ultra-Wide band. 20, 21, 24

W Social welfare of the non-cooperative game, which is the sum of all players' utilities. 106

Chapter 1

Introduction

1.1 Research Motivation

The increasing concern for people's health and well-being has led to the demand for more comprehensive healthcare systems in recent times. However, with dramatic population growth and an ageing society, healthcare resources become more scarce, while their demand is increased. Hence, a smarter healthcare system that can accommodate people's needs and provide efficient medical solutions is urgently required.

With a rapidly growing semiconductor industry, bio-sensors are now manufactured in a small form so that they can be attached to, or even implanted in, the human body without causing much inconvenience. In conjunction with advanced wireless communication technologies, the concept of Wireless Body Area Network (BAN) now becomes a reality in meeting current and future healthcare demands. A typical BAN consists of several different-purpose sensors and a central coordinator (also known as a hub) operating in a star topology. Via the hub, the system is able, for instance to connect to the external internet. This next generation personal area network is a major advance from conventional monitoring systems by unleashing new possibilities, such as: remote monitoring, real-time updates and more comprehensive scanning of complex, or even simple, physiological conditions. It is important to note that wearing a BAN may not just be limited to the time when a person is unwell, but is also beneficial for everyday use to provide insight to health conditions, as well as foreseeing any potential health problems.

In 2007, the IEEE Standards Association started to focus on standardising a low-power and short-range wireless technology for operation on, in, or around the human body. The 802.15.6 standard for BAN was then ratified in 2012 (IEEE 802.15 Task Group 6 [2012]), which defines the requirements for a BAN in terms of durability, security, complexity, mobility and reliability. BANs have a very promising future, as it is predicted that the active BAN units, worldwide, is going to increase dramatically in the next few years. It is noted that there are already various wearable technology products on the market, but the broader BAN has far greater potential. In addition to BAN's applications in healthcare, there are many other applications, such as in, e.g., consumer fitness, military and personal entertainment (Lewis [2008]). This will further enlarge the population of potential users.

An increase in the number of BAN devices has raised the critical issue of how many BANs' can gracefully coexist. The co-channel interference caused by coexistence is challenging due to: 1) its significant impact on BAN's performance, 2) the difficulty in central coordination amongst multiple coexisting BANs, and 3) the complexity of existing interference management schemes. The requirements of ultra-low power consumption and low complexity in both hardware and software in BAN has led to the simple star-topology implementation, which could make it vulnerable to any interference present at the hub. Such interference could significantly reduce Packet Delivery Ratio (PDR). This then implies that more frequent packet retransmission is required and that latency, i.e., delay, and overhead are significantly increased. The longer delay may result in late delivery of critical information, which could eventually put the BAN's human subject life at risk.

Many existing interference mitigation schemes involve congestion avoidance by medium access control with respect to time, frequency or orthogonal codes, which has been found to be effective in particular types of wireless networks. For instance, in cellular networks, coexisting mobile users access the radio channel that is directly controlled by the base-station. For wireless sensor networks the relatively static network structure and low duty-cycle requirements makes interference avoidance algorithms easy to implement. However, these methods are not suitable for BANs, given their high mobility and frequent data transmission. The group of coexisting BANs can change quickly due to difficult-to-predict random movements of BANs with respect to each other. This all implies that the competition for channel resources is both high and dynamic.

The IEEE 802.15.6 (BAN) standard indicates that it is expected that the performance of a BAN should maintain the reliability of a maximum of 10% Packet Error Rate (PER), when at least 10 BANs are co-located in a $6m \times 6m \times 6m$ space. Therefore, instead of proposing congestion and interference avoidance algorithms (that might be implemented at the link layer, for instance), all of the above discussion motivates us to design effective, fast-response and light-weight schemes for minimizing the impact of co-channel interference and to better enable multiple BANs's coexistence. This motivates the study here of both cooperative communications using relays at the MAC layer and transmit power control schemes at the PHY layer as will be investigated in this thesis — that then leads to the investigation here of suitable PHY/MAC cross-layer schemes suitable for BANs.

1.2 Thesis Statement

This thesis will investigate the performance of suitable techniques, employed in BAN, in interference mitigation for more robust BANs coexistence.

In this thesis we focus on narrowband communications around the 2.4 GHz carrier frequency, which has been included in the 802.15.6 Standard for BAN. The studies are based on realistic channel models and extensive empirical channel measurements, captured by small wearable channel sounders (Smith et al. [2012b]). These measurements can be used for various studies, e.g. human movement identification as shown in Archasantisuk and Aoyagi [2015]. These models and studies are employed to characterise subjects' everyday activities and inter-subject interactions. In this context, this thesis aims to answer the following questions:

- What is the improvement for a BAN employing two-hop cooperative communications using relays? Does it provide any benefits in inter-BAN interference management when coexisting with other BANs?
- What is the impact of relay/hub placement or diversity combining schemes on the performance of the two-hop cooperative communications?

- Is it worthwhile to jointly use simple prediction-based power control with the relays?
- Can the scenario of multiple BANs coexisting be accurately modelled as a repeated non-cooperative game?
- Does game-based power control scheme outperform the SINR-balancing or constant-power transmission for BANs coexisting?

Based on the work to be presented in this thesis, here we provide brief answers, in advance, to these questions. The detailed methodology to obtain these conclusions, as well as further elucidation of these conclusions, can be found in Chapter 3 to Chapter 6. It is noted that the energy efficiency for employing our proposed schemes is only considered at the sensor devices, since it is assumed that relays and hub are less energy-critical devices in the system design.

- When two-hop cooperative communications is employed, there is an up-to 14 dB improvement on the ratio of median channel gain to receive noise variance at the BER of 10^{-3}. When coexisting with other BANs, it is able to significantly mitigate interference by providing a maximum of 12 dB improvement in SINR outage probability.
- Depending on the hub placement, there may be some advantage in using two relays over one relay, if the added complexity is permissible. When a single relay is used, well-considered placement is important, as it shows an up-to 9 dB difference for two different single relay placement. In addition, a better outage SINR performance is shown when the hub is placed at chest than either at left or right hips.
- In the situation of coexisting with other BANs, employing the joint opportunistic relaying and prediction-based power control scheme, on the BAN-of-interest, provides about 60% circuit power consumption reduction at the same time as maintaining good reliability in terms of SINR outage probability. When not surrounded by interfering BANs, the joint algorithm's advantage is more significant.

- With the difficulties in having a global coordinator for multiple coexisting BANs, each network makes their decisions on transmission power, transmission time etc independently. Hence, this is a typical non-cooperative game, assuming selfish players. In a power control game, the choice of its transmission power influences the result of the next game repetition. Considering its mobility, a BAN can be co-located with a different group of neighbouring BANs in two consecutive time frames. Therefore, it is modelled as a finitely repeated non-cooperative game for a fixed group of coexisting BANs.
- In contrast to other power control schemes commonly applied in BAN, the game-based method with a novel utility function leads to approximately 93% of the BANs achieving the target PDR of 0.9, while the percentages for Sample-and-Hold and SINR-balancing methods are 80% and 77% respectively. In addition, it consumes less circuit power in TX mode comparing with most of other schemes. The unique Nash Equilibrium, which is the status obtained by each coexisting BAN independently choosing the optimal transmit power in response to others' choices, is also proven to be the socially optimal solution for the non-cooperative game.

1.3 Thesis Outline

The work presented in this dissertation is focused on the design of co-channel interference mitigation schemes for coexisting 802.15.6-based BANs, more specifically around two techniques: (i). Cooperative communications using relays; and (ii) distributed power control.

Chapter 2 presents literatures showing the significant impacts of co-channel interference on the reliable operation of BAN. This chapter then explains the detailed body-centric channels' characteristics and their differences from existing channel models for other types of wireless networks. This shows why many existing interference mitigation schemes cannot be directly adopted to be used in BAN without any justification. Hence, open-source body-centric channel measurements Smith et al. [2012b], are used for this thesis. At last, an overview of cooperative communications, transmit power control and game theory literature are presented with respect to general wireless networks and also particularly in terms of BAN.

Chapter 3 and 4 detail contributions in the use of relay-assisted cooperative communications for BAN. The BAN-of-interest employs the proposed two-hop cooperative communication scheme with different diversity combining technologies at the hub. In Chapter 3, we show the performance of using relays with either maximum-ratio or selection combining. Decode-and-forward relay protocol in conjunction with a suitable TDMA scheme, which enables intra-network and inter-network channel access, is used. The advantage of using cooperative communications is presented for both scenarios of an isolated BAN as well as multiple BANs coexisting. For the latter case, a simulated inter-BAN channel model consisting of the Friis path loss, Jakes' model and shadowing components is employed. The impact of relays quantity and locations to the overall performance is presented as well. In Chapter 4, an opportunistic relaying protocol is introduced that reduces power consumption by only allowing the best relay forwarding of received packets. The best relay is chosen according to the effective SINR value of the previous received packet. This scheme is investigated with the use of on-body and inter-body channel measurement sets, where the way of overlaying the two independent data sets is also explained in this chapter. In addition, an experimental study for the proposed scheme is conducted and presented in this Chapter.

Chapter 5 contributes a MAC-PHY cross-layer protocol for BANs' coexistence — that is, a joint relay selection and transmit power control scheme. The optimal path is chosen in the way as illustrated in Chapter 4. The adaptive power control is conducted on the branch which is selected as the best path for the transmission. It is performed at both sensor and selected relay for the first- and second-hop communications respectively, with respect to the required receiver sensitivity and channel quality. The performance of this joint scheme is analysed with the use of empirical on- and inter-body channel measurements, in terms of power consumption and outage statistics.

In Chapter 6, coexistence of multiple BANs is modeled as a repeated non-cooperative game, where each BAN is a rational but selfish player trying to maximum their own profit. A distributed game-based power control method is introduced. The transmit power is determined locally by maximizing a novel utility function. The SINR-modeled instantaneous PDR is adopted as the utility that a BAN is trying to maximise, with an associated cost in that utility with respect to output transmit power. The performance is analysed using empirical channel measurements and compared with other conventional power control schemes.

At last, Chapter 7 concludes the thesis and highlights the performance and feasibility of proposed schemes on co-channel interference mitigation for more robust coexistence amongst multiple BANs.

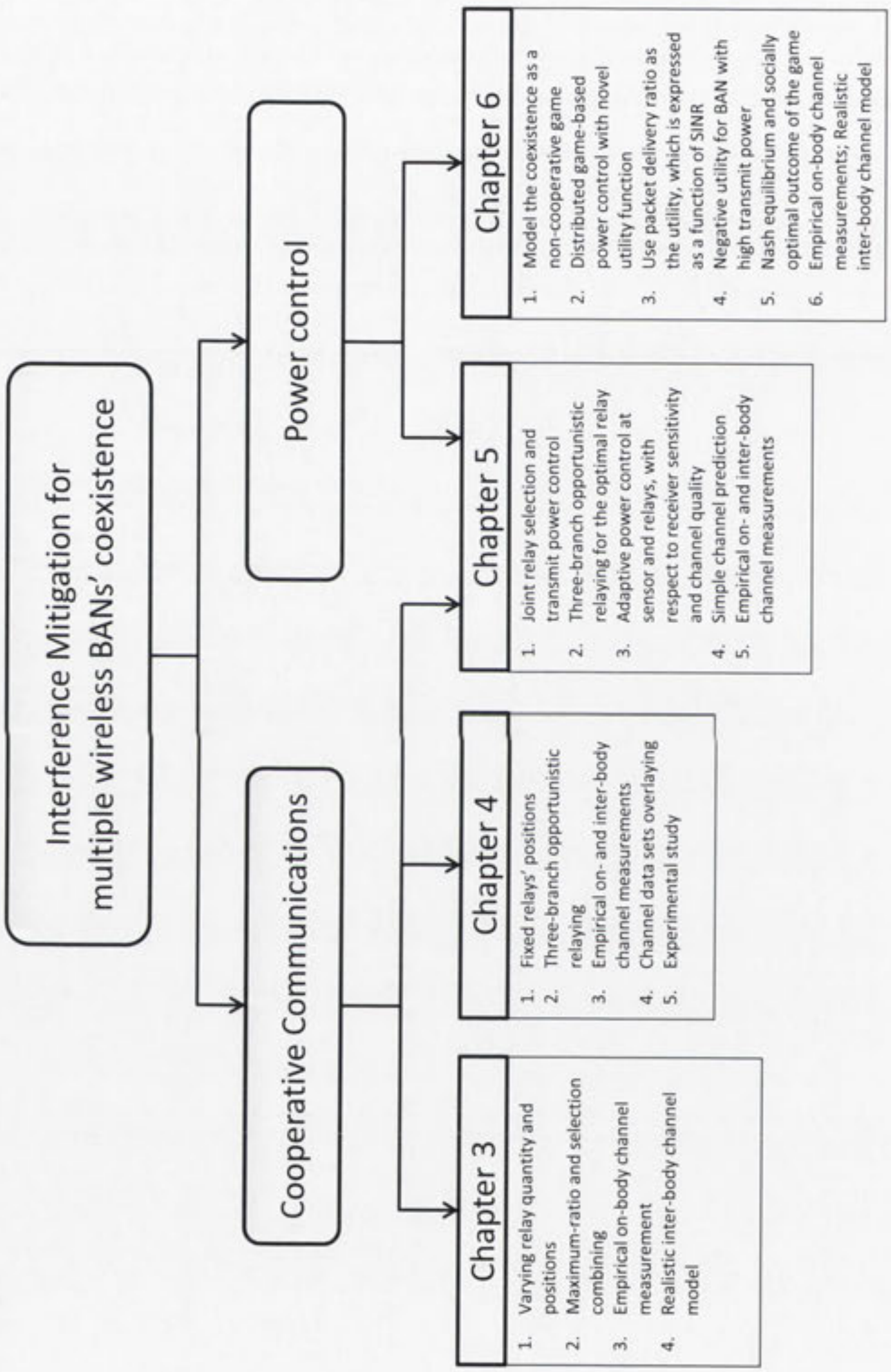

Figure 1.1: Thesis structure and key phrases for individual chapter

1.4 Research Publication

Awards

A1. Dong, J.; Smith, D.; Hanlen, L.; and Sawyer, N., "Socially Optimal Power Control for Wireless Body Area Networks", selected as a national finalist in NASSCOM Student IT Innovation Awards 2015, commendation from judges was received. http://www.nicta.com.au/publications/research-publications/?pid=8756

Journal Articles

J1. Dong, J.; Smith, D.; and Hanlen, L., "Socially Optimal Coexistence of Wireless Body Area Networks Enabled by a Non-Cooperative Game", accepted as major revision in *ACM Transactions on Sensor Networks*, revision submitted on May 30th, 2015.

J2. Dong, J.; and Smith, D., "Cooperative Receive Diversity for Coded GFSK Body-area Communications". In *Electronics letter*, vol. 47, no. 19, 2011, pp. 1098-1100.

J3. Dong, J.; and Smith, D., "Enhancing Wireless Body Area Networks Coexistence: Cooperative Communications by Opportunistic Relaying with Power Control", submitted to *IEEE Transactions on Communications* on May 22nd, 2015.

J4. Dong, J.; Ge, Y.; Smith, D.; and Hanlen, L., "Tow-hop Relay-assisted Cooperative Communication in Wireless Body Area Networks: an Empirical Study", submitted to *ACM Transactions on Sensor Networks* on Jun 15th, 2015.

Conference Papers

C1. Dong, J.; and Smith, D., "Cooperative body-area-communications: Enhancing Coexistence without Coordination Between Networks". In *Personal Indoor and Mobile Radio Communications (PIMRC), IEEE 23rd International Symposium on*. IEEE. Sydney, Australia 2012, pp. 2269-2274.

C2. Dong, J.; and Smith, D., "Opportunistic Relaying in Wireless Body Area Networks: Coexistence Performance". In *Communications (ICC), IEEE International Conference on*. IEEE. Budapest, Hungry, 2013, pp. 5613-5618.

C3. Dong, J.; and Smith, D., "Joint Relay Selection and Transmission Power Control for Wireless Body Area Networks Coexistence". In *Communications (ICC), IEEE International Conference on*. IEEE. Sydney, Australia, 2014, pp. 5676-5681.

Measurement Data Sets

D1. Smith, D.; Hanlen, L.; Rodda, D.; Gilbert, B.; Dong, J.; and Chaganti, V., "Body Area Network Radio Channel Measurement Ste". [Online] <http://opennicta.com/datasets>. 2012

Chapter 2

Literature Review

2.1 Introduction

In recent decades, rapid population growth and the changing composition of population, particularly in developed countries, from younger to older societies has brought some challenges to the current healthcare system. According to Bulatao et al. [2000], the world population reached 7 billion in 2012, and it is projected to approach almost 9 billion by 2050. In terms of Australia, the population is predicted to grow by about 65% by 2050. One phenomenon that can be observed in Australia, similar to other developed countries, is that it is generally considered that the ageing population will have a dramatic impact on society, with significant changes to the age structure of the population over the next 50 years. As shown in Fig.2.1, the population aged 65 years and over is projected to increase rapidly in terms of both numbers and proportions of the total population, from 3.2 million in 2012 to about 8 million in 2050 (Australian Bureau of Statistics [2013]). However, the health of older persons typically deteriorates with increasing age, inducing greater demand for long-term care. This could significantly increase people's expenses for healthcare, overload the current healthcare resources and degrade patients' experiences, and sometimes it could be fatal. As studied in Selvam [2012], the overcrowding issue in emergency department at hospitals not only prolongs patients' waiting time but also occasionally leads to unnecessary loss of life.

BAN offers a low-cost solution to the aforementioned problems by providing real-time updates on subject's physiological status. With employing BAN in an emergency room, it is possible to prioritise the patients and utilise the resources, which

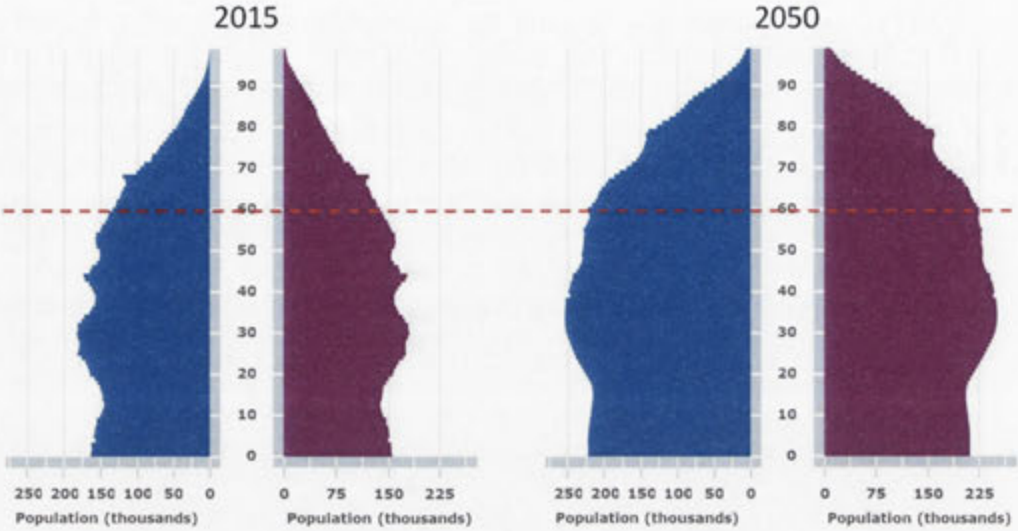

Figure 2.1: Australia Age Structure: Male and female population are indicated in blue and purple respectively; Vertical axis represents different age groups.

could eventually reduce the death rate. In addition, expenses can be substantially reduced with various applications of BAN such as remote monitoring and disability assistance (Lewis [2008]). In Au-Yeung and DiCarlo [2012], a cost comparison in anti-tuberculosis treatment shows that the cost of wirelessly observed therapy (WOT) is about 36% and 71% of 7-day and 3-day directly observed therapy (DOT) respectively. The patient's cost-to-be-treated with WOT is predicted to be 4% and 8% less. Moveover, the use of BAN is getting popular in many non-medical areas because of its flexibility, location independence and convenience, areas such as athletes training, military equipments and entertainment etc. (ABIresearch [2011]).

Considering the requirements for various applications of BAN, ultra-low power and reliability are the most priority. The needs for ultra-low power is firstly due to the safety consideration when human exposure to radio frequency field, FCC specifies a specific absorption rate limit of 1.6 W/kg measured in 1 g mass of tissue. Secondly, BAN is expected to operate for long-term use, and should requires less frequent battery replacement. This is especially the case when implant sensors are employed. Various popular low-power transmission techniques, for example WLAN, Bluetooth (IEEE Standards Association and others [2005]) and ZigBee

(IEEE 802.15 Task Group 4 [2011]), have been investigated (Takizawa et al. [2007]; Proulx et al. [2006]; Soomro and Cavalcanti [2007]). However, these wireless standards are not optimal for use in medical environment, as there is a need for a scalable data rate from 1 kbps to several Mbps for some monitoring purposes (Patel and Wang [2010]). In addition, the support for a combination of lower transmission power, higher reliability and more robust interference management should be included. Therefore, the IEEE 802.15.6 standard (IEEE 802.15 Task Group 6 [2012]) was released in 2007, which specifies the following key requirements (Zhen et al. [2008b]):

- **Topology and scalability**: typical medical network consists of 6 nodes, but should be able to support up-to 256 nodes;
- **Transmit power**: -10 dBm to 0 dBm
- **Transmission rate**: Capable for a raw data rate from 10 kb/s to 10 Mb/s;
- **Transmission range**: Maximum distance between BAN nodes should be at least 3 meters;
- **Reliability**: Within the required transmission range, the packet error rate (PER) should not exceed 10% for a 256 octet payload with a link success probability of 95% over all channel conditions;
- **Quality of service**: Latency is 125 ms and 250 ms for medical and non-medical applications respectively with a maximum jitter of 50 ms;
- **Coexistence and interference**: Support at least 10 BANs located randomly in a volume of $6 \times 6 \times 6$ meters.

2.2 Channel characteristics and measurements

The successful implementation of BAN which meets all key requirements can not be achieved without a good understanding of the characteristics of the body-centric communication channels. The wireless channel between two BAN nodes can be affected by many factors. Due to the presence of the human body in the centre of the network, there are not only wireless links formed by line-of-sight surface waves, but also more importantly links formed by on-body creeping waves (Conway and Scanlon [2009]; Akhoondzadeh-Asl et al. [2010]). The richness of multipath propagation is determined by the environment where a BAN operates in (Cotton and Scanlon [2006],Fang et al. [2014]). In addition, the scenario where a BAN is employed is also very critical. IEEE 802.15.6 standard (IEEE 802.15 Task Group 6 [2012]) has categorised its applications into 7 scenarios as shown in Table 2.1 along with their descriptions. As we can seen, these 7 scenarios can be classified into three classes based on the locations of the nodes are: implant node, body surface node and external node (up to 5 m away from the body) (Cotton et al. [2014]). The cases where an implant node is involved are fundamentally different from the others, as it uses the Human Body Communication (HBC) as specified in the standard. This PHY layer option won't be discussed here, as it is out of the scope of this thesis. For the rest of the scenarios, depending on the exact positions of the two communicating nodes, they can be further categorised into line-of-sight (LOS) or non-line-of-sight (NLOS) channels (Khan et al. [2011]). Other factors, such as subjects' movement, differences in physiology conditions and various antenna designs, further complicate body-centric channels' characteristics.

Table 2.1: Channel models for a list of scenarios and their description (Yazdandoost and Sayrafian-Pour [2010])

Scenario	Description	Frequency Band	Channel Model
S1	Implant to Implant	420-405 MHz	CM1
S2	Implant to Body Surface	402-405 MHz	CM2
S3	Implant ro External	402-405 MHz	CM2
S4	Body Surface to Body Surface (LOS)	13.5, 50, 400, 600, 900 MHz 2.4, 3.1-10.6 GHZ	CM3
S5	Body Surface to Body Surface (NLOS)	13.5, 50, 400, 600, 900 MHz 2.4, 3.1-10.6 GHZ	CM3
S6	Body Surface to External (LOS)	13.5, 50, 400, 600, 900 MHz 2.4, 3.1-10.6 GHZ	CM4
S7	Body Surface to External (NLOS)	13.5, 50, 400, 600, 900 MHz 2.4, 3.1-10.6 GHZ	CM4

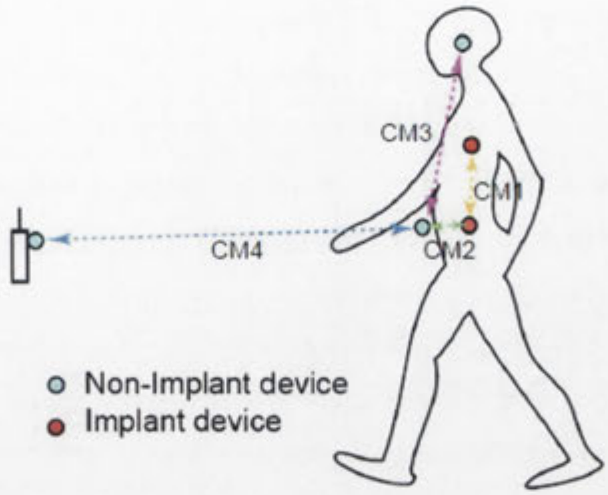

Figure 2.2: IEEE Channel models

2.2.1 BAN channel characteristics

In BAN channel modelling, various investigations have been conducted at 868 MHz and very many in the worldwide 2.4 GHz ISM bands (Cotton et al. [2014]). Distance-based path loss models have been presented in many literatures. Roelens et al. [2006] presents a empirical Friis free-space path loss model for a transmission range of up-to 40 cm above a flat, lossy human tissue model. In this case, the attenuation is more significant as the height of antenna decreases. Reusens et al. [2007] performs a measurement for deriving the on-body channel path loss on the human arm and torso. It is found that the path loss exponent is almost the same, both have $n \approx 3.3$. A higher path loss is experienced along the torso, as the author suspects the cause might be the higher absorption in the larger volume of the trunk and less flat surface. Yazdandoost and Sayrafian-Pour [2010] proposes a conventional distance-related model and a saturation model which includes the impact of operating environment. The saturation model flattens out the path loss for large distance due to the contribution of multipath components from the indoor environment.

However, as mentioned the body-centric channel is due to a combination of different factors, distance is not dominant to channel attenuation in the applications of BAN. Instead, the impact of subject movement and body shadowing are also very crucial (Alomainy et al. [2007]; Hanlen et al. [2009]; Cotton et al. [2011]). Chandra and Johansson [2013] creates an analytical model for the link loss around the torso that includes the effects of the arms. It is shown that the link loss can be underestimated by up-to 16 dB when the arms are omitted from the model. Therefore, a general distance-based model to characterise body-centric channel is inappropriate. Despite this, the Narrow Band (NB) BAN channel gain has been widely characterised by the Lognormal distribution, which combines additive effects such as diffraction, reflection, absorption and antenna losses, etc. (Cotton and Scanlon [2007]; Smith et al. [2013a]). A more realistic approach is to investigate the operation of BANs in various environments with specific user activities considered separately.

In terms of off-body and inter-body channel models, Cotton et al. [2008] studied the fading characteristics of the body-to-body channel at 2.45 GHz for the fire and rescue scenario. An experiment involving one transmitter and three receivers on four subjects respectively was conducted. The $\kappa - \mu$ distribution with $\kappa = 2.31$ and $\mu = 1.19$ is found to be a good fit. In Nechayev et al. [2010], the transmission channel between two BANs was investigated at 2.45 GHz and 5.8 GHz. The data was captured in an indoor office with subjects performing random realistic activities and orientations. The path gain envelope can be represented as a combination of a short-term Rician fading and a long-term fading component which is either a gamma distribution when distance between subjects are constant, or a lognormal distribution if varies randomly Smith et al. [2008, 2011a].

2.2.2 BAN channel measurements at NICTA

At National ICT Australia (NICTA), extensive body-centric narrowband channel gain measurements, with several hundred hours of BAN data link measurements, were captured with respect to different "everyday" activities. These involved many adult subjects of different genders, various heights, various body-sizes and various weights. Data was recorded at several carrier frequency bands, specifically 427 MHz, 820 MHz, 2.36 GHz and 2.41 GHz. These were all with narrowband communications[1]. This is the first and only open-access BAN channel measurements available

[1]The maximum bandwidth across all measurements was 10 MHz, this was when a vector signal analyser was used in an indoor-office environment. And the majority of measurements were made

for BAN-related investigation. The use of these channel measurements can be beneficial for various studies, e.g., new transmission algorithms as described in this thesis, and human movement identification as presented in Archasantisuk and Aoyagi [2015] from Tokyo Institute of Technology. The entire open-access data set is publicly available at Smith et al. [2012b] along with exact descriptions for different experiments' configurations.

The channel measurements were made at 2.36 GHz, NB 2.36–2.4 GHz (as well as 2.4–2.484 GHz) is defined in the standard (IEEE 802.15 Task Group 6 [2012]). These measurements were recorded using several small wearable channel sounders as in Hanlen et al. [2010a]. (Fig.2.3). Among all the data for subjects undertaking different activities, two specific sets are used for the BANs' coexistence performance investigation in this thesis.

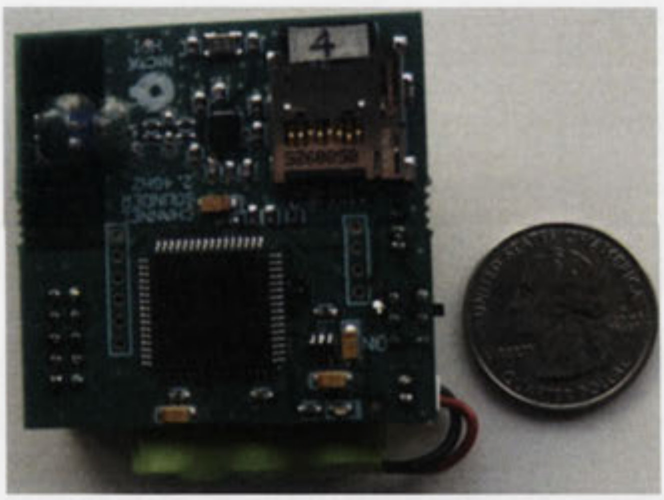

Figure 2.3: Wearable channel sounder, at 2.4 GHz ISM band. Dimension is approx 50 mm × 40 mm (Hanlen et al. [2010b])

2.2.2.1 3-star network data

In this experiment, an individual subject was equipped with 3 transceivers and 7 receivers for over a period of two hours. The experiment was repeated on eight different subjects including six males and two females with weights ranging from 60 kg to 90 kg and heights ranging from 165 cm to 190 cmSmith et al. [2011c]. A de-

with wearable channel sounders, operating with a bandwidth of 540 kHz (Smith et al. [2011a]).

tailed description of test subjects can be found in Smith et al. [2011a]; Hanlen et al. [2010a]. The transceivers were placed at the chest, right hip and left hip respectively, while the receivers' locations are highlighted in Fig.2.4[2]. Transceivers broadcasted in a round-robin fashion with a 5 ms separation at 0 dBm. While one was transmitting, the other 9 devices recorded the Received Signal Strength Indicator (RSSI) if a packet was successfully received. Hence, the RSSI values recorded at one receiver has a sampling rate of 200 Hz. It is noted that the packets recorded at each receiver are from all 3 transceivers. To obtain a specific transceiver-receiver link (as shown in Table 2.2) measurements, it is essential to extract the packets from a specific transceiver. Therefore, the resultant RSSI measurements have a sampling frequency of approximately 66.7 Hz.

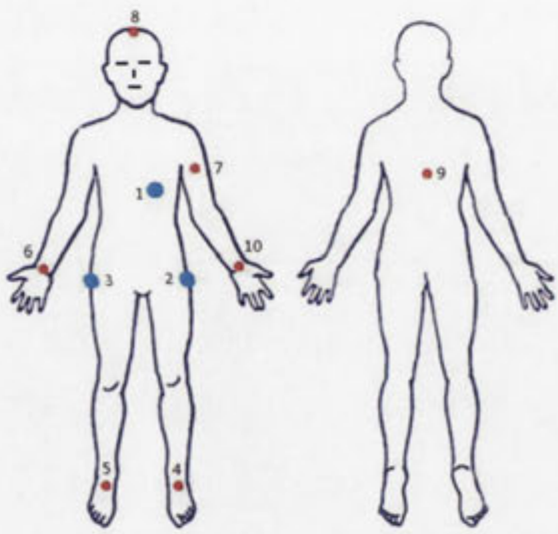

Figure 2.4: Channel sounder locations on subject's body for channel measurements capturing: 1-C, 2-Lh, 3-Rh, 4-La, 5-Ra, 6-Rw, 7-Lar, 8-H, 9-B, 10-Lw.

2.2.2.2 Multiperson interference data

Several experiments were conducted to capture inter-body interference channel data at NICTA, each of which involved different groups of subjects. The same channel sounder devices, as for capturing on-body channel data, were employed, but with

[2] The picture of body outline, which is also used in some other figures in this thesis, was found on http://www.grandhealthchiro.com

Table 2.2: Tx/Rx Radio Locations, X indicates a channel measurement. LH-Left Hip, RH-Right Hip, C-Chest, HD-Head, RW-Right Wrist, LW-Left Wrist, LAR-Upper Left Arm, LA-Left Ankle, RA-Right Ankle, B-Back

	Tx-Hd	Tx-Rw	Tx-Lw	Tx-Lar	Tx-La
Rx-Lh	x	x	x	x	x
Rx-Rh	x	x	x	x	x
Rx-C	x	x	x	x	x
	Tx-Ra	Tx-B	Tx-C	Tx-Lh	Tx-Rh
Rx-Lh	x	x	x		x
Rx-Rh	x	x	x	x	
Rx-C	x	x		x	x

only 1 transceiver and 2 receivers placed at each subject's left hip , right upper arm and left wrist respectively. For the data set used in this work, there were 8 people wearing such systems and their activities included walking together from office to a cafe and then back to the office. The placement of channel sounders used in this experiment is shown in Table 2.3. The transceiver on each subject transmitted packets at 0 dBm at 25 Hz in a round-robin fashion, i.e., each one occupies the channel sequentially for 5 msSmith et al. [2012b]. All units log the RSSI values from all packets received. Each device writes one output file as it interleaves the RSSI samples.

2.3 BAN coexistence and interference

Radio interference among adjacent wireless networks have been extensively studied for cellular networks as in Yang and Petropulu [2003]; Gulati et al. [2009]; Win et al. [2009]; Ge et al. [2011]. The unlicensed Industrial, Scientific and Medical (ISM) band has been increasingly crowded with various communication systems, for example cordless phones, bluetooth devices, NFC devices and Wi-Fi etc. It is also one of the narrowband carrier frequency bands for BAN (IEEE 802.15 Task Group 6 [2012]). Therefore, as shown in Fig.2.5 the need for coexistence of different wireless technologies is unavoidable, which creates significant heterogeneous interference. In addition, with the pervasive use of BANs, the possibility of multiple BAN coming into each others' operation range increases. For instance, in a hospital foyer or waiting area, homogeneous interference (or inter-BAN interference) can be very significant (Sun

Table 2.3: Tx/Rx Radio Locations, X indicates a channel measurement. LH-Left Hip, RH-Right Hip, C-Chest, HD-Head, RW-Right Wrist, LW-Left Wrist, LAR-Upper Left Arm, LA-Left Ankle, RA-Right Ankle, B-Back

	Tx-S1	Tx-S2	Tx-S3	Tx-S4	Tx-S5	Tx-S6	Tx-S7	Tx-S8
Rx-S1-LH		x	x	x	x	x	x	x
Rx-S1-RAR	x	x	x	x	x	x	x	x
Rx-S1-LW	x	x	x	x	x	x	x	x
Rx-S2-LH	x		x	x	x	x	x	x
Rx-S2-RAR	x	x	x	x	x	x	x	x
Rx-S2-LW	x	x	x	x	x	x	x	x
Rx-S3-LH	x	x		x	x	x	x	x
Rx-S3-RAR	x	x	x	x	x	x	x	x
Rx-S3-LW	x	x	x	x	x	x	x	x
Rx-S4-LH	x	x	x		x	x	x	x
Rx-S4-RAR	x	x	x	x	x	x	x	x
Rx-S4-LW	x	x	x	x	x	x	x	x
Rx-S5-LH	x	x	x	x		x	x	x
Rx-S5-RAR	x	x	x	x	x	x	x	x
Rx-S5-LW	x	x	x	x	x	x	x	x
Rx-S6-LH	x	x	x	x	x		x	x
Rx-S6-RAR	x	x	x	x	x	x	x	x
Rx-S6-LW	x	x	x	x	x	x	x	x
Rx-S7-LH	x	x	x	x	x	x		x
Rx-S7-RAR	x	x	x	x	x	x	x	x
Rx-S7-LW	x	x	x	x	x	x	x	x
Rx-S8-LH	x	x	x	x	x	x	x	
Rx-S8-RAR	x	x	x	x	x	x	x	x
Rx-S8-LW	x	x	x	x	x	x	x	x

et al. [2012]).

2.3.1 Heterogeneous interference

The impact of heterogeneous interference to a 802.15.6-based BAN has been explored in many literatures for both Ultra-Wide band (UWB) and NB. Dotlic [2011]; Hernandez and Miura [2012]; Wang and Wang [2011]; Martelli and Verdone [2012] investigate the scenarios where the a BAN coexists with different wireless systems. One general observation found is that the influence of interference by different wireless technologies is more significant than the interference caused by co-existing BAN.

In Dotlic [2011], the performance of a BAN operating at 4 GHz UWB under the

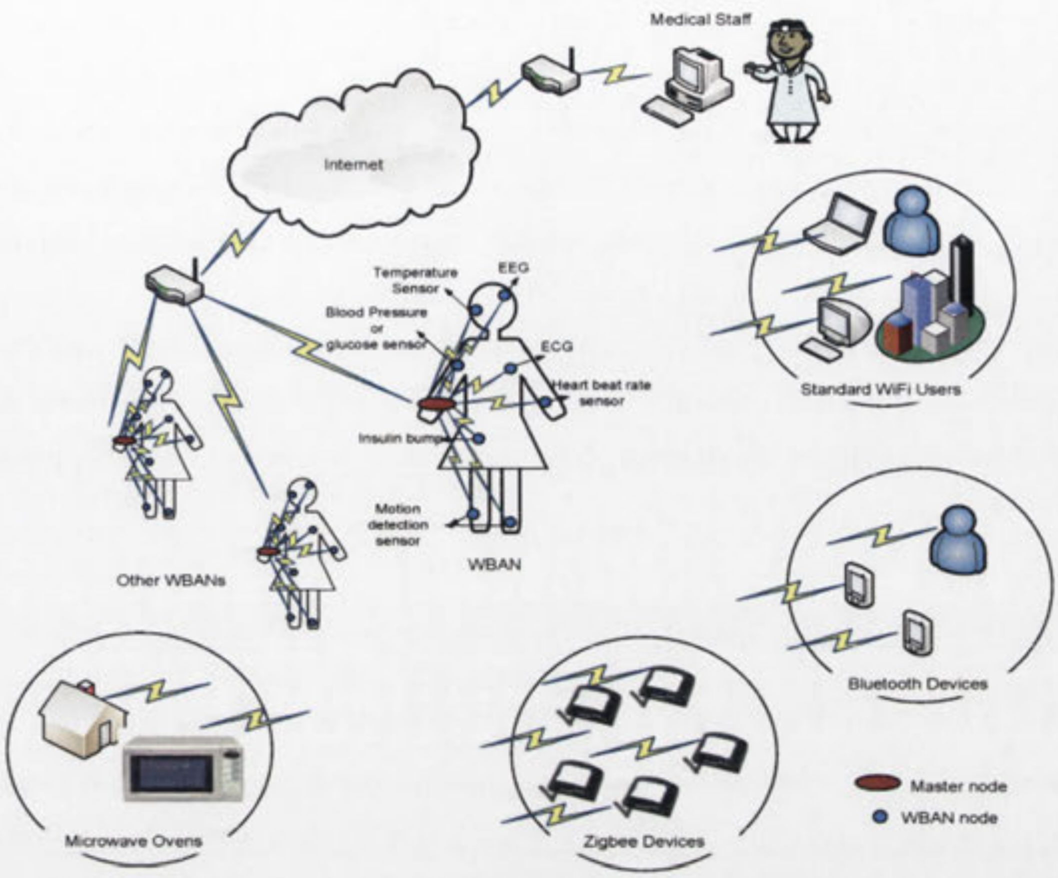

Figure 2.5: BAN coexistence: Heterogeneous and homogeneous interference (Hayajneh et al. [2014])

presence of WiMax interference is studied. Both chirp receiver and sampling receiver experience large Packet Loss Rate (PLR) when FM-UWB WiMax with 1.25 MHz or 20 MHz bandwidth coexists. While the performance of sampling receiver is less sensitive to the WiMax interference bandwidth, the chirp receiver has a better response to the interference with lower bandwidth. Hernandez and Miura [2012] simulates the case where a IEEE 802.15.6 UWB receiver in default mode coexisting with 10 802.15.4f (active RFID) interference sources. The Bit Error Rate (BER) performance degrades significantly if the desired signal power is below −30 dBm.

Wang and Wang [2011] uses the mean time to failure (MTTF) of the multi-parameter monitoring applications as a important metric to evaluate the BAN's performacne under Wi-Fi and Bluetooth interference. The distance between a Wi-Fi jamming source to the monitor should be at least 6 m to keep a MTTF of 3 hours if the distance between the electron and monitor is 0.5 m. In contrast, the Bluetooth interference has less impact, and a minimum of 0.7 m from the interference source is sufficient to maintain the same MTTF. Martelli and Verdone [2012] characterises the Wi-Fi and ZigBee interfering system in both frequency and time domain. Simulations shows that PLR is the performance metric affected the most by the interference, among which Wi-Fi is more dominant. In addition, 802.15.6-based BAN with Carrier Sense Multiple Access with Collision Avoidance (CSMA/CA) outperform the 802.15.4-based one with respect to PLR and average delay, but have a higher power consumption.

2.3.2 Homogeneous interference

Considering ambulatory patients' high mobility (Nabi et al. [2011]), discovery of proximate BANs would require exchange of additional overhead, which is potentially a waste of the valuable spectrum and can increase the probability of collision (Davenport et al. [2009]). It is generally inefficient and difficult to globally coordinate the broadcasting behaviours of several BANs in close proximity. Hence, transmission overlapping can occur in both frequency and time domain, which brings up the issue of homogeneous or inter-BAN interference. The significance of homogeneous interference in both 802.15.4- and 802.15.6-based BAN has been investigated extensively.

Hanlen et al. [2009, 2010b] studies multiple factors which could be significant to the interference between BANs. The experiment was conducted in a 6 m $\times$ 6 m in door environment with 5 male subjects wearing transceivers at various on-body location. An important discovery is that a distance-based pass-loss prediction for the interference channel is inaccurate. Same observation as found in Nechayev et al. [2010], it is the subjects' instantaneous movement and orientation that affect the dynamics of the channels. The Friis path-loss only gives a view of the long term averages of a given signal.

Deylami and Jovanov [2012] presents a theoretical analysis on the beacon loss and data loss due to the coexistence. The OPNET simulations show that the percentage of successfully transmitted beacons drops with the increase of number of BANs coexisting. The degradation is more dramatic when higher data rates are used. It can result in longer latency which is critical for medical applications. de Silva et al. [2009] experimentally investigates the impact of inter-BAN interference with respect to the packet delivery ratio (PDR), when different number of coexisting BANs and their transmission rate are employed. Each networks consists of 1 hub and 1 sensor node. It is found PDR can drop by approximately 35% if there are more than 7 high transmission rate BANs operating in the same vicinity. Similarly, Sun et al. [2012] simulates a realistic moderate-scale deployment case in a hospital's waiting area and analyses the homogeneous interference in terms of PER considering network density, traffic load and transmission power. With a duty cycle of 0.2, the reliability level of BANs' reaching the required PER of 0.05 is only 20.9% and 68.5% at peak and off-peak time respectively.

2.3.3 Summary

Both interferences are the barriers to the reliable operation of a BAN. It is recalled that IEEE 802.15 Task Group 6 [2012] specifies a maximum PER of 10% when up-to 10 BANs are co-located in a $6 \times 6 \times 6$ meters space. Therefore, effective interference management schemes for BANs coexistence are required. This thesis focuses on investigating suitable techniques to enhance multiple BANs' coexistence in NB and mitigate the homogeneous interference and its impact.

2.4 Cooperative communication

Cooperative communication techniques take the advantages of the wireless broadcasting nature, creating a virtual Multiple-input Multiple-output (MIMO) system by sharing multiple network nodes' resources, which allows user to take some of the benefits of MIMO system (Nosratinia et al. [2004]). In this concept, one or several network nodes are used as relays to provide the extra diversity gain towards the receiver (Sendonaris et al. [2003]). As shown in Fig.2.6, sequential, parallel relaying or a mixed of them can be used to form the multi-hop cooperative communications

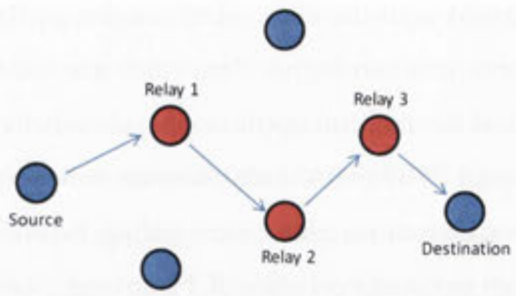

(a) Sequential relaying

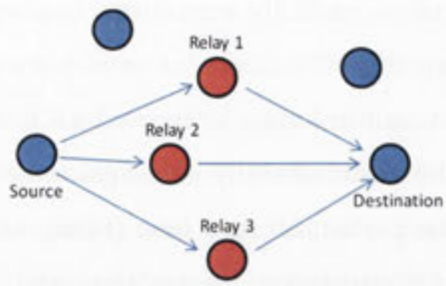

(b) Parallel relaying

Figure 2.6: Sequential and parallel relaying topologies

schemes.

Since the concept of cooperative communication technologies have been proposed, its advantages have been widely acknowledged in different types of network systems. Li et al. [2012] investigates two intra-cell coordinated multi-point (CoMP) schemes for the LTE-advanced systems, where relay nodes are taken as transmission points. Significant advantage is shown in capacity expansion. A potential drawback is that transmission from relays could possibly cause congestion to the centre-user in a cellular network. Shalmashi and Ben Slimane [2014] provides a solution by allowing a transmitter to be used an a relay at the same time as transmitting its own data with superposition coding in the downlink. In wireless ad-hoc networks, Chu et al. [2013]; Guo et al. [2014]; Lin et al. [2015] have shown that incorporating cooperative communications not only enhances the connectivity, but the network coverage is also extended significantly, both of which have a great impact on Quality of Service (QoS) of a wireless sensor network (Zhu et al. [2012]).

In terms of BAN, two-hop cooperative communication has been included in the IEEE 802.15.6 standard as an alternative implementation. Recently some two-hop cooperative communication schemes have been investigated to give significant performance benefits for BANs using either NB (Dong and Smith [2011]; Smith [2014]; D'Errico et al. [2011]; Ferrand et al. [2011]) or UWB (Chen et al. [2009]; Ding et al. [2013]; Shaban and Abou El-Nasr [2013]). Dong and Smith [2011] studied a cooperative communication scheme with either one or two relays based on the empirical channel data (Smith et al. [2011a]). Decode-and-forward strategy is employed at the relays, while maximal-ratio combining or selection combining scheme are used at the hub. An up-to 14 dB improvement in Signal to Noise Ratio (SNR) threshold is observed at the BER of 10^{-3}. In a single relay scenario, well-considered relay placement with respect to the hub can lead to an additional 9 dB performance improvement. In contrast, Smith [2012, 2014] present a similar strategy, but with switched combining used at the hub. Simulations with empirical channel data show that switching rate can reaches as low as 10% of the switching rate by using selection combining and its good outage performance is maintained. It is important to BAN, as low switching rate ensures less transmission overhead and utilities the spectrum. Shaban and Abou El-Nasr [2013] uses amplify-and-forward cooperative diversity with multiple relays and shows that one relay node is sufficient for overcoming the effect of attenuation caused by NLOS body links. The performance is improved by about 23 dB as compared to one-hop communications at BER of 10^{-3}.

Then the energy efficiency of using cooperative communications in BAN is investigated in Deepak and Babu [2015]; Madan et al. [2008]. Authors in Deepak and Babu [2015] propose a ARQ-based incremental relaying scheme where a relay link will only be active when a NACK is received from the hub. If both direct link and the first relay link fail to send a packet through, the second relay link will be active. The results show that cooperation schemes can improve the communication reliability and energy efficiency significantly. Cooperation gains can be achieved when the source-and-destination distance is above the threshold, where the threshold distance for an on-body LOS communication is 135 cm.

Sharma et al. [2011] shows that the use of an optimal relay in cooperative communication has equivalent performance to the use of all potential relays, which motivates the use of opportunistic relaying for BANs. Opportunistic relaying reduces the complexity by adopting the concept that only the single relay with the best network path towards the destination forwards per hop (Valentin et al. [2008a]). It could also potentially avoid unnecessary interferences, which is caused by all relays forwarding to the destination, to other operating nodes in the same vicinity (Stamatiou et al. [2012]). Abbasi et al. [2013] uses the broadcasting nature of the wireless transmission, and proposes a simple timer-based opportunistic routing for BAN. As soon a packet is received at a relay, a timer that considers the quality of the second-hop channel is triggered. The relay with a timer that expires first will forward its packet to the hub, and the other relays do not send when hearing its transmission.

The benefits of using spatial diversity have been emphasised in Cotton and Scanlon [2009]. Spatial diversity could also be used to overcome interference by taking advantage of the large path loss caused by body shadowing between the interference source and some relays. Little literature has investigated the effectiveness of cooperative communications in interference mitigation and enabling multiple BAN's coexistence, which underlines the importance of such a study that is made in this thesis.

2.5 Power control

One of the valuable resources in BAN is the limited power supply due to the small form factor of the sensor nodes. However, since it should be able to support long-term usage as specified in Zhen et al. [2008b], it is crucial to minimise the peak power consumption and average power consumption during its operation. Proper transmit power control schemes, which adaptively adjust sensors' transmit power to meet the minimum requirements for successful detection at the hub, are on demand. On the other hand, effective power control schemes can potentially minimise the interference levels at the other coexisting network devices (Douros et al. [2012]; Kini et al. [2014]; Chiwewe and Hancke [2012]).

2.5.1 Non-game based Power control

Various power control schemes have been studied for different wireless networks, and they can be categorised into centralised and distributed methods. A of lot work has been done for cellular networks, where some degree of central coordination can be used at the base station (Zander [1992b]; Wu [1999]). In Zander [1992b], it looks into power control algorithms for cellular radio systems, where information on all transmission and interference paths is available to all devices. The algorithms finds the Perron-Frobenius eigenvalues and its eigenvector. It is shown that the proposed method can improve the performance.

Cai et al. [2013] investigates a scheme named Energy-efficient Relay MAC with Dynamic Power Control (ERPC-MAC) for BAN which employs a relay-enabled power control algorithm. It is shown that the network lifetime is extended by up-to 106% comparing with standard IEEE 802.15.4 compliant BAN. In this scheme, multi-hop topology is enabled when a sensor indicates to the coordinator the sensor's energy shortage. Transmit power control is performed for every source-and-destination pairs, and it is trigged when the RSSI of the previous packet is out of the target RSSI threshold range. A fixed-step or a variable-step power adjustment is used, depending on how close the actual RSSI from the threshold range is to it. This strategy ensures an optimal transmission power level is reached in fewer steps. The authors define the threshold range with respect to the distance between source and destination, which is a drawback of this work due to the low correlation between distance and instantaneous channel gain in typical BAN applications (Hanlen et al. [2009]; Quwaider et al. [2010]). Therefore, Quwaider et al. [2010] considers the body instantaneous posture and determines the threshold range based on the sensitivity of the PDR as a function of the received RSSI values. The relationships between PDR and RSSI for different scenarios are found by taking the average of extensive measurements, but it's accuracy is still questionable. Smith et al. [2011b, 2012a] propose a power control scheme for star-topology BAN based on a simple short-term prediction with respect to the receive sensitivity and the previous channel gain. In addition, an enhanced power control scheme is studied, where the prediction is done over the previous 4 samples. This prediction is shown to be accurate for up-to 2 seconds, even with a nominal coherence time of 500 ms. Both power control methods with two different predictors improve the power consumption in Tx mode and outage probability.

As we found that most literatures investigate the non-game power control schemes for the situation where a BAN is isolated from any interference, to be more practical, it is essential to evaluate them in scenarios of multiple BANs coexisting.

2.5.2 Game-based Power Control

The concept of game theory firstly starts from the field of economics, and has been developed extensively in 1950s by many scholars. It has now been widely applied for behavioural relations modeling in different disciplines. Prior to investigating an efficient game theoretical power control algorithm, we should know that power control for BAN is a complex and intriguing problem since the selection of transmit power level can affect its own operation and other BANs'. Some examples include the quality of the signal received at the receiver, the interference it creates for the other receivers and energy consumption at each node. Therefore, a suitable game model with respect to BAN should be defined.

In many literatures, a system of ad hoc or sensor networks are often modeled as a repeated non-cooperative game (Long et al. [2007]; Sun et al. [2008]). In such game, each player is treated as a selfish user aiming to maximise its utility function, which could be a combination of several factors. Considering PHY layer performance, a reasonable factor for utility function could be the SINR value. The higher SINR at the receiver, the better service it can expect. However, on the other hand, the higher SINR is achieved at the expense of increased drainage on the battery consumption and higher interference to the signals of other users. Hence, if each user demonstrates totally selfish behavior, the network performance may significantly degrade, even leading to service outage. Therefore, many solutions have been proposed, and most of them rely on a pricing mechanism to facilitate cooperation among self-interested users in power control for both cellular networks (Alpcan et al. [2004]) and ad hoc networks (Heikkinen [2006]; Ileri et al. [2004]). However, such a pricing mechanism is often difficult to configure and implement in BAN. In this case, we introduce the concept of cost function for BAN, which is the amount of cost or resources a BAN needs to sacrifice in order to achieve certain utility level. Therefore, the goal of each user in the game is to maximise its utility function and meanwhile minimise its own cost function.

Details of utility function and cost function for individual BAN needs to be further studied. In terms of the solution of game, two most fundamental solution concepts will be investigated: Nash equilibrium and Pareto optimality (Leyton-Brown and Shoham [2008]). In terms of the first one, it is observed from an individual player's point of view, and there is no player want to change his strategy if he knew what strategies the other players were following. However, Pareto optimality indicates the optimal response of the overall system. In other words, the overall performance of multiple BAN system reaches its optimal point. In this process, some player may have worse experiences than others.

In the context of wireless communications, game theory has become a useful tool for modeling the interactions between cognitive radios. In general wireless sensor networks, it has been employed for purposes such as energy conservation (Felegyhazi et al. [2005]; Yuan and Yu [2006]), routing (Zheng et al. [2012]; Sun et al. [2013]), payload balancing(Sadagopan et al. [2006]; Raicu et al. [2005]), target tracking (Huang et al. [2008]; Gu [2011]) and security (Kumar et al. [2014]; Karapistoli and Economides [2014]) etc. Power control based on game theory has shown to be beneficial in both centralised (Saraydar et al. [2002]; Koskie and Gajic [2005]) and decentralised (Tushar et al. [2012]; Sun et al. [2008]) power wireless networks. Its significant capability on resource allocation, interference management and energy efficiency improvement for different types of networks has been proven when proper game models are introduced.

In the context of BAN, the use of game theory has become popular in recent years, and it has been applied in many ways. In Misra et al. [2015], a Nash Bargaining Solution (NBS) is proposed within a BAN to improve the overall network performance amongst multiple heterogeneous sensors that have different transmission priority and minimum data rate requirement. In this cooperative game, the minimum demand of data rate of all sensors are updated at the coordinator. The coordinator then optimises the data rates for all sensors based on each's criticality index, transmission failure probability and power consumption. It is shown that this approach can improve the data rate for critical sensors by an average of 10%. Similarly in Misra and Sarkar [2014], the same author proposes a priority-based time-slot allocation in BAN, considering some critical properties of a packet and its local data processing unit (LDPI). This fair game strategy can reduce the number of transmitting LDPUs by 25.97% and reduce the packet drop rate and evergy dissipation.

Not only node-level game strategies, many of the game-based schemes in BAN aim to solve the consequence of multiple uncoordinated BANs' coexistence. Shin et al. [2012] raises the issue of overlapping transmission in the contention free period (CFP) if multiple BANs occupy the same channel. In Shin et al. [2012], the authors proposes a cooperative game model based on a Cournot game, where a player knows other's information before a game repetition. Coexisting BANs select their actions, which is a certain way of channel allocation, to maximise the QoS including throughput, delay and traffic priority. It is found that by applying the proposed Gournot competition model, player's utility increases as improved throughput and delay. Wu et al. [2010] proposes a decentralised channel selection and power control method, called DISG, to reduce the effect of inter-user interference. A utility function that considers the trade-off between SINR and power utilization is provided, with which the emphasis can be altered by adjusting the weighting factor on SINR and power consumption. The Nash Equilibrium (as explained in Leyton-Brown and Shoham [2008]) is obtained with a no-regret learning strategy based on a history of previous actions. Simulation shows that the proposed non-cooperative game converges until all BANs operate on optimal channels with a suitable transmission power. Kazemi has studied some power control games for interference mitigation amongs BANs operating in the same frequency band in Kazemi et al. [2010, 2011b,a, 2012]. In Kazemi et al. [2010], a non-cooperative power control game with the following utility function is proposed for individual BANs:

$$U_i(p_i, p_{-i}) = log(1 + \frac{h_{ii}p_i}{\sum h_{ji}p_j + \sigma_i^2}) - c_i p_i^{\alpha_i} \tag{2.1}$$

where p_i and P_{-i} are the transmit powers of the BAN-of-interest and other coexisting BANs respectively. The parameter c_i can be either fixed or adaptive to channel changes and power budgets. Limited coordination is done amongst BANs by broadcasting their transmit power decision to the neighbouring networks. The existence of NE is shown. Simulations over static channels show that the aggregate throughput is improved in the presence of interference using as little power as possible. A similar power control approach – ProActive Power Update (PAPU), which incorporates limited coordination, is illustrated in Fang et al. [2010]. In Kazemi et al. [2011b, 2012], a non-cooperative power control game with reinforcement learning is proposed, which consider the results of previous actions in making the next decision. Results are given in terms of proper rewarding functions that reflect the performance and the state of operating environment. When compared with a system using a counterpart approach based on game theory without learning, a power control game with reinforcement learning can trade off throughput for transmission power and achieve lower energy consumption.

2.6 Summary

To better motivate our research on effective interference mitigation schemes for the uncoordinated coexistence of multiple BANs, we firstly reviewed important background literature about the fundamental characteristics of BAN. Together with these, the importance of this work was then highlighted with extensive literature on the significant impact of inter-BAN interference and its resultant severe performance degradation. Thus, existing interference mitigation schemes for other types of wireless communications have been described, as well as those particularly for BANs. The two most common methods of interference mitigation are using cooperative communications and transmit power control. We have reviewed the various implementations of interference mitigation for different types of wireless networks. However, the lack of consideration BANs, and particularly the distinctive properties of BANs, in the literature motivates the innovative contribution to be given in the following chapters.

Chapter 3

Cooperative Communications for Wireless Body Area Networks' Coexistence

In this Chapter, the performance of cooperative communications is extensively studied for the two cases found in any BAN implementation where: 1) a BAN is isolated from interference and, more importantly 2) multiple mobile and uncoordinated BANs coexist in close proximity to each other. A decode-and-forward protocol, with two dual-hop relay links and different combining schemes at the hub (or gateway device), is investigated when employed on the BAN-of-interest. A TDMA-like scheme is used to schedule the packet transmissions for each Tx/Rx link within the same BAN, as well as a modified TDMA-based protocol as the inter-BAN access scheme considering the uncoordinated nature of multiple coexisting BANs. For the BAN-of-interest, many hours of measured channel gain data are employed to emulate the on-body channel. Realistic inter-body channel models are employed considering large- and small-scale fading, various amounts of shadowing and additive white gaussian noise introduced between BANs. When compared to a BAN with traditional single-hop star topology, the benefits of using cooperative receive diversity for an isolated BAN is presented with an up-to 14 dB improvement in terms of the threshold SNR of 10% BER. When coexisting in a mobile and dynamic scenario, it is found that the proposed cooperative communications provides significantly better co-channel interference mitigation performance. The threshold SINR for 10% outage probability at the hub is greatly improved by up-to 12 dB. In addition, it is also demonstrated that the location of the hub, given three typical locations, has significant impact on the performance of the cooperative BAN communications.

A part of this work was presented in Dong and Smith [2011] and another part was presented in Dong and Smith [2012].

3.1 Introduction

As has already been elucidated in this thesis, with the increasing concern for human wellbeing, new technology is urgently required for the already overloaded healthcare system. BAN, the next generation personal area network, is a key solution to the existing circumstances in the medical application area, due to their convenience, flexibility, low cost, prompt response and also their high compatibility with existing network technologies and applications. Considering the nature of BAN usage, it is necessary to meet various requirements regarding safety, reliability and durability etc., which are listed and explicitly specified in IEEE 802.15 Task Group 6 [2012]; Zhen et al. [2008b].

To maximise users' convenience for BAN systems, sensors are designed and manufactured in a small form factor, which results in scarce power resources being required for sensor devices. Hence, ultra-low power consumption, particularly low transmit power, should be enabled to prolong the system operation time, which is a vital quality-of-service indicators. The potential disadvantage of low transmit power is a less robust system which is more sensitive to the subject's body posture, undergoing activities and environment change. It also leads to a BAN more vulnerable to the interference due to a decrease in SINR at the hub. The impact of both side effects is a significant degradation in performance as discussed in Nechayev et al. [2010]; Sun et al. [2012]; Hernandez and Miura [2012]. For the purpose of improving the reliability of a BAN system while minimising its power consumption, the use of cooperative communications for BANs is considered, which has been shown to provide great benefits when used in different types of networks (Li et al. [2012]; Zhu et al. [2012]). However, the significant differences between BAN and other types of networks as shown in Cotton et al. [2014]; Smith and Hanlen [2015], makes this investigation of cooperative communications' performance in BAN novel and important.

The main contribution of this chapter is to present the benefits of using cooperative communications in BAN which has, many, essentially different characteristics from other widely-studied wireless networks. To highlight the differences, extensive empirical BAN channel measurements, that captures the distinctive factors such as body movement, shadowing, human tissue absorption, etc., are employed to simulate the on-body channels for the BAN-of-interest. In accordance with an option for physical layer transmission in the IEEE 802.15 Task Group 6 [2012], BCH-coded GFSK modulation is considered at 2.4 GHz NB carrier frequency. Since the NB BAN communications is frequency non-selective, the results of this work are applicable to BAN operating at different NB carrier frequency bands and bandwidths. The performance of the proposed cooperative communications is firstly evaluated for a BAN isolated from any interference. Then, an extra BAN is adopted in the simulation, acting as an interfering source. A realistic inter-subject channel model is employed, which simulates various level of aforementioned unique factors with respect to BAN. As improvements on reliability for using cooperative communications are our major interest, metrics regarding the maximal 10% PER, as specified in the standard, are presented and then discussion follows.

The rest of this chapter is organised as follow: Section 3.2 describes the model of the BAN system used in this chapter, including BAN's configuration, intra- and inter-BAN medium access scheme. In Section 3.3, the algorithm of the proposed cooperative communications using relays, as well as its implementation, is provided. The use of empirical on-body channel data and inter-body channel model is explained in Section 3.4. Following that, we obtain the performance of the proposed cooperative communications scheme in Section 3.5, in contrast to the coexistence of multiple one-hop BANs. Section 3.6 provides some concluding remarks.

3.2 System model

3.2.1 Configuration of BAN

The model of a BAN system used in this study consists of three sensor nodes and a hub, as shown in Fig.3.1. When the system operates in a single-hop star topology, i.e. no cooperative communications are used, sensors transmit in a round-robin fashion coordinated by the hub node. Therefore, as soon as the hub sends out a beacon signal to all connected sensors, they respond by transmitting requested information back to the hub during their allocated time slots. The implementation of this scheme is achieved by utilizing the Guaranteed Time Slot (GTS) in the Contention Free Period (CFP) of the CSMA/CA protocol specified in the IEEE 802.15 Task Group 6 [2012], and it is essentially a TDMA behaviour. Alternatively, it can be implemented with the scheduled access scheme specified in the 802.15.6 standard as noted in Boulis et al. [2012]. In this thesis, it is assumed that only one packet of information is sent from each sensor during its time slot. After the completion of transmission from all sensors, the system becomes idle till the next beacon period starts. When cooperative communications scheme is employed, the transmission sequence of sensors follows the same TDMA scheme. However, instead of switching to idle mode when not actively transmitting, sensors act as relays to forward the transmission from the active sensor to the hub. The two-hop cooperative communications algorithm is also demonstrated as in 3.1.

Besides using TDMA as the access scheme within any BAN, it is also adopted as the co-channel access scheme across multiple BANs in the coexisting scenario, considering its capability of co-channel interference mitigation and power consumption minimization (Zhang et al. [2010]). Assuming there are total m BANs co-located (or in close proximity) and the number is fixed during the period of simulation, then the shared channel can be evenly divided into m time slots each with a superframe length of T_d. Therefore, each BAN goes into idle status for a period of $(m\text{-}1)\times T_d$ after it completes transmission. However, due to the lack of a global coordinator amongst multiple BANs, the execution of TDMA scheme is slightly different from a traditional pattern. In the simulated TDMA scheme, the coordinator in each BAN

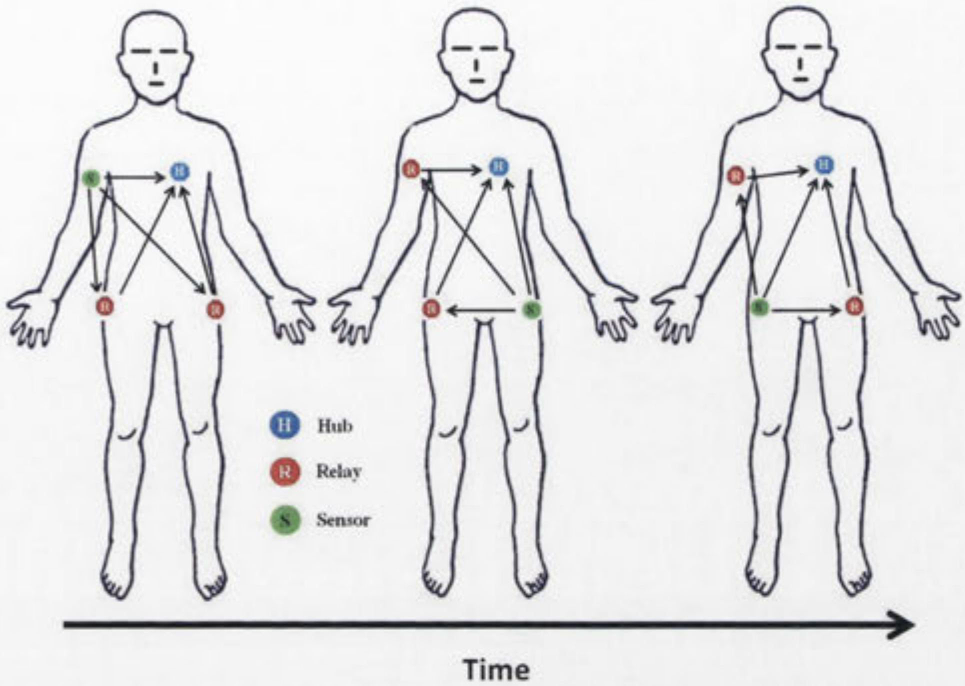

Figure 3.1: BAN configuration: varying relay topology. This figure shows the sequential transition, in time, of three non-hub devices becoming active sensors.

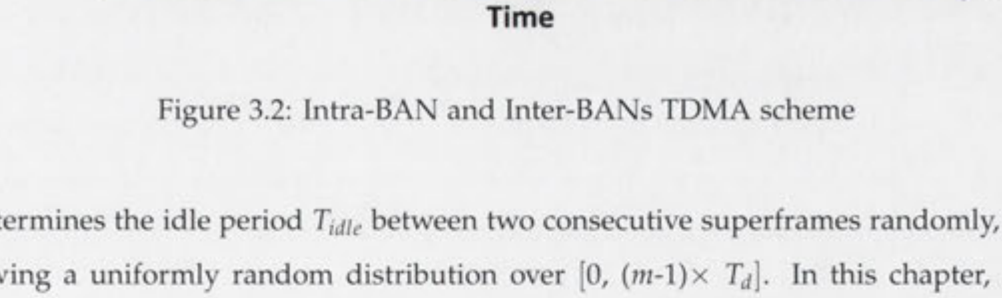

Figure 3.2: Intra-BAN and Inter-BANs TDMA scheme

determines the idle period T_{idle} between two consecutive superframes randomly, following a uniformly random distribution over $[0, (m\text{-}1)\times T_d]$. In this chapter, two BANs employing this same configuration are used for simulation. Both intra- and inter-BAN TDMA schemes are illustrated in Fig.3.2.

In terms of physical location, a real scenario is emulated, which may occur in an open indoor or outdoor environment as shown in Fig. 3.3. In such scenario, two people both wearing an on-body BAN system walk approach each other, passing by

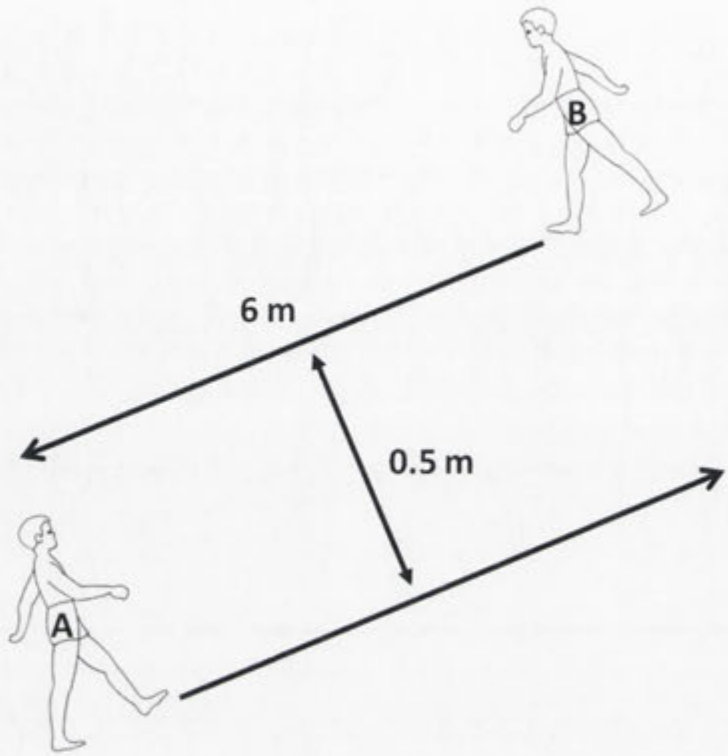

Figure 3.3: Inter-BAN motion model of two human subjects

and then move apart. In this case, they start with a 6-meter separation (corresponds to the guidelines of IEEE 802.15.6 specifying reliable operation for BAN in Zhen et al. [2008a]). Over the simulation period, the distance between BANs as the subjects move towards each other gradually decreases to 0.5 meters and then increases to 6 meters by the end of the simulation period. We simulate each subject's motion with a constant slow walking speed of 0.5 m/s. Therefore, the two subjects approach each other with a relative speed of 1 m/s. Hence the time it takes for the distance between two subjects to decrease to 0.5 m is 6 s. This model simulates an ideal scenario, in contrast, a more pseudo-dynamic case is considered in Chapter 6.

3.3 Relay-assisted cooperative communications scheme

In the proposed two-hop relay-assisted cooperative communications scheme, decode-and-forward protocol is assumed whereby all received signals at any given relay are decoded and forwarded to the destination. Two-branch and three-branch coherent

Maximal Ratio Combining (MRC) and Selection Combining (SC) are adopted (where one of the branches is the direct link, and the other branches are the decode-and-forward relay links). In terms of SC, the best branch is chosen based on comparing the effective SINR of all source-and-destination links. The receive SINR γ_{SC} of the selected branch, and hence the selected received signal y_{SC} for any packet, is determined in the following manner

$$y_{SC} = \mathbf{y}(j), \text{where } j = \arg\gamma_{SC}, \tag{3.1}$$

$$\gamma_{SC} = \max[\gamma_{\mathbf{i,min}}, \ \gamma_{sd}], \tag{3.2}$$

$$\mathbf{y} = [\mathbf{y_{r_i d}}, \ y_{sd}],$$

$$\gamma_{i,\text{min}} = \min[\gamma_{r_i d}, \gamma_{sr_i}], \text{ with } i \in K. \tag{3.3}$$

For MRC, y_{MRC} is determined as:

$$y_{MRC} = h_{sd} * y_{sd} + \sum_i h_{i,min} * y_{r_i d}, \tag{3.4}$$

$$h_{i,min} = min[h_{r_i d}, h_{sr_i}], \text{ with } i \in K$$

Here, the notation y_{SC} and y_{MRC} represent the processed signals after employing selection and maximal ratio combining respectively. $\gamma_{i,min}$ indicates the effective SINR for the ith relay path, and its value is taken as the minimum value of the first-hop SINR γ_{sr_i} and the second-hop SINR $\gamma_{r_i d}$. Similarly, $h_{i,min}$ is the effective average channel gain for the ith relay path, and h_{sd} is the average channel gain for the direct path between the source and destination. The subscripts s, r_i and d represent source, ith relay and destination respectively; The value of K is either 1 or 2, corresponding to the number of relays employed.

The analysis of the intra-BAN cooperative scenario considered here is performed based on effective SINR of individual packets. For relay branch, it is the minimum SINR value between the first- and second-hop links (Equ. (3.3)). The calculation of the SINR γ of a received packet at a receiver node is as follows:

$$\gamma = \frac{p_{sig} * |h_{sig}|^2}{|\sigma_{\text{noise}}|^2 + \sum(p_{int,i} * |h_{\text{int},i}|^2)} \tag{3.5}$$

where p_{sig}, $p_{int,i}$ are the average transmit powers of packet-of-interest and interfering packet from ith coexisting BAN respectively. h_{sig},$h_{\text{int},i}$ are the average channel gain of the signal channel and interfering channel across the length of the received packet. At last, σ_{noise} is the average power of noise at the receiver across the same time frame. In the scenario where no interferer is presented, the calculation of SNR is the same as Equ. (3.5) with interference power equals to 0.

3.4 Channel model

3.4.1 Intra-BAN channel

Prior to simulation, extensive on-body channel gain measurements are used to examine the proposed cooperative communications strategy, as described in Section 2.2.2.1. The data set was measured with small wearable channel sounders operating at 2.36 GHz over several hours of normal "everyday" activity of an adult subject (Hanlen et al. [2010b]). Their locations are highlighted in Fig. 2.4. According to the experiment setup as shown in Table 2.2, samples were taken over a period of two hours with 7 receivers and 3 transceivers (at chest, right hip and left hip). Three transceivers broadcasted in sequence with space between individual transmissions of 5 ms. While one was transmitting, the other 9 receivers recorded the received signal strength indictor (RSSI) if a packet was successfully detected.

Due to the characteristics of channel stability and channel reciprocity for everyday BAN (Smith et al. [2009]; Hanlen et al. [2010b]; Smith and Hanlen [2015]), this data can be used as the intra-BAN two-hop communication channel gain in the study of co-existence of multiple BANs. It also allows to investigate the impact of different hub placements at chest, right and left hips respectively. These 3 locations are chosen as typical hub and relay placements, as they allow for larger devices than a dtandard small on-body sensor.

A block fading model is used whereby the Tx-Rx channel gain, $\mathbf{h}_{TxRx}$ is constant over each period of transmission of a packet[1], and the next channel gain block magnitude is based on the subsequent RSSI measurement. For all scenarios simulated, Additive White Gaussian Noise (AWGN) is injected into the system with receive noise variance from -90 dBm to -110 dBm.

3.4.2 Inter-BAN channel

3.4.2.1 Large scale fading model

Considering the distance between the two wearers of the BAN, a free space path loss (FSPL) model is applied to derive the mean path loss, without shadowing, between the two BANs at any given distance. The free space path loss model suggests that this mean path loss is proportional to the distance between two subjects with path loss exponent of $n = 2$. In this case for BAN, the path loss exponent of 2 is chosen corresponding to a relatively 'open' environment (few objects nearby causing reflection or diffraction).

$$FreeSpacePathLoss = \left(\frac{4\pi d f}{c}\right)^2 \tag{3.6}$$

where d indicates the distance between objects in meters, f is the frequency of transmitted signal in Hz (in this case, 2.4 GHz) and c is the free-space speed of electromagnetic wave propagation (3.0×10^8 m/s).

Shadowing effect While subjects are moving randomly with respect to each other, there will not always exist a line of sight path between the interfering BAN and the BAN-of-interest. Instead, there will be an obstructed line-of-sight or non-line-of-sight in most cases (Yazdandoost and Sayrafian-Pour [2010]). In the simulation, a reasonable shadowing offset is applied to a free-space line-of-sight path loss. Based on the on-body channel measurement data at 2.4 GHz analyzed in Smith et al. [2011a], it can be observed that the median channel gain of on-body channels at 2.4 GHz is around -71 dB, where the high path loss is principally due to significant shadow-

[1] without loss of generality this could also be a codeword

ing and effects of body-movement. Given typical on-body distances this implies a degradation of approximately 40 dB due to shadowing. In the scenario considered here this shadowing effect of one body should be similar between bodies, thus we apply an offset, i.e., an increase in path loss due to shadowing, of 40 dB. We consider varied amounts of shadowing[2] corresponding to three types of channels:

1. *No shadowing:* We first consider the "no shadowing" channel that is the worst case scenario, where there always exists a line of sight path between the interfering BAN's sensor and the gateway of the BAN-of-interest. This gives a lower bound (i.e., in fact an extreme lower bound, as the interference is the maximum among all the three types) for SINR.

2. *Partial shadowing:* For this channel, the interfering sensors only part-of-the-time have line of sight paths to the gateway of the BAN-of-interest. Because of independent motion between the BAN-of-interest and the interfering BAN, some line-of-sight paths will be partially, or fully obstructed, for part of the time. Partial shadowing simulates this randomness by introducing shadowing some portion of the time. Here, it is half of the total transmitting time. Based on the assumption of 0.5 m/s movement speed mentioned above, shadowing is included for 6 s of the total 12 s transmitting time. This gives a somewhat more typical approximate (just above, or close to) lower-bound for SINR.

3. *Full shadowing:* In the concept of full shadowing, which is the closest to most practical scenarios, a 40 dB shadowing offset, with appropriate small-scale fading around this offset, is added over the entire period of interest for interference. This gives the best mitigation of interference from other BANs and typically results in the highest SINR.

3.4.2.2 Small scale fading model

Based on the large scale shadowed mean path loss, Jakes model with a Doppler spread, f_D of 2 Hz (Doppler fading parameter $f_D/f_s = 0.01$, where $f_s = 200$ Hz is the

[2]The shadowing mentioned in the remainder of this chapter represents the inter-body shadowing components, and does not include on-body shadowing factor.

sampling rate at the receiver), and Rayleigh fading with fading coefficients that are $\mathcal{CN}(0,1)$ distributed around the shadowed path-loss (hence the mean power of the fading coefficients is the shadowed path loss), is used as a small scale fading model for communication channels between two BANs (Jakes [1974]). *Please note that this does not mean the small-scale fading for any given BAN is modeled well by Rayleigh fading. On any given BAN a far better model is Gamma fading (Smith et al. [2011a, 2013b]).*

3.5 Numerical Analysis

Based on the setup described above, simulations are repeated for many times, each of which using a random segment of the on-body channel measurements and an independently generated inter-BAN channel model. For the transceiver simulated in the investigation, it is assumed that BCH(31,19) coding scheme and GFSK modulation (with a modulation index of 0.5, i.e. GMSK) were employed, which corresponds to one of the implementations specified in IEEE 802.15 Task Group 6 [2012]. The performance of the proposed cooperative communications scheme is validated by averaging the results of all simulations. Its benefits are shown for both scenarios where one interfering BAN coexists and where no interfering BAN exists.

3.5.1 Multiple BANs coexisting

We first simulate the case of a hub at chest with three sensors communicating with it, following the TDMA manner described in Section 3.2.1. Two of the sensors are located at left and right hips separately, and the third sensor is placed at one of the locations 4 to 10 as shown in Fig.2.4. Among all three sensors, any two idle ones are used as relays in one transmitting period (i.e., all three sensors send packets to the hub). Effective SINR value for each packet received at the hub using SC is obtained following Equ 3.5 and 3.2, and hence outage probabilities at given SINR thresholds are determined. It is defined as the probability of SINR value smaller than a given threshold

$$Pr(\gamma < \gamma_{threshold}) \tag{3.7}$$

Table 3.1: SINR Threshold (in dB) at Outage Probability of 1% when full shadowing is included, hub at chest

Sensor location	Single Link	Cooperative links	Gain
Left ankle	-4.5dB	3.1dB	7.6dB
Right ankle	-3dB	2.5dB	5.5dB
Right wrist	-2dB	5.1dB	7.1dB
Upper left arm	-1.7dB	5.7dB	7.4dB
Head	-1.3dB	12.2dB	13.5dB
Back	-5.3dB	1.3dB	6.6dB
Left wrist	-3dB	3.2dB	6.2dB
Overall	-3.1dB	3.7dB	6.8dB

The performances of different communication schemes are compared with respect to SINR threshold values at 1% and 10% outage probability.

As seen in Fig. 3.4, shadowing influences system performance significantly. The partial shadowing model has a large improvement of 29 dB when compared with no shadowing at 10% outage probability. Full shadowing gives a further 6 dB improvement at 10% outage probability. Shadowing mitigates interference from the interfering BAN and therefore helps the BAN-of-interest achieve better SINR performance. Given many scenarios, of orientation of interfering hubs/sensors to the BAN-of-interest, full shadowing may be the most realistic assumption, hence the remainder of the analysis here is based on the case of full shadowing.

Overall, a significant improvement in outage probability performance is demonstrated using cooperative receive diversity. As seen in Fig. 3.4, when full shadowing is introduced, the use of two relays provides an average 6 dB performance improvement over single-link communication schemes at 10% outage probability. At 1% outage probability, the average improvement across all sensor locations is about 7 dB. Table 3.1 and Table 3.2 contain a full list of the 1% and 10% outage probability statistics when the third sensor is at different locations. They show an up-to 14 dB and 11 dB gain respectively in the case of the third sensor at the head.

Next, we perform the same simulations but with the hub alternately placed at the left hip and right hip. The results are plotted in Fig.3.5 and Fig.3.6. Their full lists of SINR threshold values are included in Tables 3.3–3.6. We can see from these tables and Fig.3.5 and Fig.3.6 that cooperative communications provides a similar amount

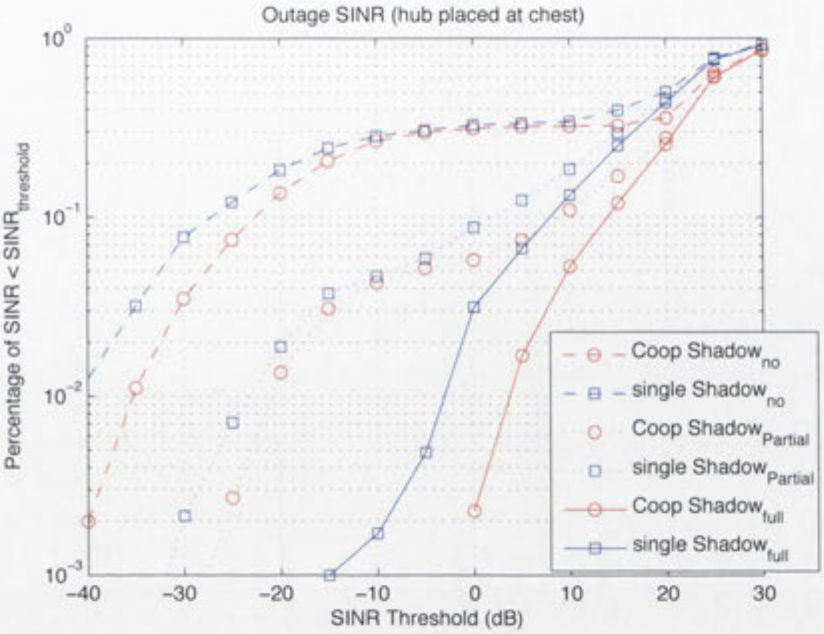

Figure 3.4: Outage SINR for Hub at chest

Table 3.2: SINR Threshold (in dB) at Outage Probability of 10% when full shadowing is included, hub at chest

Sensor location	Single Link	Cooperative links	Gain
Left ankle	6.4dB	12.5dB	6.1dB
Right ankle	6.8dB	11.9dB	5.1dB
Right wrist	9.3dB	14.8dB	5.5dB
Upper left arm	10.3dB	15.5dB	5.2dB
Head	11.1dB	21.2dB	10.1dB
Back	5.7dB	11.6dB	5.9dB
Left wrist	7dB	13.2dB	6.2dB
Overall	7.9dB	13.9dB	6dB

of improvement in SINR performance, an average of about 7 dB, in terms of outage probability regardless of the hub location. However, when outage SINR performance is compared for the hub at the chest with that for the hub at either the left or the right hip in Fig.3.7 and 3.8 (only considering the case of full shadowing), outage SINR performance is considerably improved with the hub at the chest. Thus, importantly interference has less impact on BAN coexistence performance when the hub of the BAN-of-interest is located at chest. In addition, there is no real performance advantage for hub at right hip over hub at left hip, or vice-versa.

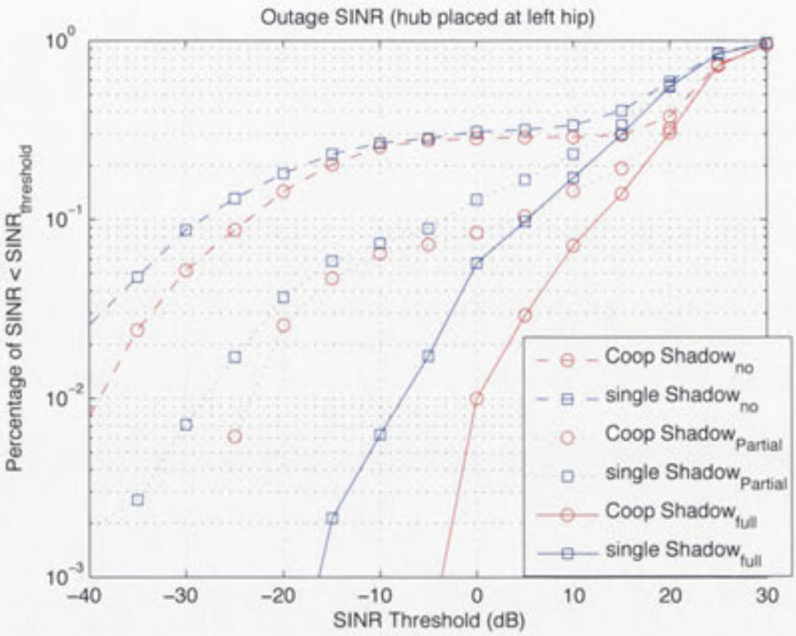

Figure 3.5: Outage SINR, Hub at left hip

Table 3.3: SINR Threshold (in dB) at Outage Probability of 1% when full shadowing is included, hub at left hip

Sensor location	Single Link	Cooperative links	Gain
Left ankle	-5.8dB	0.4dB	6.2dB
Right ankle	-8.2dB	-0.2dB	8dB
Right wrist	-7.4dB	-1dB	6.4dB
Upper left arm	-7.7dB	-2dB	5.7dB
Head	-5.4dB	1.3dB	6.7dB
Back	-12.4dB	-0.5dB	11.9dB
Left wrist	-5dB	2.7dB	7.7dB
Overall	-7.7dB	0dB	7.7dB

Importantly in Fig. 3.4 with single-link communications to the chest, even with full shadowing, the 10% outage SINR value is relatively low at 9 dB, emphasizing the need for cooperative communications. This value is even lower, around 5 or 6 dB, for the hub at the left hip in Fig.3.5, and for the hub at the right hip in Fig.3.6.

Table 3.4: SINR Threshold (in dB) at Outage Probability of 10% when full shadowing is included, hub at left hip

Sensor location	Single Link	Cooperative links	Gain
Left ankle	8.6dB	13.3dB	4.7dB
Right ankle	4dB	11.6dB	7.6dB
Right wrist	5.3dB	12.2dB	6.9dB
Upper left arm	5dB	11.3dB	6.3dB
Head	8.5dB	14.3dB	5.8dB
Back	-0.9dB	10.6dB	11.5dB
Left wrist	9.6dB	15.8dB	6.2dB
Overall	5.2dB	12.5dB	7.3dB

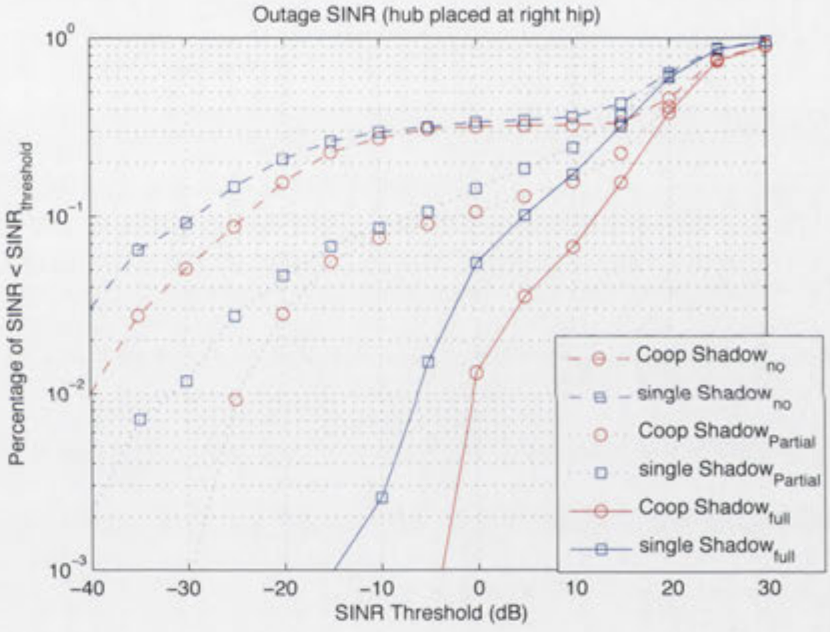

Figure 3.6: Outage SINR, Hub at right hip

3.5.2 Single BAN

The average BER performance, versus the ratio of median channel gain to receive noise variance, is determined with respect to all 7 Tx-only locations (as Location 4 to 10 in the on-body channel measurements experiment shown in Fig.2.4). We alter the hub placement between chest and left hip and vary number of relays between 1 and 2. The locations of hub and relays will be chosen among chest, left and right hip. For example, if the hub is at chest, then: 1) either left or right hip is a relay location

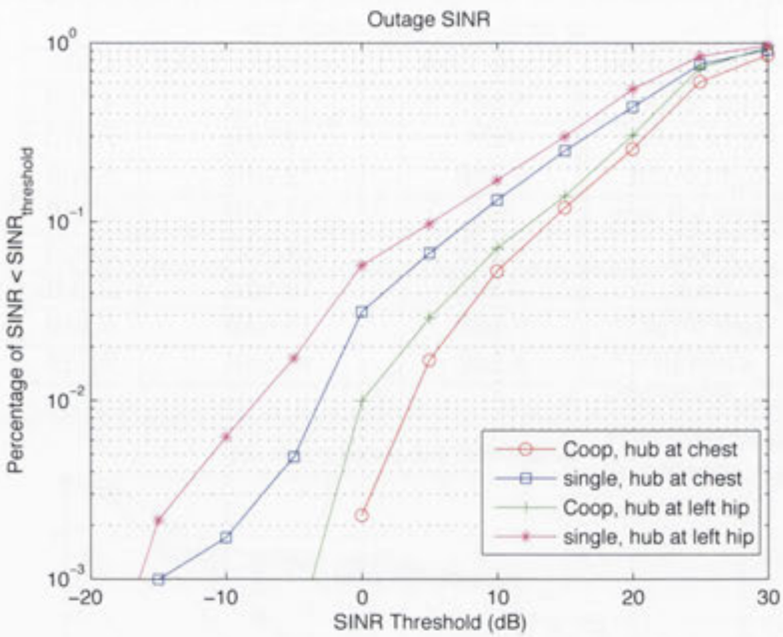

Figure 3.7: Outage SINR, Hub at chest and left hip respectively

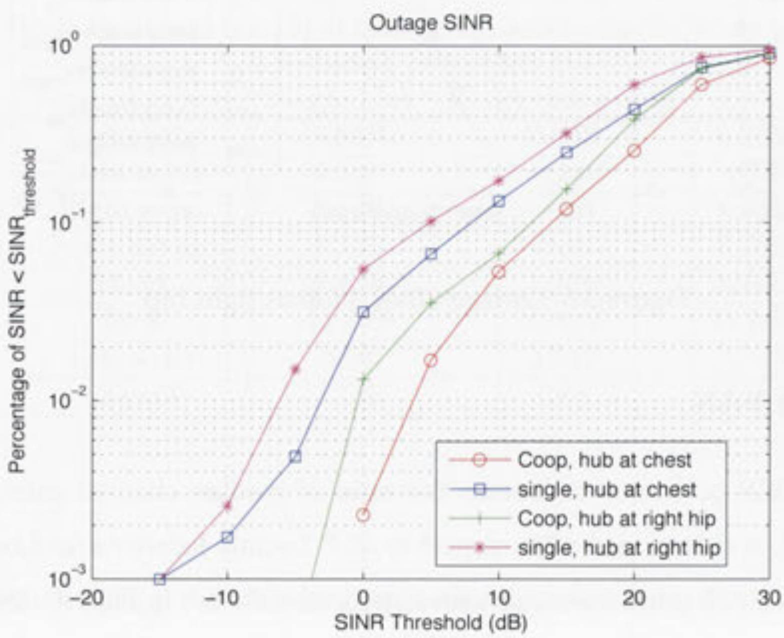

Figure 3.8: Outage SINR, Hub at chest and right hip respectively

Table 3.5: SINR Threshold (in dB) at Outage Probability of 1% when full shadowing is included, hub at right hip

Sensor location	Single Link	Cooperative links	Gain
Left ankle	-7.1dB	-1.7dB	5.4dB
Right ankle	-5dB	7.5dB	12.5dB
Right wrist	-4.6dB	10.3dB	14.9dB
Upper left arm	-6.7dB	-1.5dB	5.2dB
Head	-5.3dB	2.1dB	7.4dB
Back	-5.9dB	-0.5dB	5.4dB
Left wrist	-8dB	-1.3dB	6.7dB
Overall	-6.1dB	-0.4dB	5.7dB

Table 3.6: SINR Threshold (in dB) at Outage Probability of 10% when full shadowing is included, hub at right hip

Sensor location	Single Link	Cooperative links	Gain
Left ankle	3.4dB	10dB	6.16B
Right ankle	8.7dB	16dB	7.3dB
Right wrist	9dB	19.3dB	10.3dB
Upper left arm	3.6dB	11.1dB	7.5dB
Head	4.9dB	12.9dB	8dB
Back	4.4dB	10.3dB	5.9dB
Left wrist	2.9dB	10.2dB	7.3dB
Overall	4.9dB	12.4dB	7.5dB

when 1 relay is in use, or 2) both left and right hips are relay locations when 2 relays are in active. The performance of non-cooperative one-hop transmission is provided as reference.

One general observation can be seen from both Fig.3.9 and 3.10 that MRC performance is only marginally better than that of SC and no real benefit of using one than the other. Furthermore, with the hub at the chest, there are significant performance gains in all cases of cooperative receive diversity in Fig.3.9. At a BER of 10^{-3}, there is 4 dB gain of both SC and MRC with single relay at left hip over the one-hop communications scheme. The gain is 11 dB and 13 dB for SC and MRC respectively when single relay right hip. In contrast, marginal performance improvement is shown for using two relays over one relay, 14 dB gain for both SC and MRC compare to one-hop communications. When the hub is placed at the left hip, even though improvement over one-hop communication strategy is still significant, but not as much as placing

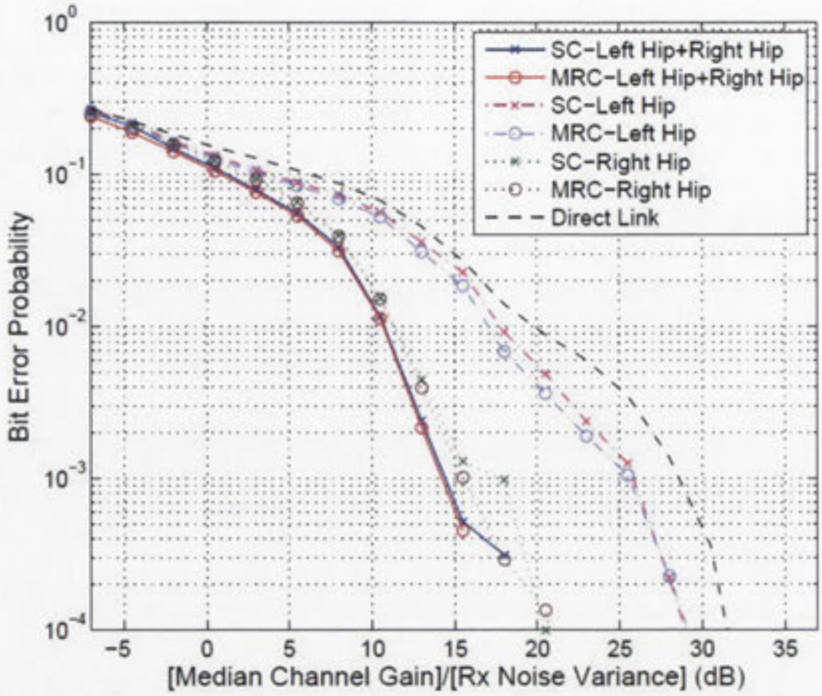

Figure 3.9: Single BAN with no interference. Hub at chest.

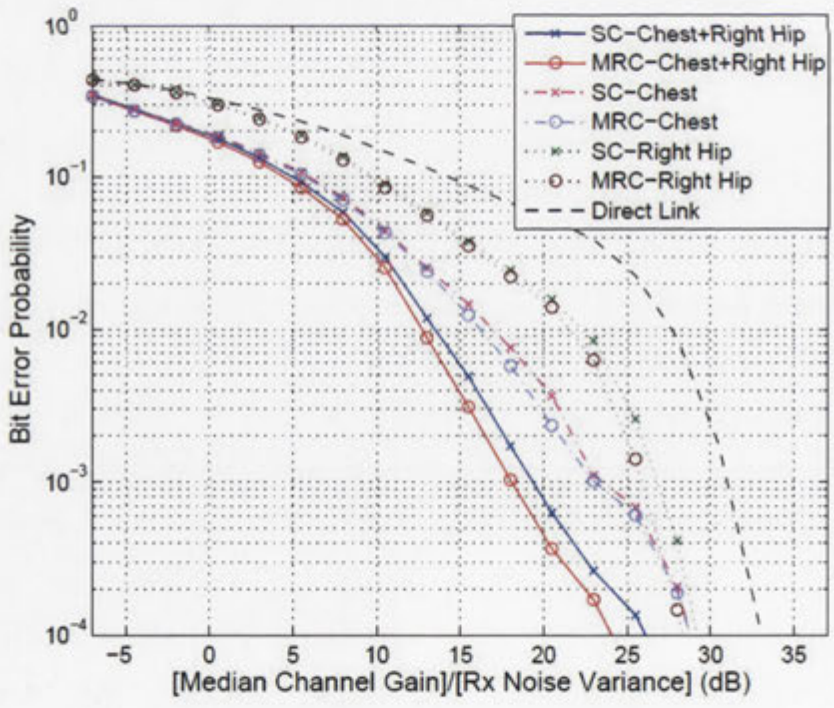

Figure 3.10: Single BAN with no interference. Hub at left hip.

the hub at the chest. At the same BER of 10^{-3}, there is about 4 dB and 5 dB gain for SC and MRC with relay at the right hip; and 8 dB gain for both combining schemes with one relay at the chest. The use of two relays provides additional 4 dB gain over the better performing one-relay strategy.

In general, it is encouraged to include relay-assisted cooperative communications scheme in the design of BAN, as significant improvements are demonstrated over traditional single-hop star-topology BAN. There is no real performance gain of cooperative MRC over SC. Depending on the hub placement, there are advantages to use two relays than one relay, if the added complexity is permissible. The extra complexity in this case can be computational complexity, increased latency, additional power consumption etc. Well-considered relay placement with respect to the hub is important.

3.6 Concluding remarks

In this chapter, cooperative communications using on-body relays have been developed for BAN. A varying relays scheme was proposed, where as a sensor node is transmitting, the other idle sensors work as relays to forward the overhearing packet. Hence, all sensors acted as relays in turn to assist transmission. Two typical scenarios were investigated: 1) a BAN was isolated from any interference and 2) two BANs were coexisting in a close range. The BAN-of-interest used a [31,19] BCH-coded Gaussian Frequency Shift Keying (GFSK) modulation scheme and a TDMA-like inrea-BAN access protocol. Empirical on-body channel measurements were employed to better simulate the dynamic body-centric channel. For the latter scenario, a realistic inter-BAN channel model incorporating path loss, small-scale fading and shadowing was used.

The numerical results validated the performance of our proposed two-hop relay-assisted cooperative communications method to be used in BAN for both scenarios. The improvement in reliability by employing the scheme was substantial in terms of average BER and SINR threshold corresponding to specific outage probability. In addition, it was observed that enabling relays in the scenario for BANs coexisting can make use of the body shadowing effect to more significantly mitigate the impact of co-channel interference.

Furthermore, simulations with three different common hub locations were conducted, among which a better outage SINR performance was shown when the hub was at the chest than when it was at left or right hips. Moreover, there was some advantages to using two relays over a single relay if the added complexity of doing so was neglected. At the hub, the difference of using MRC and SC were studied, and no real performance gain is found for using one over the other. This result agrees with the statement made by Nessa et al. [2008], which claimed the use of a single best relay is equivalent to use of all potential relays. It motivates us to employ an opportunistic relaying scheme for BAN, which will be discussed in the next chapter. To reduce extra overhead for switching between sensor and relay mode and simplify the complexity for typical sensors, fixed relay-only nodes (i.e., not typical sensors) will be considered in the following chapters.

Opportunistic Relaying for Coexisting Wireless Body Area Networks

In the previous chapter, it was observed that the performance gain of employing MRC and SC in BAN was very similar. This inspires us to introduce and study the use of opportunistic relay schemes for BANs' coexistence in this chapter. In addition, considering the extra overhead for switching between sensor and relay modes, we introduce a fixed-relay scheme, which assigns the relay function to less energy-constrained location-fixed radio devices and therefore reduces the added complexity to sensors and prolongs their operation time.

More specifically, in this chapter, we first investigate the effectiveness of cooperative communication with opportunistic relaying, in terms of interference mitigation for the non-coordinated BAN coexisting scenario. A suitable TDMA scheme is adopted as both an intra-network and also an inter-network access scheme. For this work, both extensive on-body and off-body channel gain measurements are employed to gauge performance, which are overlaid to simulate a practical BAN working environment. Then as the other important contribution of this chapter, an experimental study for the two-hop cooperative communications scheme is conducted based on two IEEE 802.15.4 BAN systems located closely in an indoor environment. These systems are realised with several MICAz motes running the TKN15.4 version of the Medium Access Control (MAC) protocol, specifically using a beacon-enabled mode and GTS Guaranteed Time Slot (GTS) scheduling. This setup enables the observation of two-hop cooperative communications operation in a coexistence scenario in real-time. Numerical results are provided for both aforementioned studies. Significant advantages of the proposed scheme over the traditional star-topology BAN are demonstrated with respect to the first and second order statistics of the received packets' quality.

A part of this work was presented in Dong and Smith [2013]. The second part of the work was done in collaboration with Dr. Yu Ge, of the Institute for Infocomm Research, Singapore; and is being submitted to ACM Transactions on Sensor Networks (Dong et al. [2015a]) for consideration for publication therein.

4.1 Introduction

In the previous chapter, the performance of cooperative communications, with multiple relays participating in transmission, was evaluated and this showed substantial improvement over the reliability of a BAN operating in an isolated or interfering scenario. Considering the finding that similar improvements were presented with either MRC or SC, the use of a single optimal relay instead of having all relays actively cooperating is inspired. This idea follows the concept of opportunistic relaying, which has been demonstrated in Bletsas et al. [2007]; Valentin et al. [2008a]; Hwang et al. [2008]; Cui et al. [2009]. It has shown no performance loss compared to schemes involving all potential relays in general slow-fading wireless relay channels (Nessa et al. [2008]; Sharma et al. [2011]). In BAN, a reasonable hypothesis is that using opportunistic relaying can potentially mitigate the interference created to coexisting BANs as the number of transmitting relays is reduced (Stamatiou et al. [2012]), but whether the reduction in the number of active relays degrades reliability improvements is unknown. The key to this question and also to the effectiveness of opportunistic relaying is whether the correct optimal relay can be determined before a packet is sent. As mentioned in Valentin et al. [2008b], this requires to establish reliable control channels for optimal path selection and the channels of the selected path to remain stable over the period-of-interest. According to Smith and Hanlen

[2015], it is generally the case in BAN, as most of the BAN channels are stable for typically more than 0.5 seconds, which is sufficiently longer than the duration of a packet length in BAN transmission. This chapter simulates BANs' coexistence, and provides numerical results about the actual performance of opportunistic relaying in terms of interference mitigation.

The first part of this work presented here is extended from Chapter 3, some similarities with that are:

1. Intra- and inter-BAN access scheme: TDMA across multiple BANs is employed as well as the intra-BAN access scheme since it provides better interference mitigation with respect to power consumption and channel quality (Zhang et al. [2010]);

2. Three-branch cooperative communication: A BAN system in this chapter uses two relay nodes to provide extra diversity gain at the receiver. Three branches are used with one direct link from sensor to gateway node and two additional links via two relays;

3. Intra-BAN channel model: Extensive on-body channel gain measurements are adopted as the intra-BAN channel model for the analysis by simulation (Smith et al. [2012b]).

There are also some major differences in our simulation setup:

1. Diversity combining scheme: Instead of a three-branch MRC and SC schemes at the gateway node, an opportunistic relaying method is simulated, which reduces complexity by adopting the concept that only a single relay with the best network path towards the destination forwards a packet per hop;

2. Fixed relay placements: Considering the additional complexity to the sensor when the relay function is integrated, a fixed-relay scheme is used. In this case, sensors' functions are more simplified than the ones described in Chapter 3 and there are extra relay-only nodes at well-considered locations.

3. Inter-BAN channel model: A major contribution for this part of the work is that the performance of cooperative BANs using opportunistic relaying with

no cooperation amongst them is investigated with real inter-body channel gain measurements as described in Section 2.2.2.2.

Besides a simulation study of opportunistic relaying with respect to interference mitigation, a thorough experimental investigation is conducted to validate the performance of relay-assisted cooperative communication for BAN. The major contributions are:

1. A light-weight real-time two-hop relay-assisted communication scheme is implemented for BAN in real life. Our scheme considers two parallel low complexity relay nodes and provides three-branch diversity gain to the hub.

2. The BAN-of-interest contains multiple sensors distributed over various places where typical sensors are placed at real BAN products.

3. We empirically demonstrate, through extensive radio propagation measurements, the significant improvement of the two-hop cooperative communications compared to the single-hop BAN.

In a multiple BANs coexistence scenario, a BAN's performance is more interference limited. Therefore, the performance is analysed with respect to the SINR values of the received packets at the hub in both the simulation and experiment work. Since the duration of outage is more critical than the probability of outage in analyzing the performance of a communication system with multiple co-channel interferers (Annavajjala and Zhang [2010]), here our analysis shows both the first-order and second-order statistics of the SINR. Statistics are compared with respect to a traditional star topology BAN with the same channel data employed.

The rest of this chapter is organised as follows. In Section 4.2, the opportunistic relaying scheme used in this work is explained. Section 4.3 and 4.4 describes the setup for the coexistence simulation. In Section 4.3, system models such as the fixed-relay scheme, composition of the BAN-of-interest, intra- and inter-BAN access schemes are explained, while the inter-personal channel measurements and its joint usage with on-body channel data are provided in Section 4.4. Section 4.5 presents numerical results for both the simulation investigations, and highlights the performance of proposed schemes for BAN. Section 4.6 provides a detailed descriptions on the hardware and software used in the coexistence experiment as well as the numerical results of the experiments. Finally, some concluding remarks are made in Section 4.7.

4.2 Opportunistic Relaying Scheme

In the simulation, three-branch opportunistic relaying is adopted. Among three branches, one of them is the direct link from the active sensor to the gateway node, and the other two are decode-and-forward links via two relays, which are located at left and right hips respectively. The best relay is chosen prior to each packet's transmission. This requires each relay to know the SINR for each packet it receives from the active sensor, as well as the SINR for each packet received from it at the hub, i.e. an indication of first- and second-hop channel quality. In practice, the proposed opportunistic relaying scheme can be implemented using timers at relays, as illustrated in Bletsas et al. [2006]. In this chapter, it is achieved by selecting the link with the best effective SINR which is essentially the minimum of the weighted SINR between sensor to relay and relay to hub links. SINR γ is defined as follows:

$$\gamma = \frac{p_{sig} * |h_{sig}|^2}{|\sigma_{\text{noise}}|^2 + \sum(p_{int,i} * |h_{\text{int},i}|^2)} \tag{4.1}$$

where p_{sig}, $p_{int,i}$ are the average transmit powers of packet-of-interest and interfering packet from ith coexisting BAN respectively. h_{sig},$h_{\text{int},i}$ are the average channel gain of the signal channel and interfering channel across the length of the received packet.

With opportunistic relaying, each decode-and-forward relay evaluates the minimal instantaneous received SINR among two hops in the beginning of a superframe. With SINR γ defined above, the selected j_{OR}th relay is hence determined by the following:

$$j_{OR} = \arg\max[\gamma_{1,min}, \gamma_{2,min}], \qquad (4.2)$$
$$\gamma_{k,\min} = \min[\gamma_{r_k h}, \gamma_{sr_k}], \text{ with } k = 1 \text{ or } 2.$$

The subscripts s, r_k and h represent sensor, kth relay and hub respectively.

At the receiving end, i.e. hub, the relayed copy is then compared with the one received via the one-hop source-to-destination link. The decision is also based on the SINR value, and the larger one will be used for decoding and demodulation.

4.3 System model

4.3.1 Configuration of BAN

The model of a BAN system used in the simulation consists of one hub (gateway node), two relay nodes and three sensor nodes, which are organised in a star topology. In order to cooperatively use measured channel data, the hub and two relays are placed separately at one of three locations: chest, left and right hips. Fig. 4.1 shows the situation where hub is at chest and relays are at left and right hips respectively. In terms of sensor devices, they are at any three locations from the Rx places listed in Table 2.2. Within each BAN, sensor nodes are coordinated by the hub using TDMA. Therefore, as soon as the hub sends out a beacon signal to all connected sensors, they respond by transmitting required information back to the hub in a pre-defined sequence during their allocated time slots. During the transmission period, one of the relays assists transmission by providing another copy of the signal to the hub. The choice of relay is based on the opportunistic relaying scheme explained in previous section. In this part of the work, it is assumed that only one information packet is sent from each sensor during its allocated time slot. After completion of transmission from all sensor nodes, the system becomes idle until the next beacon period.

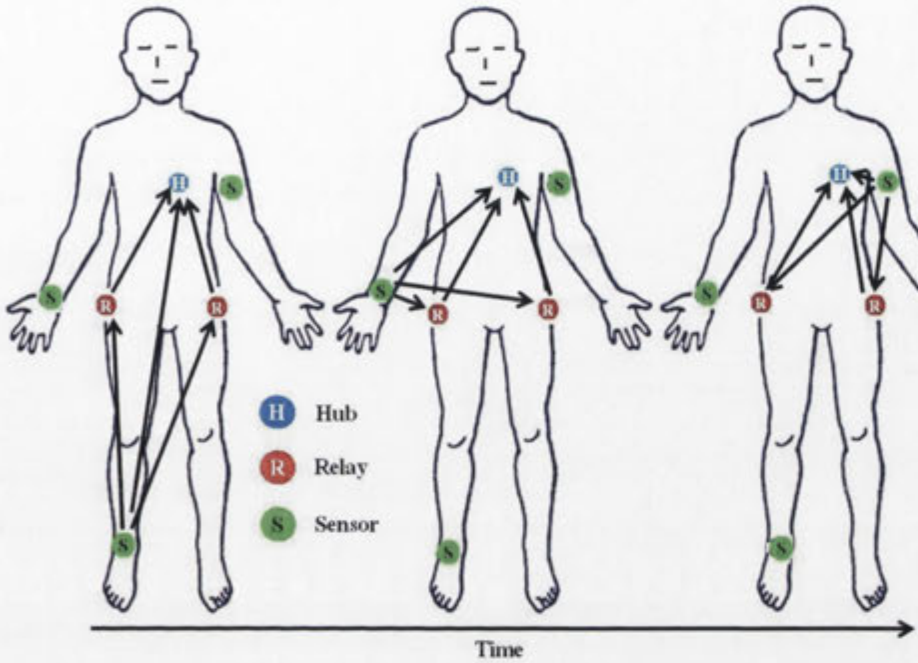

Figure 4.1: BAN configuration: fixed relay topology

4.3.2 Two BANs coexistence

For optimal co-channel interference mitigation and reduction in power consumption, TDMA is adopted as the co-channel access scheme across BANs, as well as being the access scheme within any BAN. Assume there are total m BANs co-located (or in close proximity) and the number is fixed during the period of simulation, then the shared channel can be evenly divided into m time slots with a length of T_d. Therefore, each BAN goes into idle status for a length of $(m-1)\times T_d$ after it completes transmission. However, due to lack of a global coordinator among multiple BANs, the execution of the TDMA scheme used here is slightly different from the traditional implementation of TDMA. Here, in our TDMA scheme the coordinator in each BAN chooses the idle period T_{idle} between two consecutive superframes randomly, following a uniform random distribution over $[0,(m-1)\times T_d]$. In this chapter, two BANs employing this same configuration are used in analysis, i.e. $m = 2$.

4.4 Channel model

4.4.1 Inter-BAN channel model

In order to study the impact of an opportunistic relaying scheme on a BAN while multiple collocated BANs work non-cooperatively, a well-defined and reliable inter-BAN channel model is employed. NICTA has performed several measurements to capture such multi-person interference channel data (Smith et al. [2012b]). The experiment ran for many times with different number of subjects involved, each wearing channel sounders that were the same as for measuring on-body channel data as described in Section 2.2.2.1. Each subject had a transceiver and two receivers, working at 2.36 GHz, attached to their body. In the experiment, the transceiver was at left hip and two receivers were at right upper arm and left wrist respectively. For the data set used in the simulation, there were 8 people wearing such systems, and their activities included walking together from office to a cafe and then back to the office. The transceivers on all subjects transmitted packets in sequence at 0 dBm every 40 ms in a round-robin fashion, i.e., each one occupies the channel sequentially for 5 ms. All units log the RSSI value from all packets received. Each device writes one output file when it interleaves the RSSI samples.

4.4.2 Overlaying two data sets

With these two data sets, a realistic multi-BAN coexistence scenario can be simulated. However, we recall from Section 2.2.2 that the on-body channels and off-body interfering channels were sampled every 15 ms and 40 ms respectively. Therefore, in order to use these two data sets together, it is critical to synchronise them at the same sampling rate. Since the coherence time of both on-body and off-body channels is around 500 ms (Smith et al. [2012a]), it is possible to down sample both types of channel gain coefficients to 120 ms per sample that is within the period while the channel is stable. In addition, a block fading model is used whereby the Tx-Rx channel gain is constant over each packet transmission period. Therefore, the time between each packet transmission is effectively 120 ms.

Table 4.1: Interfering channels

Channel index	Interfering BAN	BAN-of-interest
1	Left Hip	Left Hip
2	Left hip	Right Hip
3	Left Hip	Chest

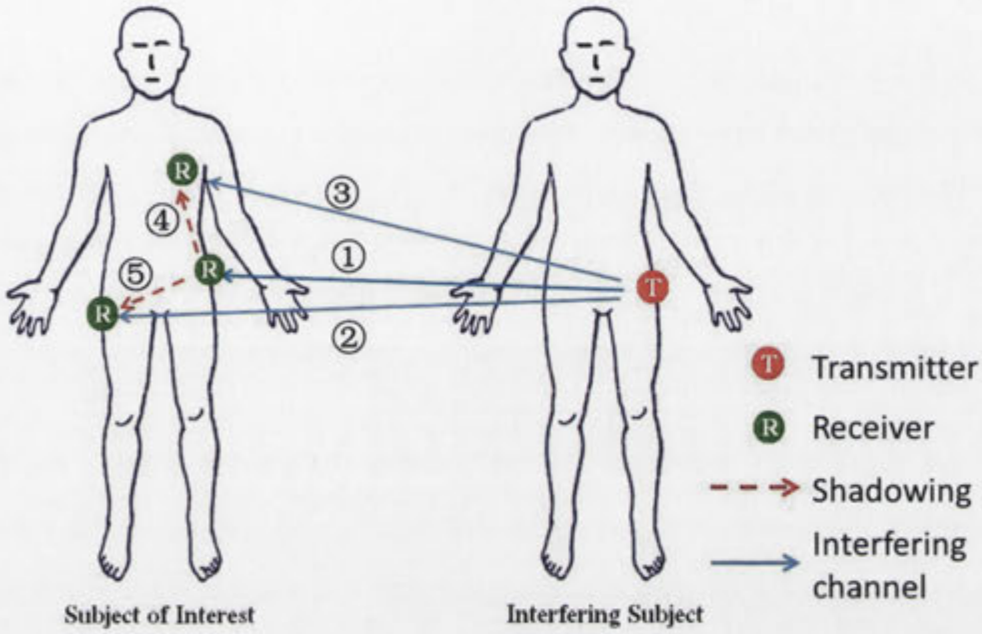

Figure 4.2: Channel overlaying map

Besides overlaying fading profiles in the time domain, it is also crucial to consider spatial overlaying. Assume the person-of-interest is named Subject One, and an interfering transmitter is attached to Subject Two. Gateway node and relays are placed on Subject One at the chest, left and right hips respectively (three common locations for these two types of devices). Since opportunistic relaying used in this part of the work is based on the SINR value at the relays, interference is considered at three locations, i.e. one hub node and two relay nodes. Then these three devices on Subject One can all hear the interference from the interferer, i.e. Subject Two's transmitter. Thus the interfering system can influence operation of the opportunistic relaying for the BAN-of-interest. Channels 1, 2 and 3 shown in Fig. 4.2 are the resultant interfering channels described previously. Based on this, the three interfering channels specified in Table 4.1 were used in simulation.

Table 4.2: In the table, (Intf) represents the person of interfering, and (I) indicates the person-of-interest. Numbers in each cell represent indicated channel in Fig.4.2

Final channel	Part 1	Part 2
1: LH(Intf) - LH(I)	1: LH(Intf) - LH(I)	
2: LH(Intf) - RH(I)	1: LH(Intf) - LH(I)	5: LH(I) - RH(I)
3: LH(Intf) - C(I)	1: LH(Intf) - LH(I)	4: LH(I) - C(I)

However, because the interference channel data was measured with devices at left hip, right upper arm and left wrist, there is no direct channel data for the cases of right arm and left wrist (in Table 4.1). Thus, it is necessary to overlay two data sets spatially to form a good model of interfering channels between two subjects. Details of overlaying can be viewed from Table 4.2. It can be seen that the shadowing components of Part 2 channels are combined with channel gain measurements listed in the Part 1 column. The shadowing components are abstracted by removing the corresponding free space path loss from the original channel gain data.

4.5 Simulation results

Here, we simulate the case of a hub placed at chest with two relays at the left and right hips, following the simulation configuration described in Section 4.3. We present performance analysis with respect to the system's first order statistics - outage probability of SINR, and its second order statistics - Level Crossing Rate (LCR). Their concept will be defined in following sections. As shown in Table 4.3, simulation is duplicated using different combinations of the person-of-interest and the interferer. Simulation for every combination is run 10 times with a varied starting time for the channel data. In the following figures, the notation of "SX - SY, schem" indicates experiment using Subject X as BAN-of-interest and Subject Y as interfering BAN, with either a single-hop or a cooperative communication scheme. In the following analysis, we also used the term "overall" outage probability or level crossing rate. The overall results are obtained by calculating the corresponding metrics using the SINRs formed by stacking SINR series of all simulation repetitions and different subject combinations.

Table 4.3: Simulation combination: X indicates a simulation is performed.

Subject Index	#1	#2	#3	#4	#5	#6
#1		x	x	x	x	x
#2	x		x	x	x	x

4.5.1 Analysis of SINR outage probability

Outage probabilities at given SINR thresholds are defined as the probability of SINR value being smaller than a given threshold

$$Pr(\gamma < \gamma_{threshold}) \tag{4.3}$$

The performance of single link communication and two-hop cooperative communication schemes are compared with respect to SINR threshold at 1% and 10% outage probability. Here, 10% outage probability corresponds to a guideline for 10% maximum packet error rates in Astrin et al. [2012].

Fig. 4.3 shows the outage probability for situations when different subjects are treated as the person-of-interest. Note that in Fig. 4.3(a), the relevance of choosing a starting sample index $n = 45000$ is explained in the next paragraph. For Subject One, the cooperative communication scheme provides about 5 dB improvement over traditional single link communications at 10% outage probability. At 1% outage probability, the improvement is even more significant, there is, in fact, more than 15 dB improvement. In contrast, simulation on Subject Two shows similar results, with 4 dB and 6 dB improvement at 10% and 1% outage probabilities respectively.

However, while running simulations using a different starting channel sample index, it is found that channel stability has a significant impact on the performance of the cooperative communication scheme. Fig. 4.4 is a typical on-body channel gain plot for Subject One. It is clear that there is a significant change in operating environment for the sample where the red line is placed in Fig. 4.4. Subject One's on-body channels become more unstable after that point, i.e. channel coherence time decreases rapidly. Hence, simulation is also performed with channel sample taken from $n = 1000$, and result is plotted in Fig. 4.5. Compared to Fig. 4.3(a) where channel sample is taken from $n = 45000$, cooperative communication scheme

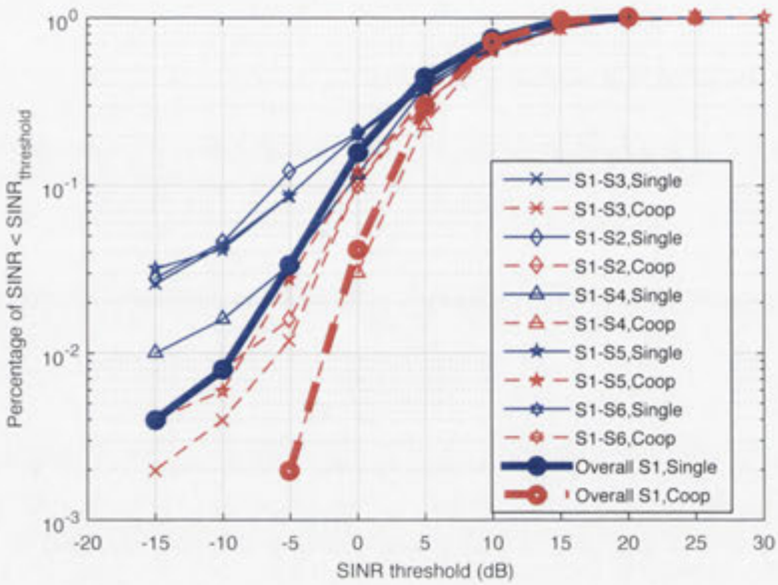

(a) Outage probability of Subject One with channel sample starting at n=45000

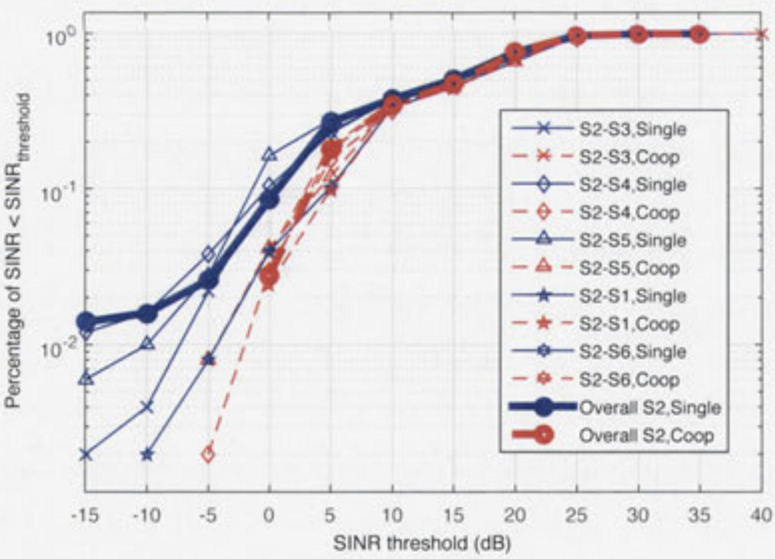

(b) Outage probability of Subject Two with channel sample starting randomly

Figure 4.3: Outage probability of SINR for two subjects

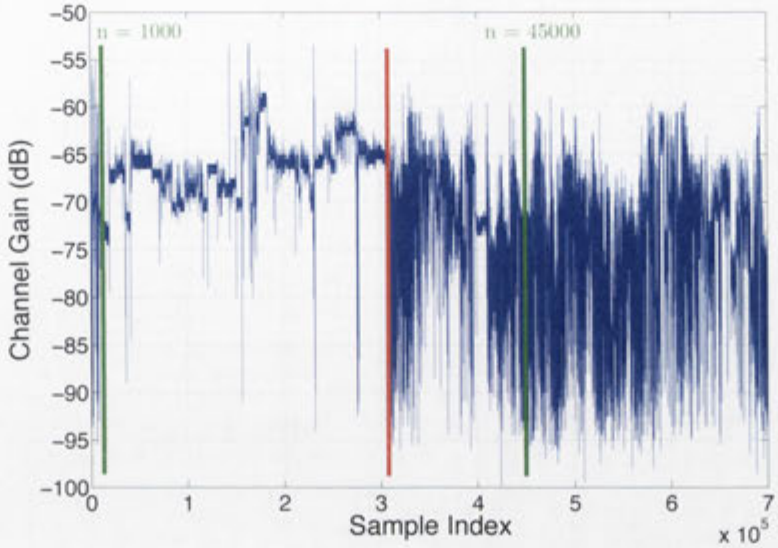

Figure 4.4: A typical on-body channel gain plot of Subject One

provides little SINR improvements at both 10% and 1% outage probabilities in this situation. As a result, two-hop cooperative communication schemes can provide even more improvement in system performance when the environment, in which the BANs are operating, changes rapidly.

4.5.2 Level crossing rate

LCR is defined as the average rate at which a received packet's SINR value going below a particular threshold in the positive going direction. It provides an important insight into the severity of the rate of packet dropping. A high LCR indicates frequent unsuccessful packet reception, which can eventually lead to increased retransmission, decreased throughput, inefficient channel usage and energy wastage. In the simulation, the LCR value at threshold γ_{th} is calculated as

$$LCR_{\gamma_{\text{th}}} = \frac{n}{\sum_{i=1}^{n-1} t_{i,i+1}}, \tag{4.4}$$

where n is the total number of crossings at threshold γ_{th}, and $t_{\text{i,i+1}}$ indicates the time between two consecutive crossings.

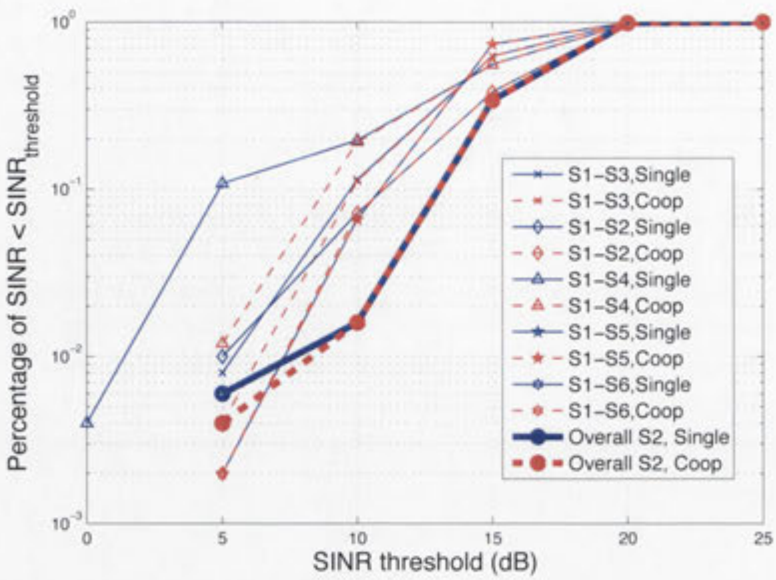

Figure 4.5: Outage probability of Subject One with channel sample starting at n=1000

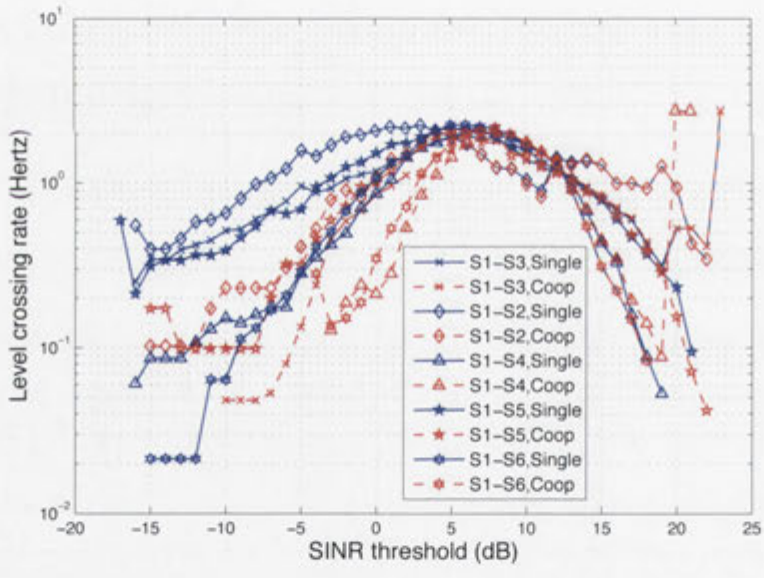

Figure 4.6: LCR of Subject One with channel sample starting at n=45000

Fig. 4.6 and Fig. 4.7 both show that cooperative two-hop communications are able to reduce LCR at low SINR threshold values significantly. At a LCR of 1 Hz, the SINR threshold value for Subject One rises by an average of 6 dB as shown in Fig. 4.6 with the use of cooperative communications. For Subject Two, the improvement, as shown

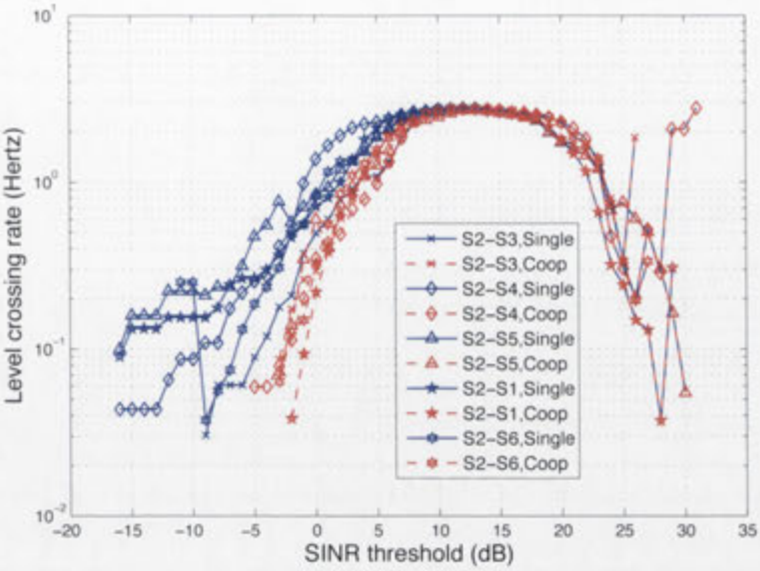

Figure 4.7: LCR of Subject Two with channel sample randomly

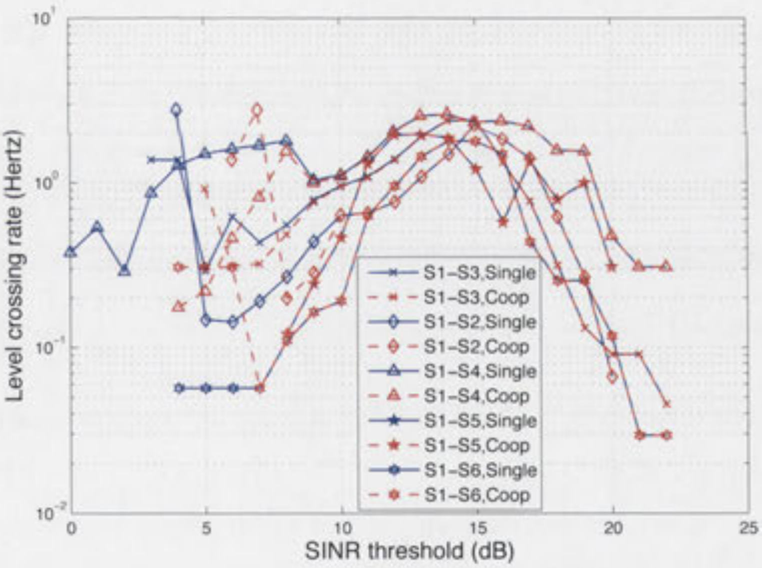

Figure 4.8: LCR of Subject One with channel sample starting at n=1000

in Fig. 4.7, is about 4 dB. System performance remains similar at high SINR threshold values. In addition, a similar observation to that made for outage probability in Fig. 4.5 can be made from Fig. 4.8, when coherence time of the on-body channels in the BAN-of-interest is large (i.e., channels are more stable). In the case of Fig. 4.8, the

LCR curves overlap most of the time for single-hop and cooperative communications schemes. Therefore, in such a case, there is no real performance advantage in terms of LCR to use our proposed cooperative communication scheme.

4.6 Experimental Study

4.6.1 System implementation

The configurations of our experiments to investigate relay-assisted communications are as follows:

Sensor node configuration: multiple MICAz motes[1], as shown in Fig.4.9, running modified TKN 15.4[2] MAC protocol were employed to form an IEEE 802.15.4 BAN. A fixed transmission power of 0 dBm is set on all operating motes. It is noted that due to the memory capacity of the MICAz motes, a limited amount of data can be saved. In addition, there is some probability that data was lost while saving to the memory. Therefore, we repeated the experiment several times to capture enough measurements and also mitigate the impact of losing data.

Locations of on-body nodes: Three types of network nodes were implemented, *coordinator*, *device* and *relay*. The term *device* here stands for the sensor nodes that collect information (such as sensors) and transmit to the coordinator. The coordinator was placed at the chest while two relay-only nodes are placed at the left/right hips as in Fig.4.10.

Network architecture: In the BAN-of-interest, the proposed two-hop cooperative topology is adopted, where the device sends data through the direct link and relay links. For performance comparison, traditional single-hop communication, where only direct transmission between the coordinator and device is available, is also experimentally implemented in the same environment. Both the BAN-of-interest and

[1]The MICAz with MPR2400 radio chip operates over 2.4 to 2.48 GHz, a globally compatible ISM band. It supports a link transmission rate of up-to 256 kbps, and the transmission power range is from −24 to 0 dBm (dat [2006]). With an internal 512K bytes measurement flash, it is able to store all data for later extraction and analysis. Even though the MICAz mote is a simple off-the-shelf device, it is able to adjust its sampling rate by varying the beacon order in its implementation.

[2]TKN 15.4 is the first open-source empirical implementation of the 802.15.4 MAC protocol, based on the TinyOS 2.1.x operating system (Hauer [2009]). It is platform-independent and can be widely used for BAN studies.

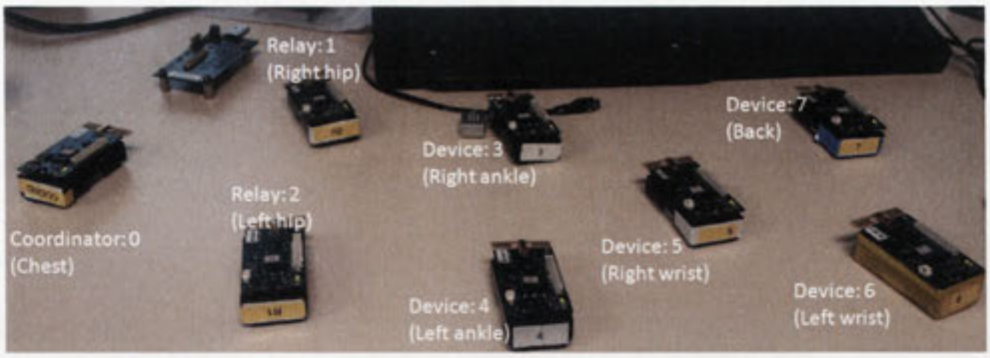

Figure 4.9: MICAz motes to be used in the BAN testbed.

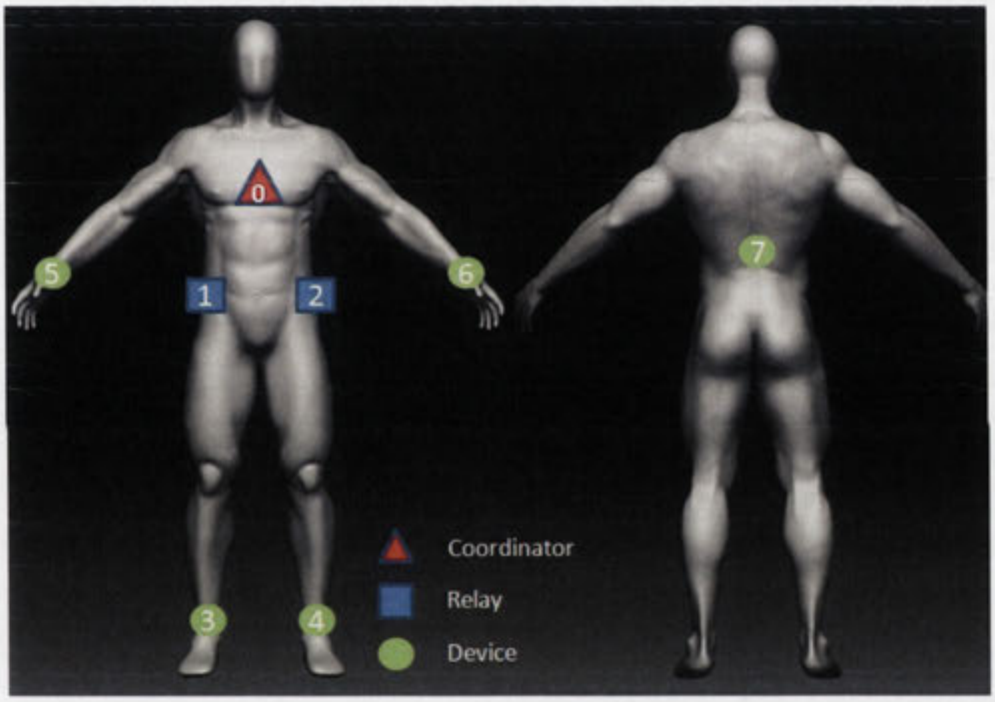

Figure 4.10: Nodes placement in BAN testbed.

the interfering BAN (in the coexisting scenario) operate in the same physical radio channel at all times.

MAC mode: It follows the slotted CSMA/CA MAC mode specified in IEEE 802.15 Task Group 4 [2011]. The GTS mechanism in the Contention Free Period (CFP) is used in scheduling. For the needs of periodic data acquisition at the coordinator, the beacon-enabled mode is used. Fig.4.11 shows the superframe structure of the measuring system in the beacon-enabled mode. Relays and devices transmit

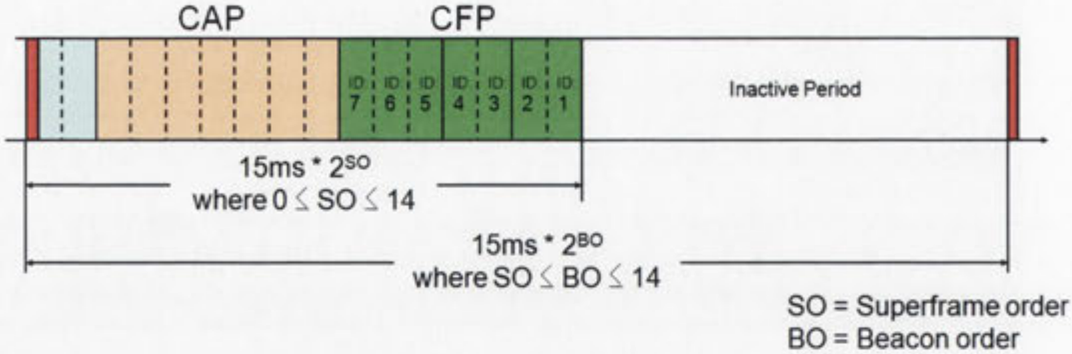

Figure 4.11: IEEE 802.15.4 beacon-based superframe structure.

their packets in the allocated GTS during the CFP.

Revised GTS scheme: In this experiment, the number of devices is fixed and each device only requires one unit in CFP. Each relay node also requires one unit in CFP. Both relay and device request GTS from the coordinator and transmit during their allocated GTS. The difference is, instead of only waking up at its own GTS (like a device), a relay remains active snooping throughout the entire CFP. This allows relays to capture the device nodes' transmission, and therefore record the channel gain between each device and the relay. It is noted that the snooping function at relays can draw additional current and hence consume extra power, but at a much lower level than the current solution. In addition, relays are less energy-constrained since relays and hub can be more frequently recharged than sensors. Therefore, the added power consumption is negligible.

Scenarios: Two different experiments were conducted and each one was repeated on three occassions. Every run of the experiment lasted for approximately 10 minutes.

- In the first experiment, a male subject, with height of about 1.80 meter and weight of 80kg, wore a complete BAN (Network 1) that consisted of 1 coordinator, 2 relays and 5 devices (locations and ID are as shown in Fig.4.10). This subject walked randomly indoors in a 10m×10m room.

- In the second experiment, in addition to the same configuration of the first

Table 4.4: Parameters for the experiments

Parameter	Network 1	Network 2
Frequency	2.450 GHz	2.450 GHz
Channel	20	20
Network ID	0x1FF1	0x0531
Superframe Order (SO)	4	2
Beacon Order (BO)	4	2
Sample frequency f_s	245.8 ms	61.4 ms
packet payload size	20 bytes	20 bytes

experiment, a simplified network (Network 2), acting as an interfering source, was placed at the centre of the same room. It only consisted of a coordinator and a device.

The key parameters for the two networks are listed in Table 4.4.

4.6.2 Experimental results

The performance of the two-hop cooperative communication scheme, with/without interference in the vicinity, is presented. The results are averaged across all 3 occasions of each experiment. The proposed scheme is compared with a BAN using a one-hop star topology operating in the same environment. Therefore, we exam four different scenarios, i.e., the combination of "Direct/Coop and Isolated/Interfering". These terms will be used in the rest of this section, which corresponds to the following description:

- Direct: The BAN system on the subject uses a traditional star topology;
- Coop: The BAN system on the subject employs the proposed two-hop cooperative communications;
- Interfering: An interfering BAN is in operation locating closely to the BAN-of-interest;
- Isolated: No interfering BAN is closely located to the BAN-of-interest.

The performance is presented from the perspectives of the first- and second-order statistics of the effective channel gains of all device-to-coordinator links. In the context of one-hop communication, the effective channel gain of a device-to-coordinator link within a superframe is simply the channel gain h_{direct} of the direct link. In contrast, for the case of using two-hop communication scheme, it is the resultant channel gain h_{SC} of the best path among three available branches, which is determined as Eq.(4.2).

4.6.2.1 Onbody channel characteristics

Table 4.5 summarises the median values of all source-to-destination channel gains (TX power is fixed at 0 dBm). There are two situations in which a packet lost can occur and the coordinator fails to record the RSSI value: the RSSI drops below the receive sensitivity; or a received packet cannot be correctly decoded. The median values of channel gain, which is a preferable guide for BAN applications (Hanlen et al. [2009]), are shown in Table 4.5, and the median gain across all channels is -73 dB. These are generally close to the typical on-body channel gain given as -70 dB in Hanlen et al. [2010a]. The mean of all the channel gain samples captured is found to be -59 dB. With respect to the channel gain normalised to the mean gain for each Tx/Rx link, a lognormal distribution with parameters, log-mean $\mu = -1.64$ and log-standard deviation $\sigma = 1.46$ is found to match the data quite well.

4.6.2.2 Outage probability

First, we show the outage probability at the given channel gain thresholds. It is defined as the probability that a channel gain sample is lower than a threshold value $Pr(h > h_{threshold})$

From Fig.4.12, we can see that interference from other coexisting BANs significantly affects the operation of the target BAN. When interference exists in the environment, if the outage probability of 10% is required for a system, the threshold channel gain requirement decreases by approximately 7 dB(from -83 to -90 dB) and 4 dB(from -76 to -80 dB) for systems with star topology and cooperative communication respectively. Therefore, BAN using cooperative communications is more effective at reducing the performance impact of interference than a star-topology

Table 4.5: The channel gains, for Tx and Rx located correspond to those shown in Fig.4.10

Rx ID	Tx ID	median, dB
#0	#1	−76
	#2	−61
	#3	−71
	#4	−73
	#5	−67
	#6	−56
	#7	−73
#1	#3	−75
	#4	−72
	#5	−74
	#6	−52
	#7	−73
#2	#3	−79
	#4	−85
	#5	−70
	#6	−75
	#7	−82

system. In the isolated operations,if the outage probability of 10% is required for a system, cooperative communications provides an 7 dB improvement(from −83 to −76 dB), while the improvement is up to 10 dB(from −90 to −80 dB) for the system in the presence of interference. In addition, interestingly the performance of 'Coop, interfering' is even better than 'Direct, isolation' by about 4 dB.

4.6.2.3 Level crossing rate

Firstly, the impact of interference can be similarly observed as in outage probability, which leads to more frequently dropping below the required threshold. For example, at the channel gain threshold value of −80 dB, the presence of interference increases the LCR by twice, from approximately 0.14 Hz to 0.28Hz. Fig.4.13 shows that by employing the proposed two-hop cooperative communications, the LCR is significantly reduced in the threshold range from −75 to −100 dB. For instance, at a threshold of −100 dB channel gain, LCR drops from 0.2 Hz to 0.04 Hz when the network configuration switches to the proposed scheme.

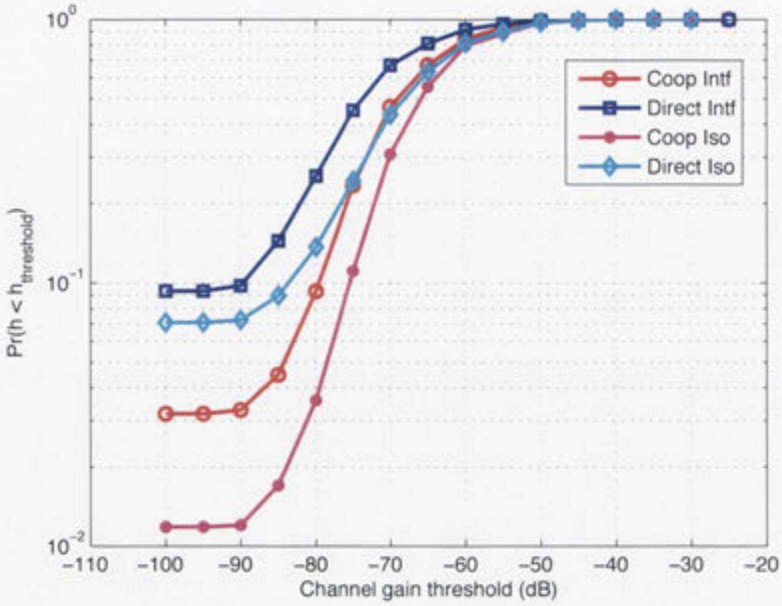

Figure 4.12: Outage Probability at different channel gain thresholds.

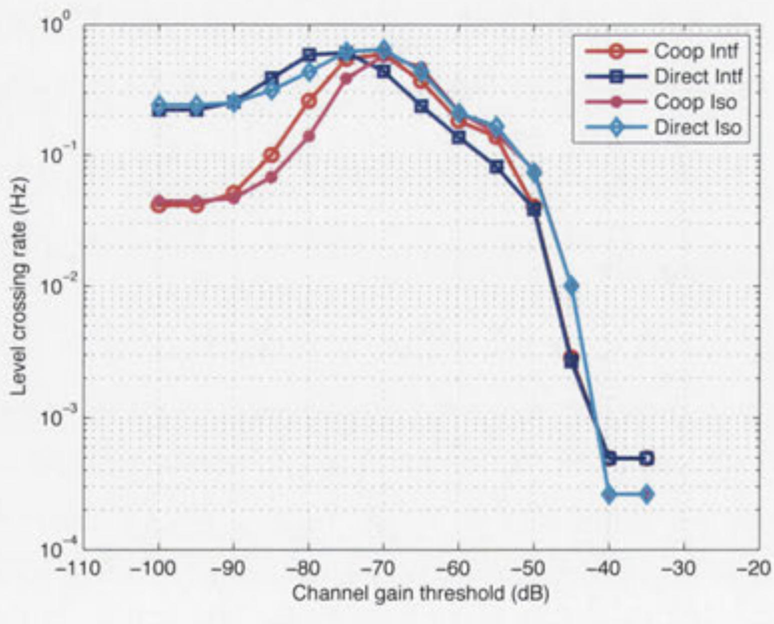

Figure 4.13: Level crossing rate at different channel gain threshold.

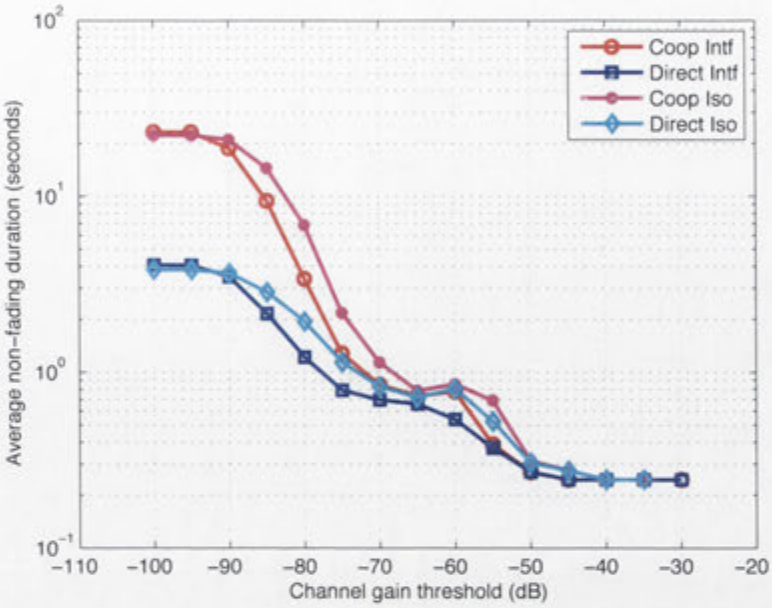

Figure 4.14: Average non-fading duration at different channel gain threshold.

4.6.2.4 Average non-fade duration

Similar improvement can also be observed in terms of average non-fade duration as shown in Fig.4.14. The average time of a device-to-coordinator link remaining above a threshold, particularly in the range of −75 dB to −100 dB, is remarkably prolonged with the use of relays. The benefits are consistent regardless of the presence of the interference. The longer non-fading duration, together with smaller LCR as shown in Subsection IV.C., ensures more time for successful packet transmission and reduces the overhead required to re-transmit packets. Hence, two-hop cooperative communication can increase the effective throughput and reduce latency (delay).

4.6.2.5 Average fade duration

Average fade duration (AFD) of time varying channel gain is defined as the average period of continuous time that the channel gain stays below a threshold value across one-or-more superframes. Fig.4.15 presents the empirical results of AFD of all different scenarios. Slight improvement is shown using cooperative communication scheme when an interfering BAN is coexisting. Otherwise, no significant perfor-

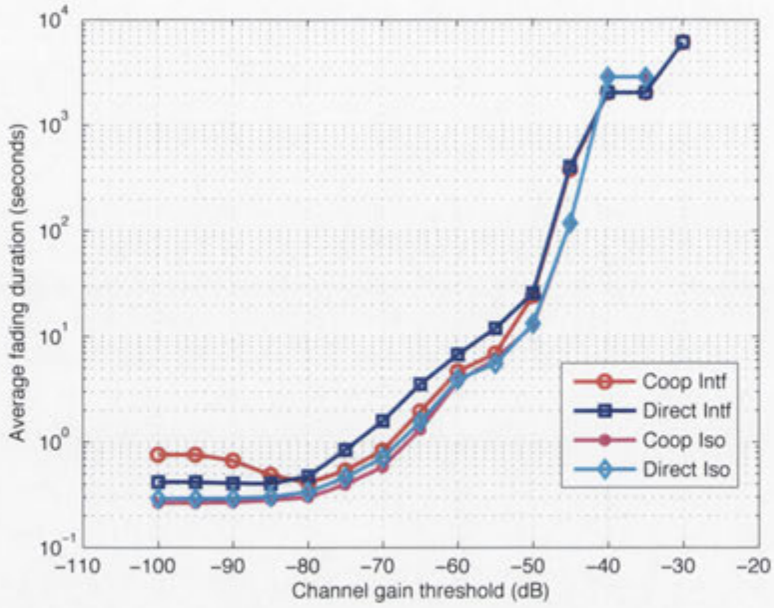

Figure 4.15: Average fading duration at different channel gain threshold.

mance advantage is found in terms of average fade duration.

4.6.2.6 Branch switching rate

At last, the switching rate for the proposed cooperative communication scheme is examined. The switching rate is the frequency at which the selection of any branch changes at the coordinator. It is found that the switching rate is 1.76 Hz when the BAN-of-interest is isolated from any interfering BANs. In comparison, the rate increases to 1.79 Hz when another BAN comes into its proximity. To further reduce the switching rate, switched combining design can be employed (Smith [2012]).

4.7 Concluding remarks

In this chapter, the effectiveness of two-hop cooperative communication with opportunistic relaying has been investigated in terms of interference mitigation in a multiple BAN coexistence scenario. For the purpose of reducing complexities on sensor nodes, two fixed relay-only nodes have been integrated into the traditional star-topology BAN system. Within the sufficient channel coherence time of typical

BAN channels, the three-branch opportunistic relaying only activates the optimal relay that has been predicted prior to the transmission. In this chapter, both intra- and inter-body channel measurements have been employed and overlaid for a more realistic simulation capturing various unique characteristics of body-centric channels. Meanwhile, a thorough experimental study has been conducted, which enables the real-time study of cooperative communication scheme in various situationss under various scenarios. Two low-complexity relays were placed in the BAN-of-interest to provide three-branch diversity over the body. The experiment was constructed with several MICAz motes executing the modified TKN 15.4 MAC protocol. We employed cooperative communications using relays in both cases, whether an interfering BAN was present or not, and compared its performance with the case of a BAN using no relays.

Promising advantages of using opportunistic relaying in BAN have been demonstrated in this chapter, and they are consistent for both our simulation and experimental studies. The comparison with traditional star-topology BAN network has shown improvements in outage probability of SINR of the received packets at the hub, and hence this ensures that the BAN system will be more reliable and robust in a crowded environment. In addition, LCR and average non-fade duration are significantly reduced. This increases the chance of successful receptions of consecutive packets, which is critical to data transmitted across multiple frames. We also found that the benefits of using opportunistic relaying is even more promising when the operation environment is more dynamically varying, i.e., channel coherence time is small, or significant interference is present.

When opportunistic relaying improves the SINR of received packet at the hub by taking advantages of spatial diversity, it was also observed that packets that already have high SINR achieved in slightly higher throughput. But this provides unnecessary growth in "good" packet' SINR values that has no real, overall, system reliability benefit and furthermore it is cost inefficient in terms of power consumption. Therefore, a joint relaying selection and power control scheme is presented for BAN in next chapter, which adaptively adjusts the transmit power according to the selected transmission-like quality and hub's receiver sensitivity.

Joint Relay Selection and Transmit Power Control Scheme for Interference Mitigation

The advantages of using relays in BAN has been demonstrated in the previous chapter 4, in terms of its efficiency in interference mitigation when multiple BANs are coexisting. The resultant significant higher SINR of the received packets leads to a better network reliability, but also reflects the potential cost-inefficient issue. For transmission links which have good channel qualities, transmitting at maximum power level is not necessary and is a waste of precious energy in BAN's sensors and hence degrades their battery longevity. Based on this idea, a joint relay selection and transmit power control scheme is presented for the coexistence of BANs in this chapter. The transmit power control is performed based on light-weight channel prediction with respect to the selected direct/relay link. Considering the environment of BAN use, signal transmission and hence the prediction accuracy are sensitive to typical non-line-of-sight propagation and multipath fading. To include these influences in our study, a large set of empirical on- and inter-body channel data is employed to model various scenarios of BAN communications. The number of interfering BANs in the simulated coexistence scenario is scaled up from 1 , as shown in the previous chapter, to up-to 9 as specified in the Zhen et al. [2008a]. Our study shows that relay assisted power control can reduce significant amount of circuit power consumption from that of constant transmission at 0 dBm, without loss in reliability.

Further,the ability of interference mitigation is enhanced over constant transmission at −5 dBm, which has a similar power consumption as the proposed joint scheme. The reliable performance is maintained with various number of BANs coexisting. In addition, the performance of a joint algorithm is also validated for an isolated BAN. A trade-off between power saving and interference mitigation is motivated, taking remaining sensor-battery level, amount of interference and on-body channel quality into account.

A part of this work was published in Dong and Smith [2014], and the full-work has recently been submitted for consideration for publication in IEEE Transactions on Communications (Dong and Smith [2015]).

5.1 Introduction

The current design of BAN, which uses a simple star topology consisting of a central hub and multiple sensor devices around the body, faces two main constraints on operation: radio-sensor battery capacity and lifetime; and radio co-channel interference from closely located BANs. For small low-complexity sensors, typical to BAN in healthcare, battery constraints are significant, with small battery size and long life-time required. Moreover, BANs communications generally experience large path loss (Yazdandoost and Sayrafian-Pour [2010]), and robust transmission with battery-constrained limitations on transmit power is a big challenge. With respect to co-channel interference, this is due to other, closely-located, BANs with no coordination between them. The number of BANs coexisting can vary according to scenario and application, in conjunction with a range of BAN mobility (Astrin et al. [2012]), and it is generally difficult to find a coordinator in a dynamic BAN communications environment. The IEEE 802.15.6 BAN standard specifies the demand for reliable performance when up-to 10 BANs are all located within a $6 \times 6 \times 6$ m space (Astrin et al. [2012]). As the use of BANs becomes more pervasive, efficient interference mitigation becomes even more important.

To prolong network lifetime and improve the robustness of BAN communications, various different strategies have been proposed. Among them, cooperative communications and transmit power control are prominent. The advantages of two-hop cooperative communications have been demonstrated in both narrowband (e.g., D'Errico et al. [2011]; Ferrand et al. [2011]), and ultra-wideband (e.g., Chen et al. [2009]) BAN systems. Such relay assisted communications can also reduce co-channel interference from other BANs in the vicinity, by increasing the SINR of packets received at the hub as shown in Chapter 4. In terms of power control, the potential of extending sensor battery lifetime and improving a BAN's reliability by using a simple prediction-based power control scheme has been shown in Smith et al. [2011b]. This leads to the following questions:

1. Is it possible to use cooperative communications together with power control as a potential implementation for BAN?
2. Does the combination of these schemes provide any advantage in terms of performance reliability, interference management and power consumption?

As an answer to these questions, here we present an effective joint relay selection and transmit power control algorithm based on selection combining and prediction-based power control. Improved interference mitigation is verified based on large sets of empirical on-body and inter-body channel gain data measured across many hours of "everyday" mixed activities (Smith et al. [2012b]).

The rest of this chapter is organised as follow. In Section 5.2, the proposed joint power control and relay selection scheme is explained. Following that, the system model for this investigation and channel model employed are shown in Section 5.3 and 5.4 respectively. The performance of the proposed scheme is demonstrated in terms of interference mitigation and power conservation in the scenario of multiple BANs coexisting. At last, Section 5.6 provides some concluding remarks.

5.2 Algorithm

The BAN-of-interest in this chapter has a configuration consisting of three sensors, two relays and a hub. The hub is placed on the chest, while the two relays are located at the right and left hips respectively. The locations of three sensor nodes are chosen

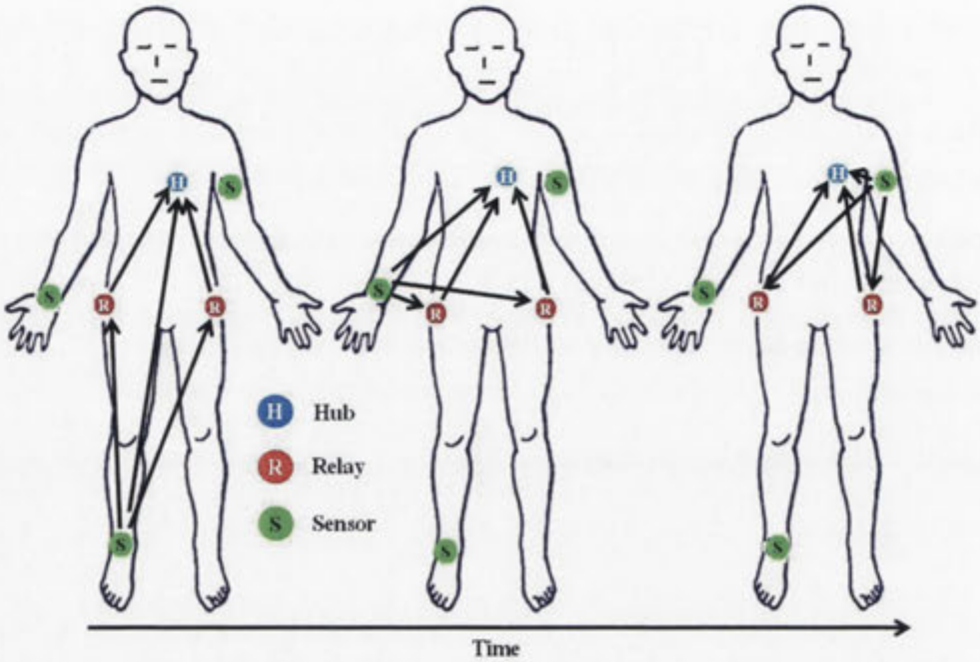

Figure 5.1: BAN configuration

from 7 other locations, as listed in Table 2.2 at which long periods of on-body channel gain data was captured experimentally (Smith et al. [2012b]).

Three-branch selection combining is employed, using a direct link from the sensor to the hub and two links via relays. It is assumed that hub broadcasts with a constant transmission power of 0 dBm as it is not power constrained. In conjunction with this combining, a simple prediction-based power control is employed at the sensors and relays. By keeping the prediction function only at relays and the hub, it is ensured that there are not additional computational and storage complexities for the more-energy-sensitive sensor nodes. It is assumed that the transmission power at these nodes can vary from −30 dBm to 0 dBm in 2 dB steps. Prior to transmission, the active sensor is informed of the best link chosen from its previous transmitted packet, a link choice that can be broadcast by the hub within it's beacon. The sensor then adjusts its transmission power according to receiver sensitivity and the best link's previous channel gain sample across the relevant packet. If the best link was dual-hop using a relay, prediction and power control is performed on the first hop of the relay link, i.e., between the sensor and relay. The same process is used at each relay, but this time on the second hop. After receiving signals via these three links, the hub chooses the best copy of signal based on the SINR of the received packet, which is calculated as shown in Equ. (2) in Algorithm 2. A detailed description of the proposed scheme is shown in Algorithm 1 with respect to transmit power control and in 2 with respect to joining relay selection with power control. Note that in Algorithm 1, the variable $offset$ provides the flexibility of adjusting transmitting power according to the current channel conditions and remaining energy level at sensor and relay nodes. In this chapter, we simply use different fixed offsets for different receiver sensitivities.

Algorithm 1 : Power control using simple channel prediction based on previous channel gain sample

Variable Definition:
Rx_{sens} is receiver sensitivity (at relay or hub)
$h(\tau)$ is the current channel gain sample
$h(\tau - 1)$ is the previous channel gain sample
$p = [-30, -28, -26, -24, \dots, -2, 0]$ dBm

```
function POWER CONTROL(h, τ)
    C = Rx_sens − h(τ − 1);
    Find index k so p(k − 1) < C ≤ p(k);
    p_out = p(k) + offset;
    if p_out > max(p) then
        p_out = 0 dBm;
    else if p_out < min(p) then
        p_out = −30 dBm;
    end if
end function
```

5.3 System model

To investigate the performance of the proposed scheme, we simulate a scenario for multiple BANs coexistence, with the BAN-of-interest employing the joint algorithm (as shown in Fig. 5.2), along with the case of an isolated BAN. Large sets of empirical everyday activity channel data are used as a model of a realistic environment for BAN use, which was illustrated in Section 2.2.2

Algorithm 2 : Joint relay selection and transmit power control algorithm

Variable Definition:
Rx_{sens} is the receiver sensitivity at the hub
Five channels: h_{sh}, h_{sr_1}, h_{sr_2}, h_{r_1h}, h_{r_2h}
Aggregate interference and noise at hub, Relay 1 and Relay 2: $\mathbf{IN}_h$, $\mathbf{IN}_{r_1}$, $\mathbf{IN}_{r_2}$
Link active indicator: a_1, a_2. Initialised with 0 prior to a packet's transmission; (*0 means inactive*)
Current channel gain index: τ

% Power control at sensor
if $h_{sr_1}(\tau - 1) \geq Rx_{sens} - max(p_{sensor})$ **then**
  Active the first relay link; $a_1 = 1$;
end if
if $h_{sr_2}(\tau - 1) \geq Rx_{sens} - max(p_{sensor})$ **then**
  Active the second relay link; $a_2 = 1$;
end if

Find index k, so
$k = \arg\max \left[\frac{h_{sh}(\tau-1)}{IN_h(\tau-1)}, a_1 \frac{h_{sr_1}(\tau-1)}{IN_{r_1}(\tau-1)}, a_2 \frac{h_{sr_2}(\tau-1)}{IN_{r_2}(\tau-1)} \right]$ (1)
$p_{sensor}(\tau)$ = **Power Control**(Channel, τ) , where
  $k = 1$, Channel $\Rightarrow h_{sh}$
  $k = 2$, Channel $\Rightarrow h_{sr_1}$
  $k = 3$, Channel $\Rightarrow h_{sr_2}$

% Power control at relay
if *i*th Relay is active, $i = 1, 2$ **then**
  $p_{r_i}(\tau)$ = **Power Control**(h_{r_ih},τ)
end if

% Branch selection at the hub
SINR $\gamma = \frac{p_{sig} * |h_{sig}|^2}{|\sigma_{noise}|^2 + \sum(p_{int,i} * |h_{int,i}|^2)}$ (2)

Find the best branch ℓ at time τ so,
$\ell(\tau) = \arg\max \left[\gamma_{direct}(\tau), a_1 * \gamma_{r_1}(\tau), a_2 * \gamma_{r_2}(\tau) \right]$ (3)

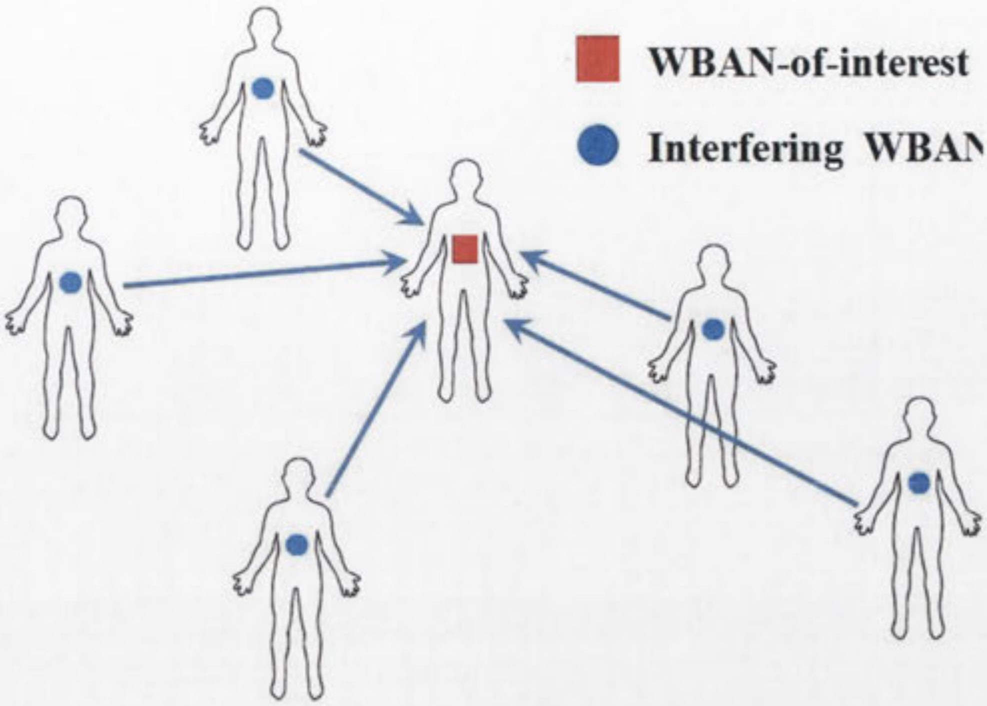

Figure 5.2: Multiple BANs coexistence - Diagram

5.3.1 Intra- and inter- BAN configuration

A major difference from the system set-up employed in previous chapter is that here there is a varied number, from 0 to 9, of BANs interfering with the BAN-of-interest. This setup allows us to simulate coexistence, for from 2 to 10 BANs, as well as simulate for an isolated BAN. Each BAN has the configuration specified in Section 5.2, i.e., a hub at the chest, two relays at right and left hips, and three sensors at other suitable locations. All possible nodes locations are given in Table 2.2. An example is shown in Fig.5.1, where sensors are placed at the right wrist, right ankle and left upper arm. Within a BAN, i.e., intra-BAN, TDMA is adopted. Sensors transmit the collected information to the hub in a pre-defined sequence after receiving the beacon signal from the hub. This process is shown in Fig. 5.3, in which the labels indicate node numbers. While each sensor is transmitting, two relays assist as described. We denote the time period starting from the beacon signal to when all nodes within the network finishing transmission of their current packets as a superframe. It is assumed that each sensor only transmits one information packet

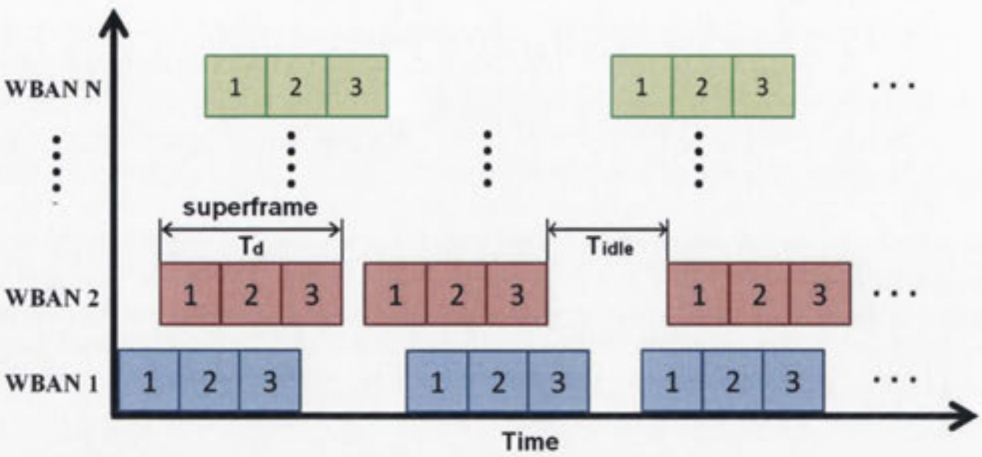

Figure 5.3: Multiple BANs coexistence - TDMA use

in a single superframe. At the end of a superframe, the current BAN becomes idle and waits until the next beacon period. The length of the idle period depends on the expected number of BANs co-existing and also the inter-BAN access scheme.

In the consideration of co-channel interference mitigation and power consumption, TDMA is employed as co-channel access scheme across all BANs (Zhang et al. [2010]). In conventional TDMA, the channel will be divided equally into time slots and allocated to each BAN without overlap. However, as we recall that it is generally not feasible to have global coordination across coexisting BANs, the implementation of inter-BAN TDMA is different. As shown in Fig. 5.3, if we assume the number of BANs coexisting is N and the length of a superframe is T_d, then a BAN chooses the starting time of every superframe randomly, following a uniform distribution over $[0, (N-1) \times T_d]$. In the case when $N = 1$, the BAN-of-interest is an isolated BAN.

5.4 Channel model

Prior to simulation, extensive BAN channel data was measured using small wearable channel sounders operating at 2.36 GHz (close to the 2.4 GHz ISM band), developed at NICTA (Hanlen et al. [2010b]). The experiments were conducted in many different environments, involving subjects doing a mix of distinctive everyday activities (Smith et al. [2012b]). In this work, comprehensive on-body and multi-person inter-body channel data sets from Smith et al. [2012b], captured in realistic environments and scenarios, are utilised.

With respect to the on-body channel gain data used here, 3 transceivers were placed at the chest, left and right hips respectively and 7 receivers were placed at other typical sensor locations (as shown in Table 2.2). Throughout the entire experiment, transceivers operated in a round-robin fashion broadcasting every 5 ms at 0 dBm. During one transceiver's transmission, the remaining channel sounders, including the idle transceivers, recorded the received signal strength indicator (RSSI) upon successful detection of a packet. This experimental process was repeated on different subjects.

For the capturing of inter-body channel data, multiple subjects were involved in the experiment. For the data set used in the simulation, there were 8 people walking together to a cafe, sitting there for a while and then walking back to the office. Each subject wore only 1 transceiver at the left hip and 2 receivers at the right upper arm and left wrist respectively. Similar to the on-body channel experiments, each transceiver broadcast every 5 ms in round-robin sequence at 0 dBm. Hence on-body and inter-body channel data sets have unmatched sampling rates, 15 ms per sample and 40 ms per sample respectively, because there is a different number of transceivers in each of these data sets.

Therefore, before applying them in our system simulation, temporal synchronization and spatial overlaying are required. A more detailed description of this process can be found in Section 4.4.2. As the coherence time of both on-body and off-body "everyday" channels is around 500 ms (Smith and Miniutti [2012]), both of them can be downsampled to 120 ms per sample, well within the period of channel temporal stability. In addition, considering the channel stability, a block-fading channel model over each transmitted packet, either within the BAN-of-interest or from interfering BANs, is adopted.

Further, as described in Algorithm 2, we take interferences heard at hub and two relays into account while perform power controlling and relay selection. Therefore, three inter-body channels are required between a single interfering BAN and the BAN-of-interest, i.e., from an interferer to BAN-of-interest's chest, left and right hips.

However, due to the selected channel sounder placement in the inter-body channel capturing experiment, there is no explicit data for some of the interfering channels. As a result, random offsets for spatial overlaying are added onto the available channel data to simulate the required interference channel.

5.5 Numerical Analysis

Performance of the proposed joint relay selection and transmit power control algorithm is analysed based on extensive simulations employing empirical BAN channel data. Comparison is made with other algorithms specified in Table 5.1. The legends, 'Coop' and 'No Coop', represent using two-hop relay-assisted cooperative communications and traditional single-link communications respectively. In the following analysis, algorithms will be referred to as 'Coop/No Coop, $0/-5/-10$ dBm', with the numerical values representing the constant transmission power. In the case of 'Coop, power control', it is the proposed joint relay selection and transmit power control algorithm. Four receiver sensitivities, $[-86, -90, -93, -95]$ dBm, are employed, which correspond to different, BAN compliant, data rates when operating at 2.4 GHz IEEE 802.15 Task Group 6 [2012]. Additive constant received noise power of -100 dBm is assumed in all cases. In addition, as mentioned before, there are 7 possible sensor locations to choose from. Therefore, different permutations of the three sensor node locations are simulated, and the results are averaged across all tested permutations.

Here, the performance is compared with respect to outage probability of SINR values of packets received at the hub, and average circuit power consumption for every sensor node in Tx mode. To map changes in sensor transmit power to circuit power consumption, the related mapping provided in Sagan [2009] is used. According to the MedWin alliance (Davenport et al.), -10 dBm transmit power Tx_{out} corresponds to *a* circuit power consumption, Tx_{cons}, of 2.9 mW at 2.4 GHz. Therefore, Tx_{out} from -30 to 0 dBm is mapped to Tx_{cons} from 1.76 mW to 5.97 mW according to the relation in Sagan [2009] and the reference value in Davenport et al.. The $offset$ variable, as used in Algorithm 1, is chosen so that whenever power control is used,

Table 5.1: 8 Algorithms simulated for performance analysis; X indicates a simulated algorithm

	Power Control	Constant Transmit Power		
		0 dBm	−5 dBm	−10 dBm
Coop	X	X	X	X
No Coop	X	X	X	X

there is similar power consumption to transmitting at a constant −5 dBm power level.

In Fig.5.4, the outage probabilities when using algorithms specified in Table 5.1, with different receiver sensitivities, are compared. In this case, the number of BANs needing to coexist is 5. We note that the performance differences for 5 coexisting BANs are similar to any number from 2 to 10 BANs needing to coexist. It is observed that for each receiver sensitivity, performance variations between algorithms are very consistent. Therefore, our analysis will focus on the case of −90 dBm receiver sensitivity as shown in Fig.5.4(b). It can be observed that the proposed joint 'Coop, power control' algorithm has the third (together with 'Coop, −5 dBm') and second best performance, at outage probabilities of 10% and 1% respectively. At these two levels, the only two algorithms which are better than our proposed scheme involve transmitting at 0 dBm constant power. (But we note that the proposed scheme performs better than 'No Coop, 0 dBm' at 1% outage probability by 2.7 dB). However, if we look at the average circuit power consumption in Tx mode, at the sensors, as shown in Fig.5.5, transmitting at 0 dBm consumes about 60% more power than our joint algorithm. In addition, we can also see that employing transmit power control consumes a similar level of circuit power as −5 dBm constant transmission, but provides 4.1 dB improvement at an outage probability of 1%. Finally, although transmitting constantly at −10 dBm from the sensors saves a large amount of power in Fig. 5.5, reliability shown in Fig.5.4 is significantly degraded.

Fig.5.6 shows the SINR threshold values at 1% outage probability when the number of coexisting BANs varies. As more BANs come into each other's vicinity, the proposed algorithm consistently out-performs all but one case. It is better than all other algorithms, apart from performing an average of 3.4 dB lower than the best

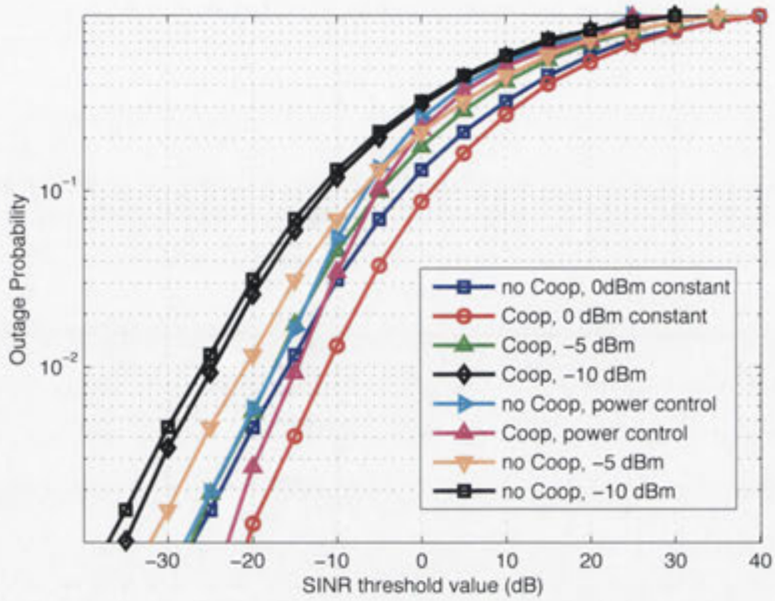

(a) Receiver Sensitivity of −86 dBm

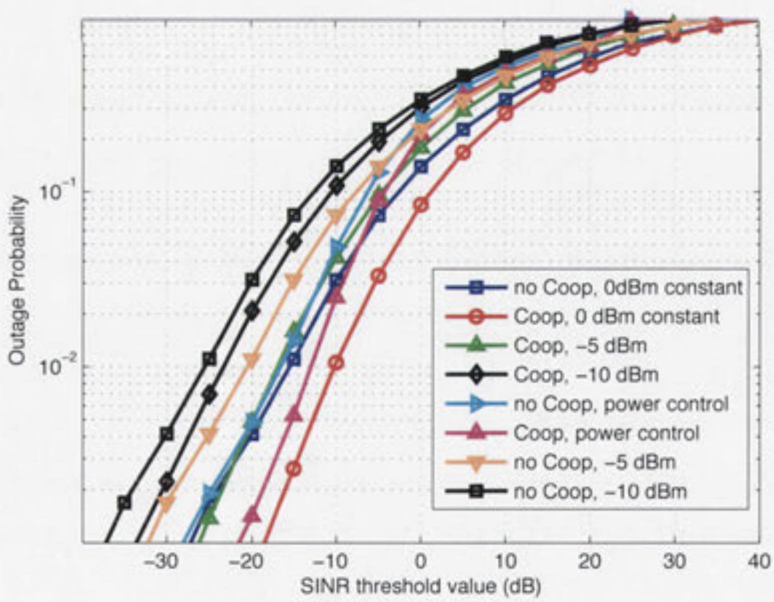

(b) Receiver Sensitivity of −90 dBm

Figure 5.4: Outage Probabilities for 5 coexisting BANs

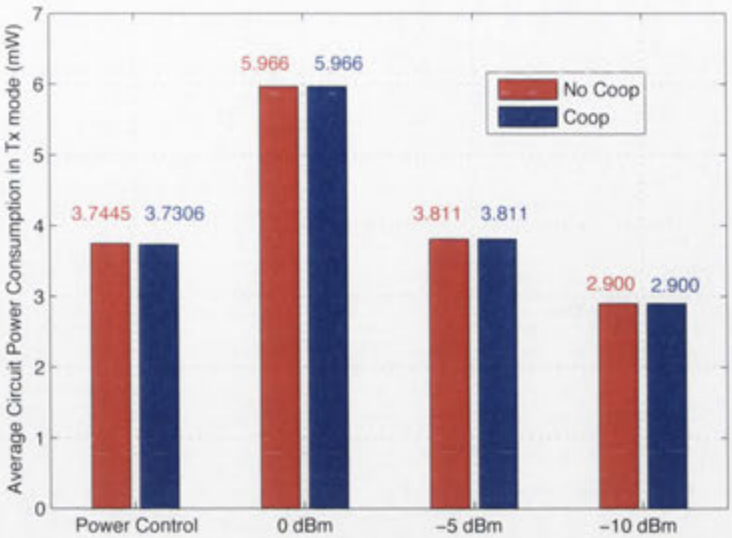

Figure 5.5: Average circuit power consumption of sensors in Tx mode

'Coop, 0 dBm', although the latter case has significantly larger power consumption. In addition, the SINR performance of all tested schemes degrades from 2 BANs up to 7 BANs coexisting, from 7 to 10 BANs coexisting the performance is approximately constant.

In terms of an isolated BAN, Fig.5.7 shows that the proposed joint algorithm is even more valuable. Although 'Coop, 0 dBm' still has the best performance, the performance gap to the joint algorithm for SINR threshold values at 10% and 1% outage probabilities reduces significantly. In addition, the joint algorithm leads 'Coop, −5 dBm' and 'No Coop, 0 dBm' by 4.2 and 2.9 dB respectively at an outage probability of 10%, while the improvement is 5 and 12 dB respectively at an outage probability of 1%. All these improvements are observed for the same power consumption as given in Fig.5.5.

At last, to simulate the use of these algorithms when a subject is undertaking different activities, we divide the on-body channel into smaller segments across time. Fig. 5.8 shows a typical measured on-body channel. The channel stability notably varies in different parts of the captured channel gain data. The proposed joint algorithm employed for the on-body channel, under different subject activity, has very

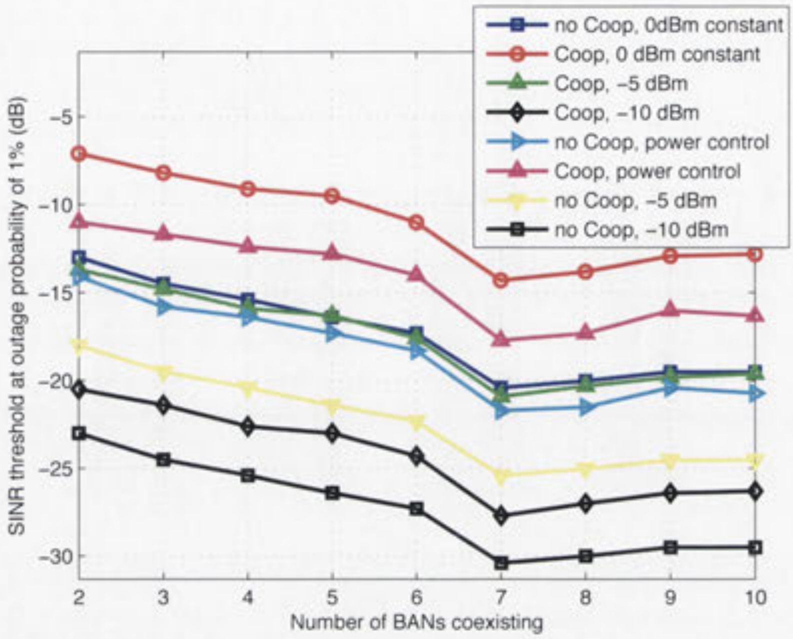

Figure 5.6: SINR Threshold Value at Outage Probability of 1% for different number of BANs scenarios

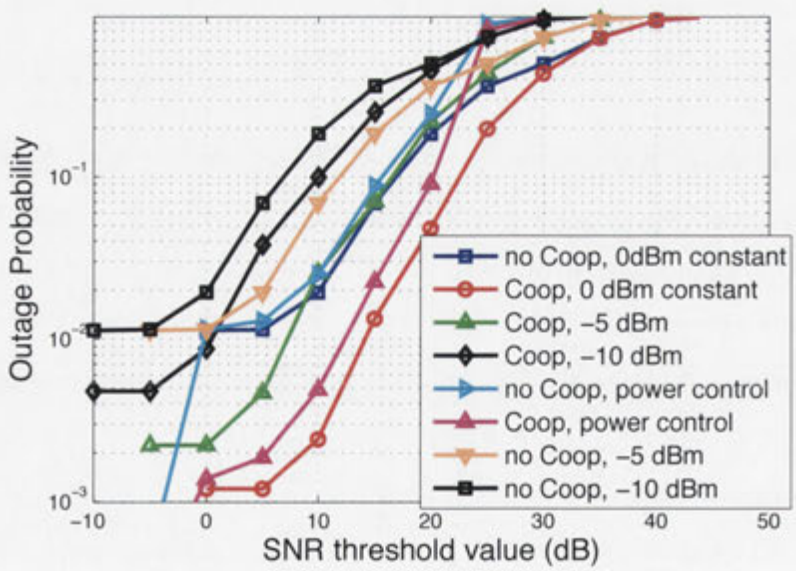

Figure 5.7: Isolated BAN SNR outage probability (no interference). Receiver Sensitivity −90 dBm

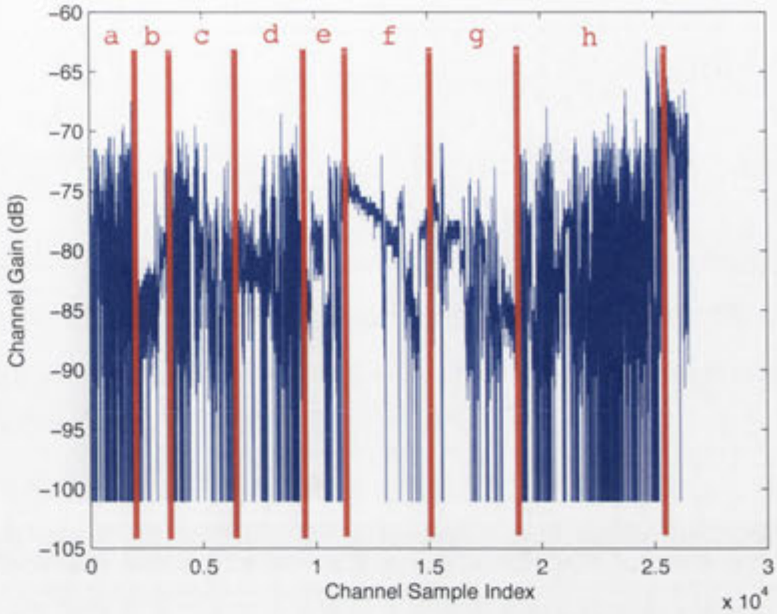

Figure 5.8: Typical on-body channel gain as measured for a subject used in the simulation, with segmentation into subject's varied activities across measurement timespan

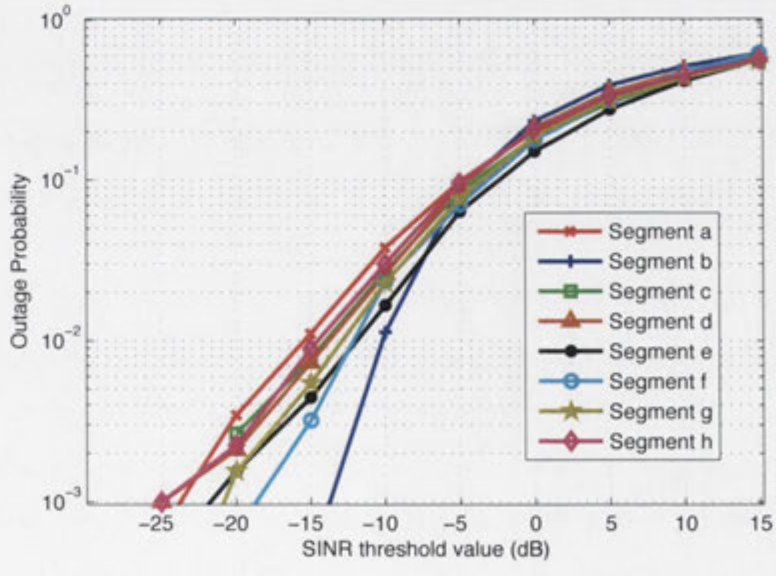

Figure 5.9: Simulation Results for 5 BANs coexistence with −90 Receiver Sensitivity across segmented activities, represented in Fig. 5.8, of the on-body channel

consistent performance across activities, as shown in Fig. 5.9.

5.6 Concluding remarks

In this chapter, a joint relay selection and transmit power control scheme was proposed for BAN. In this joint algorithm, two dual-hop relay links were added to the direct-link to hub for a BAN to provide diversity gain, and radio transmit power control was also integrated into sensor and relay nodes. Prior to the transmission, the optimal path is selected. Based on the chosen transmit path, the light-weight prediction-based power control scheme is performed. This simple channel predictor provides a relatively good estimation of the channel quality, as the on-body channel is stable for at least hundreds of milliseconds. According to the required receiver's sensitivity, sensor and relay (if a relay link is chosen) adjust their transmit power with respective to the first- and second-hop channel quality respectively.

By employing extensive simulation using the empirical on- and inter-body channel data, the joint algorithm has been demonstrated to significantly prolong sensor battery lifetime and mitigate interference when multiple BANs need to coexist. In contrast to single-hop communication with 0 dBm constant transmission, the joint scheme has shown a similar reliability in terms of SINR outage probability, but an approximately 60% circuit power consumption reduction. In addition, it has provided a better SINR outage performance, but used similar power consumption to −5 dBm constant transmission protocol. Its effectiveness in power saving and improving reliability is promising regardless of the presence of inter-BAN interference and the activities undertaken by the BAN user.

Finally, the proposed joint scheme has been demonstrated to be effective when employed in the BAN-of-interest. However, it will lead to a potential resource competition and thus global transmission failure if many of the coexisting BANs implement this scheme. Therefore, in the next chapter, a non-cooperative game model will be adopted to model the coexistence scenario, where each BAN is a self-interested game player at least obtaining target reliability while minimising Tx power consumption.

Chapter 6

Non-Cooperative Game-Theoretical Power Control for Socially Optimal Coexistence

In this chapter, we enable the coexistence of multiple BANs using a finite repeated non-cooperative game for transmit power control, in which each coexisting BAN is modeled as a self-interested player. It is noted that there is no relay involved in the work presented in this chapter. With no coordination amongst these personal sensor networks, the proposed game enables more coexisting BANs reaching the target PDR. In this context we propose a local novel utility function at each BAN, which gives reduced benefit to the player with higher transmission power, and a subsequent reduction in radio interference to other coexisting BANs. Considering the purpose of inter-BAN interference mitigation, PDR is expressed as a compressed exponential function of inverse SINR, so it is essentially a function of transmit powers of all coexisting BANs. It is shown that a unique Nash Equilibrium (NE) exists, and hence there is a subgame-perfect equilibrium, considering best-response at each stage independent of history. In addition, the postulate of social optimality is demonstrated with the given unique NEs obtained by maximising the utility function at each BAN. Realistic and extensive on- and inter-body channel models are employed. Results confirm the effectiveness of the proposed scheme in better interference management, greater reliability and reduced transmit power, when compared with other schemes that can be applied in BANs.

A part of this work is pending major revision in ACM Transactions on Sensor Networks (Dong et al. [2015b]). This work was selected as a finalist and presented in NASSCOM Student Innovation Awards 2015, receiving a judges' commendation [1].

6.1 Introduction

With the increasing concern for interferences in various types of wireless networks, there have been more and more studies on effective interference management schemes presented in the literatures (Douros and Polyzos [2011]). Many techniques involves transmission power control that is based on a centralised (Zander [1992b]; Wu [1999]) and partially distributed (Zander [1992a]) approach. They are effective in the context of cellular networks and general large-scale ad-hoc networks (Lin et al. [2006]) as these networks have fewer resource constraints and a stabler network topology. However, these methods are difficult to apply to BANs due to their high mobility. In Lee and Lin [1996] and Foschini and Miljanic [1993], fully distributed power control schemes were proposed, which we refer to as SINR-balancing in this chapter. SINR balancing works well for distributed cellular mobile systems, but their performance is unknown for BANs. More recently, game-theoretic based resource allocation schemes have been widely proposed for general wireless networks, from spectrum allocation (Candogan et al. [2010]; Seneviratne and Leung [2011]) to transmit power control algorithms (Ozel and Uysal-Biyikoglu [2009]).

To better model the scenario of multiple BANs coexistence as shown in Fig.6.1 and considering the difficulty in finding a global coordinator among BANs, they are modeled as rational players competing for resources (common channel) in a non-cooperative game. We employ a local non-cooperative game-based power control scheme at each BAN. It uses a novel price-dependent utility function to determine the next superframe's transmission power, which provides a unique Nash Equilibrium. As IEEE 802.15 Task Group 6 [2012] clearly specifies a maximum packet error rate of 10%, PDR is used as the target utility. Hence, by maximizing the utility function, a

[1] The full presentation slides can be found at http://www.nicta.com.au/publications/research-publications/?pid=8756

higher PDR can be achieved. The instantaneous PDR is expressed as a compressed exponential function of SINR, which is essentially a function of all transmit powers of coexisting BANs. Obviously, by raising its transmit power, a self-interested BAN can achieve a better utility outcome if the other BANs keep their transmit powers unchanged. However, if every BANs in the range do so, both local and aggregate utilities get worse due to larger interference experienced. Therefore, a proper pricing function is employed to restrain this behavior by penalizing utilities of BANs with high transmit power. In Kazemi et al. [2010], Kazemi also presented an interference mitigation scheme using game-based power control games for BANs with limited cooperation amongst networks over static channels. In our work, the dynamic body movement and shadowing are taken into consideration, which is typically experienced on BANs(Zhang et al. [2009]; Smith et al. [2009, 2011a]; Cotton and Scanlon [2006](, and no coordination exists amongst networks.

This chapter makes the following novel contributions:

- We introduce a non-cooperative game theoretic transmit power control scheme for BANs to maximise the local packet delivery ratio across multiple BANs while reducing average transmit power.
- We model the packet delivery ratio in terms of instantaneous SINR using a compressed exponential function for a typical BAN system with BCH coding.
- The performance of the proposed power control scheme is evaluated using realistic on- and inter-body time-selective channel models, which is the typical operating environment for the BANs.
- The implementation of this game results in a unique Nash equilibrium that additionally provides a socially optimal outcome across all coexisting BANs.

The rest of this chapter is organised as follows. In Section 6.2, the details of the system models are explained. Section 6.3 defines the non-cooperative game for multiple BANs coexistence. Our novel utility function is also provided in this section, together with the existence of unique Nash equilibrium, as well as the socially

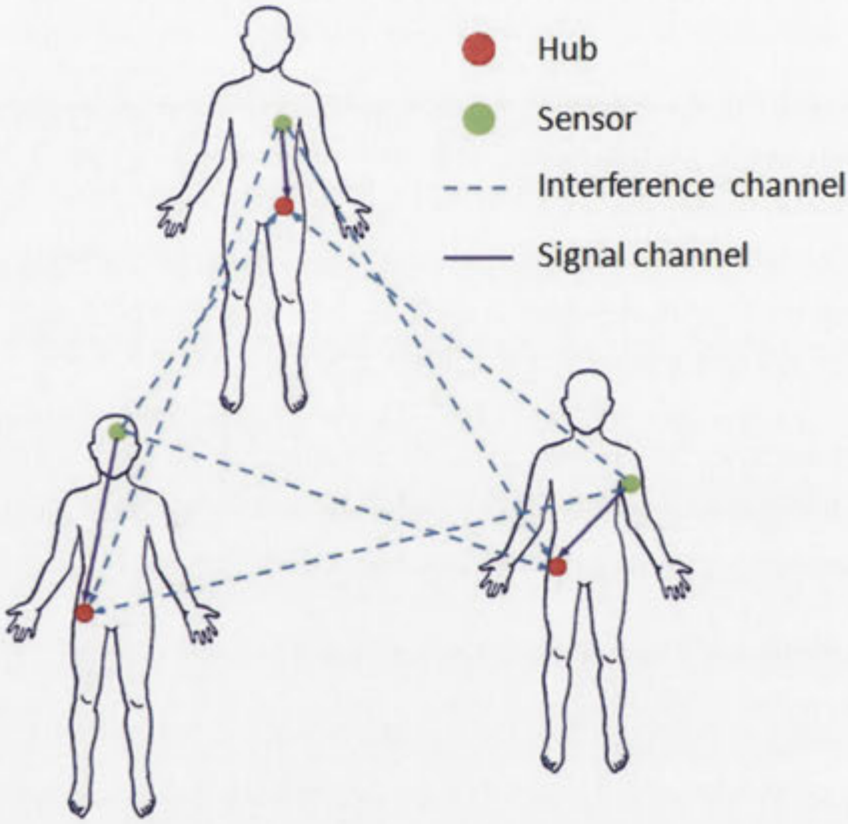

Figure 6.1: The coexistence of multiple BANs, and the interference amongst non-cooperative BANs

optimal outcome of the game. In Section 6.4, the channel models used for this investigation is introduced. Then the performance of the proposed power control method is assessed and compared with other schemes in Section 6.5, and numerical results are provided. Finally, in Section 6.6 some concluding remarks are made.

6.2 System model

6.2.1 BANs coexistence based on probability of overlapping

We consider multiple subjects in the proximity of each other, each wearing a typical star-topology BAN. As the IEEE 802.15.6 standard does not only limit the medium access to CSMA/CA, it also provides a great flexibility to adapt the medium access according to various requirements (IEEE 802.15 Task Group 6 [2012]). As in classical health-care BAN systems, TDMA is employed as the intra-BAN access scheme for each BAN. In practice, this can be implemented with the scheduled access scheme specified in the 802.15.6 standard as noted in Boulis et al. [2012]. Here, the period of time, between hub broadcasting a beacon and all sensors completing transmission in a round-robin fashion, is defined to be a superframe T_d. It is followed by an idle period T_{dile}, during which sensors are inactive and waiting for next beacon. In terms of the inter-BAN access scheme, a unsynchronised TDMA scheme is used as we assume no coordination exists amongst networks (Zhang et al. [2010]). In this concept, the channel is temporally divided into N_c orthogonal channels (time slots) and each time slot has a length of T_d. BAN i chooses its transmission starting time of a superframe independently and randomly following a uniform distribution over [0, $(N_c - 1)T_d$].

$$T_{beacon,i} = T_d + T_{idle,i}, \tag{6.1}$$

$$Pr(T_{idle,i} = t) = \begin{cases} \frac{1}{(N_c-1)T_d}, & t \in [0, (N_c-1)T_d] \\ 0, & t \text{ otherwise} \end{cases}, \tag{6.2}$$

where $T_{beacon,i}$ is the time between two consecutive beacons from the hub of BAN i. Here, we assume S is the set of all M BANs located in close proximity, which consists of a subset of all active BANs S_{active} and a subset of all idle BANs S_{idle}.

$$S = S_{active} \cup S_{idle}, \qquad (6.3)$$
$$and\ |S| = |S_{active}| + |S_{idle}| = M.$$

where $|\cdot|$ represents the number of element in a set. Therefore, the probability of m BANs transmitting concurrently $Pr(|S_{active}| = m)$[2] is calculated as follow:

$$Pr(|S_{active}| = m) = \binom{M}{m} \left(\frac{1}{N_c}\right)^m \left(1 - \frac{1}{N_c}\right)^{M-m}, \qquad (6.4)$$
$$\text{where } m \in [1, M], N_c \geq 2$$

Fig.6.2 shows the probability of m BANs transmitting concurrently with 8 BANs ($M = 8$) coexisting. Different colors correspond to the varying number of orthogonal channels available. In this study, the proposed power control game is simulated over many occasions with different channels, wherein each occasion the value of m is chosen randomly following the probability distribution $\{Pr(|S_{active}| = m)\}$. By introducing this probability distribution, it also models the mobility of BANs for multiple networks coexistence as BANs can leave and also enter the area of interest.

6.2.2 SINR-based packet delivery ratio

At any time, a sensor in each BAN transmits concurrently with sensor nodes in other $m - 1$ BANs. Hence, for each BAN, the hub receives not only the signal packet from its own sensor node, but also $m - 1$ interfering signal packets. Therefore, the SINR over a signal packet at the hub of BAN i, $\gamma_i(\tau)$, is calculated as follows:

$$\gamma_i(\tau) = \frac{p_i(\tau)|h_i^i|^2}{\sum_{j=1, j\neq i}^{m} p_j(\tau)|h_j^i|^2 + \sigma^2}, \qquad (6.5)$$

[2]When $m = 1$, only 1 BAN is transmitting and there are no interfering (coexisting) BANs; when $m \in [2, M]$, concurrent transmission of m BANs is represented

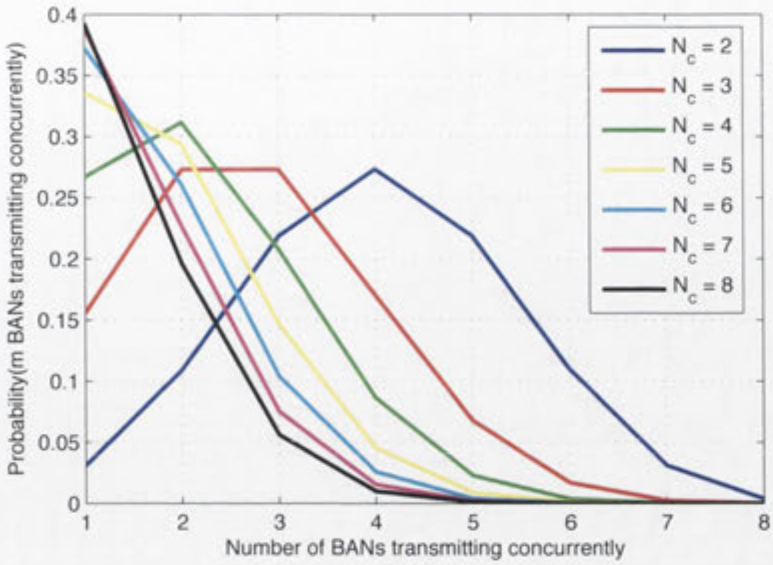

Figure 6.2: Multiple BANs coexistence probability

where $p_i(\tau)$ is the transmission power of a sensor in the ith BAN at time τ; h_j^i represents the average channel gain across a packet time from the sensor in BAN j to the hub in BAN i, in other words, the interference channel from interferer j to network i. In terms of $h_{i'}^i$, it is the average on-body channel gain from the sensor to its connected hub in BAN i in the same time interval.

Observing that the graph of general PDR vs. SINR is a sigmoidal function, it is possible to express the PDR, denoted by pdr, as a compressed exponential function of inverse SINR, $1/\gamma$ (Smith et al. [2014]). In (6.6), γ is calculated as (6.5) and a_c and b_c are constant parameters depends on particular modulation, coding scheme and packet length. Complying with the (Astrin et al. [2012]), BCH(31,19) coding and DPSK/BPSK modulation scheme are applied with a packet length of 256 bytes. It is found that BCH(31,19) provides about 2 dB channel coding gain as shown in Fig.6.3, this advantage is considered when estimating the PDR vs. SINR relation.[3] With a root-mean-square error of the approximation less than 0.006, Fig.6.4 shows the comparison between approximated and simulated PDR vs. SINR relation for DPSK and BPSK respectively. For later simplicity of analysis, we can rearrange the

[3]BCH(31,19) is used as an example here. There are other non-IEEE 802.15.6 compliant coding schemes which can provide higher coding gain.

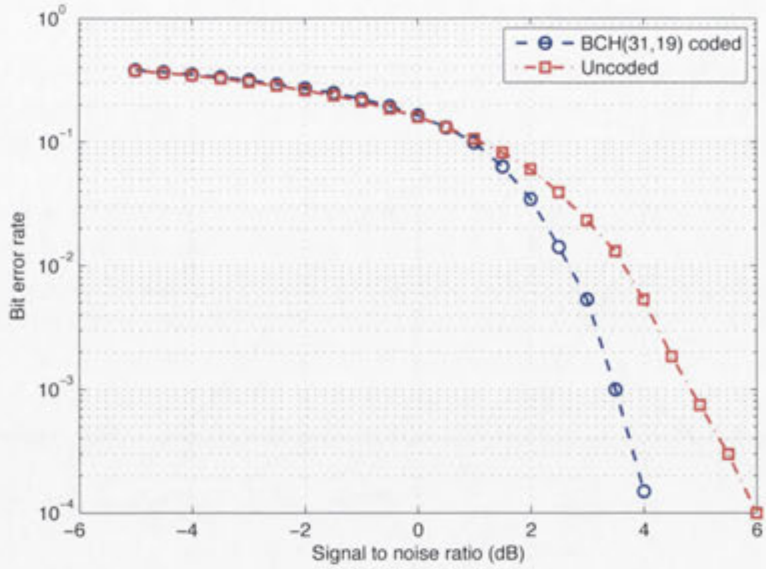

Figure 6.3: BCH coding gain

Table 6.1: Estimated parameters in the compressed exponential function (6.6) and its simplified form (6.7)

Modulation	a_c	b_c	a	b
DPSK	0.230	7.409	−337.2164	−7.4540
BPSK	0.293	6.358	−30.0512	−6.3470

equation to be expressed as (6.7), where $a = -(1/a_c)^{b_c}$ and $b = -b_c$. The values of a and b are given as in Table 6.1 for both DPSK and BPSK.

$$pdr = \exp\left(-\left(\frac{1}{\gamma a_c}\right)\right)^{b_c} \tag{6.6}$$

$$= \exp\left(a\gamma^b\right), \tag{6.7}$$

6.3 Non-Cooperative Power control Game

6.3.1 Game Definition

In this multiple BANs coexistence game, each BAN network makes an independent decision on the transmit power of the next packet based on its current SINR. Here

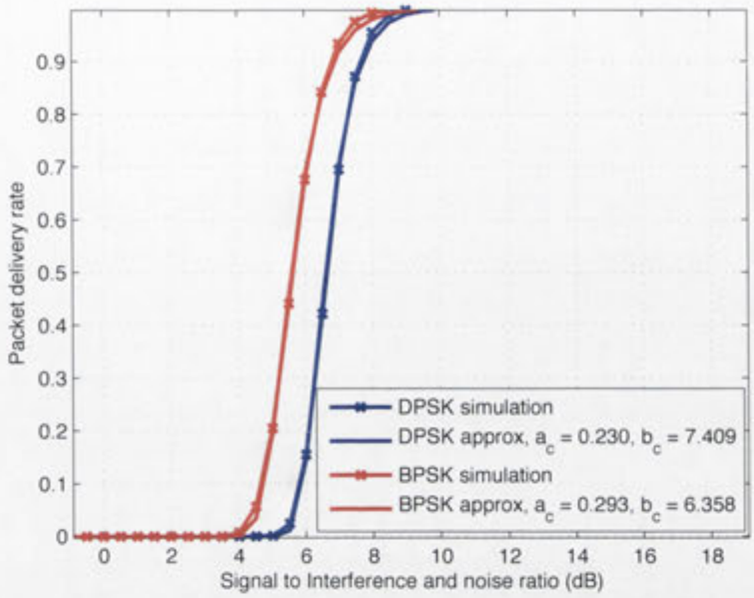

Figure 6.4: Simulated SINR vs. Approximated SINR

each BAN is treated as a player in a non-cooperative repeated game $G = \{N, \mathbf{p}, U\}$, where:

1. $N = \{1, 2, ..., m\}$ is a finite set of players whom indexed by i. N represents the same set as S_{active};

2. $\mathbf{p}$ represents the global strategy space, which is the Cartesian product of all players' strategy spaces, i.e. $\mathbf{p} = \mathbf{p}_1 \times \mathbf{p}_2 \times ... \times \mathbf{p}_m$. The pure strategy set of player i, $\mathbf{p}_i$, is a finite set of discrete transmit powers in the range of $[P_i^{min}, P_i^{max}]$. The action of player i at any time(stage) τ is denoted by $p_i(\tau) \in \mathbf{P}_i$, and $\boldsymbol{p}_{-i}$ stands for the choice of transmission power of other players except player i;

3. The utility function $U(\cdot)_i$ is defined in terms of the current transmission power $p_i(\tau)$ and PDR. Its objective is to maximise the PDR while minimizing the transmit power. It is defined as follow:

$$U(p_i, pdr_i) = -p_i^{w_i} - \frac{d_i}{pdr_i^{v_i}}, \tag{6.8}$$

where pdr_i is a function of SINR and thus a function of the transmit powers of all players according to (6.6) and (6.5). Hence, $U(p_i, pdr_i)$ can be rearranged and expressed as $U(p_i, p_{-i})$. The exponents $v_i > 0$ and $w_i > 0$ depend on the particular network configuration, and can be varied accordingly. The weighting factor $d_i > 0$ can be adjusted depending on the current network status. At the end of every time slot, players (BANs) update their transmit power levels to maximise the outcome from applying the utility function based on the latest transmit power and the current SINR:

$$p_i(\tau+1) = \arg\max(U(\mathbf{P_i}, p_{-i})), \tag{6.9}$$
$$\text{where } \mathbf{P}_i = \{p_i | p_i \in [P_i^{min}, P_i^{max}]\}, \forall i \in N$$

6.3.2 Nash Equilibrium

An important condition for the non-cooperative game to converge is that a unique Nash Equilibrium (NE) exists. The existence and uniqueness of the Nash Equilibrium of the defined game are proved as follow.

Definition 1. *The action profile $\mathbf{p}^* = (p_1^*, p_2^*, ..., p_m^*) \in \mathbf{P}$ is a Nash Equilibrium if, for all players, p_i^* is a best response to $\boldsymbol{p}_{-i}{}^*$. In the other words, there exists $U_i(p_i^*, \boldsymbol{p}_{-i}{}^*) \geq U_i(p_i, \boldsymbol{p}_{-i}{}^*)$ for any choice of $p_i \in \mathbf{P_i}$.*

Theorem 1. *At least one Nash Equilibrium exists for the non-cooperative finite repeated game $G = \{N, \mathbf{P}, U\}$ proposed here.*

Proof.

1. $[P_i^{min}, P_i^{max}]$ is a nonempty, convex and compact subspace of a Euclidean space $\mathbb{R}^m$.

2. The utility function (6.8) is continuous in the domain $[P_i^{min}, P_i^{max}]$. This can be shown by taking the first derivative of the utility function and substituting (6.7) and (6.5):

$$\frac{\delta U_i}{\delta p_i} = -w_i p_i^{w_i-1} + \frac{d_i v_i}{pdr_i^{v_i+1}} \frac{\delta pdr_i}{\delta p_i}, \tag{6.10}$$

$$= -w_i p_i^{w_i-1} + \frac{d_i v_i}{pdr_i^{v_i+1}} pdr_i ab\gamma_i^{b-1} \frac{\delta \gamma_i}{\delta p_i}, \tag{6.11}$$

$$= -w_i p_i^{w_i-1} + ab\gamma_i^{b-1} \frac{d_i v_i}{pdr_i^{v_i}} \frac{|h_i^i(k_i)|^2}{I_{-i}}, \tag{6.12}$$

where I_{-i} is the interference and noise power experienced at the hub of player i. Based on (6.5), we can derive the relation $\frac{\gamma_i}{p_i} = \frac{|h_i^i(k_i)|^2}{I_{-i}}$. Therefore,

$$\frac{\delta U_i}{\delta p_i} = -w_i p_i^{w_i-1} + ab\gamma_i^{b-1} \frac{d_i v_i}{pdr_i^{v_i}} \frac{\gamma_i}{p_i} \tag{6.13}$$

Since $p_i \in [P_i^{min}, P_i^{max}]$ is real and pdr_i is non-zero according to the approximation shown in (6.7), the first derivative function is defined. Therefore, Theorem 1 is proved.

□

Theorem 2. *The Nash Equilibrium at each stage in the non-cooperative power control game G is unique, when $d_i > 0$. With the unique Nash equilibrium at each stage, which is independent of history, there is a unique sub-game perfect equilibrium.*

Proof. To show the Nash Equilibrium point p_i is unique in the range of $[P_i^{min}, P_i^{max}]$, it is sufficient to check the concavity of the utility function $U(p_i, pdr_i)$ by taking the second derivative.

$$\frac{\delta^2 U_i}{\delta p_i^2} = -w_i(w_i-1)p_i^{w_i-2} + c_i \frac{\gamma_i^{b-2}}{pdr_i^v} \{(b-1) - abv_i\gamma_i^b\}; \tag{6.14}$$

where $c_i = abd_i v_i \frac{|h_i^i|^4}{I_{-i}^2}$. Due to the fact that p_i is always positive, the first part of (6.14) has a negative value as long as the constraint of exponent $w_i >= 1$ is satisfied. In addition, since $v_i > 0$, and a and b are both negative and SINR,c_i and PDR are always positive, the second part of (6.14) is always negative. The addition of these two parts means the second derivative $\frac{\delta^2 U_i}{\delta p_i^2} < 0$ in the range of $[P_i^{min}, P_i^{max}]$. Therefore, the function $U(p_i, pdr_i)$ is concave and has a local maximum at p_i^* which occurs at the point $\frac{\delta U}{\delta p_i} = 0$. In other words, the Nash Equilibrium at each stage of this game is unique. Furthermore at any given stage, it can be seen that this equilibrium is independent of the history, hence there is a sub-game perfect equilibrium. □

6.3.3 Social Optimality and Pareto Optimality

As the existence and uniqueness of the Nash Equilibrium (NE) of the defined non-cooperative game has been proved, the efficiency of operating at the NE now needs to be determined. It should be noted that a NE, as per definition 1, is the best response in a single player's point of view, given the decisions of the other players. However, in the proposed non-cooperative game, here is imperfect information as the other BANs' transmit power for the current time slot is unknown. Therefore, it predicts other BANs' actions based on the latest aggregate interference power received. Additionally, as players in the game act in their own self interest, there is no guarantee that the decision is optimal from a social point of view, or even from an individual BAN's perspective. Here we define the social welfare W of a game as the sum of all individuals' utility with respect to a joint action profile $\mathbf{p}^* = (p_1^*, p_2^*, ..., p_m^*)$:

$$W = \sum_{i=1}^{m} U_i(p_i, \mathbf{p}_{-\mathbf{i}}). \tag{6.15}$$

Therefore, the efficiency of the unique NE solution is characterised as follows:

Definition 2 (Pareto Optimality). *A joint action profile* $\mathbf{p}^* = (p_1^*, p_2^*, ..., p_m^*) \in \mathbf{P}$ *is a Pareto optimal (efficient) outcome to user i if there is no other joint action profile* $\mathbf{p} \in \mathbf{P}$ *such that* $U_i(\mathbf{p}) \geq U_i(\mathbf{p}^*)$.

Definition 3. *A joint action profile* $\mathbf{p}^* = (p_1^*, p_2^*, ..., p_m^*) \in \mathbf{P}$ *is a socially optimal (efficient) outcome if there is no other joint action profile* $\mathbf{p}$ *such that* $W \geq W^*$.

As $\mathbf{p}^*$ leads to the maximal social welfare, it is socially optimum and therefore is also Pareto efficient (Bemporad et al. [2010]). In this chapter, we would like to show

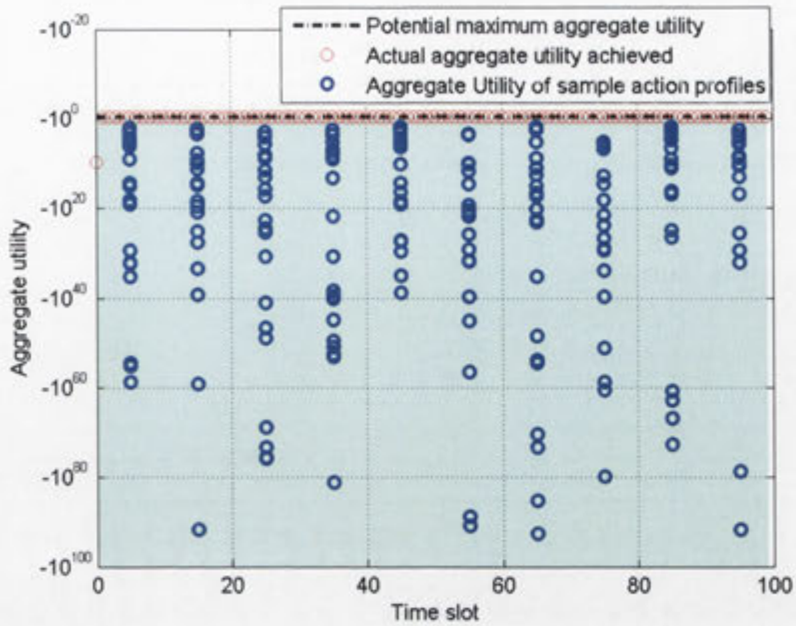

Figure 6.5: Social welfare outcome of the game

that the action profile $\mathbf{p}^* = (p_1^*, p_2^*, ..., p_m^*)$ at the NE point is indeed socially optimal. This can be observed by comparing the social welfare, i.e. aggregate utility outcome of (6.8), obtained with all different action profiles $\mathbf{p} \in \{\mathbf{P} = \mathbf{P}_1 \times \mathbf{P}_2 \times ... \times \mathbf{P}_m\}$.

Conjecture 1. *When all BANs are operating at the unique Nash equilibrium shown in Theorem 2, then according to Definition 3 the outcome of the proposed power control game is socially optimal.*

Proof. Following (6.8), it may appear that the maximum social welfare that the game can achieve is when all BANs transmit at the lowest power, i.e. −30dBm, and meanwhile achieve a PDR of 1. However, due to the on-body channel attenuation and inter-BAN interference, it is generally impossible to achieve this. With exhausted comparing among all possible action profiles $\mathbf{p}$ at each time slot, the maximum possible social welfare is plotted as the black dashed line in Fig.6.5. It matches the social welfare reached with actual action profile $\mathbf{p}^*$ determined at the unique NE, which is indicated as red dots in Fig.6.5. Additionally, Fig.6.5 also shows the social welfare of a large agglomerate of randomly sampled action profiles in the blue shaded area, which are all below the actual social welfare of the game. It is noted that the aggregate utility achieved at time slot 0 is not the optimal social welfare, since the initial transmit power of all BANs are randomly chosen in the range of $[-30, 0]$ dBm. According to all possible observations, the Nash Equilibrium is therefore conjectured as socially optimal, and hence also Pareto optimal. □

6.3.4 Algorithm Description

In this section, an iterative and distributed power control game that determines each BAN's transmission power at time τ is described as in Alg.3.

Algorithm 3 The proposed distributed non-cooperative power control game

1. In BAN i, a sensor transmits a packet with $p_i(\tau)$. When $\tau = 0$, $p_i(0) \in [P_i^{min}, P_i^{max}]$ is randomly chosen. If $\tau > 0$, $p_i(\tau - 1)$ is determined in the previous iteration at $\tau - 1$;

2. Hub in BAN i ($i \in N$) calculates the SINR $\gamma_i(\tau)$ of the received packet as (6.5);

3. Estimate the instantaneous PDR $pdr_i(\tau)$ with $\gamma_i(\tau)$ based on the PDR vs. SINR approximation (6.7);

4. As (6.9),determine the transmission power at $\tau + 1$, $p_i(\tau + 1) \in [P_i^{min}, P_i^{max}]$, which gives the maximum value of $U(p_i, pdr_i(\tau))$;

6.4 Channel model

To evaluate the performance of the proposed game-based power control algorithm, extensive on- and inter-body channels are modeled for narrowband communications at a carrier frequency of 2.4 GHz. Each BAN consists of any number of wireless nodes, with sensors at suitable locations on the body, with one hub centrally located, such as at the chest or left/right hips, and single-hop communication. . We simulate the scenarios in which a random number of BANs are coexisting and moving in arbitrary directions. Since the same network topology is used in each BAN, it is a reasonable assumption that on-body channels are independent and identically distributed for all players. The gamma distribution can characterise the general everyday on-body channel of a BAN (Smith et al. [2011a]), so gamma fading, for any given sensor to hub link, is employed with a mean 60 dB attenuation, and as in (Smith et al. [2011a]) with a shape parameter of 1.31, and a scale parameter of 0.562, which considers the effect of body shadowing and BAN channel dynamics.

In terms of the inter-body interfering channel, we start with representing the movement of a player by a series of $(x(\tau), y(\tau))$ coordinates updated every 20 ms, with total of 10000 samples are modeled, which is equivalent to 200 seconds simulation time. The initial positions of players are randomly chosen within a $6 \times 6\text{m}^2$ square area[4] which corresponds to the requirements in (Astrin et al. [2012]). During their movement, a random small turning angle is introduced to model a realistic walking pattern of an individual. In addition, an average walking speed of 3m/s with 0.2m/s standard deviation is applied. This walking model enables us to calculate the distance between two players i and j at any instant throughout the simulation. The channel attenuation is then calculated based on path loss model, body shadowing and also small scale fading,

$$h_i^j = A_t(dist_0/dist_{ij})^{(2.7/2)} A_{BS} A_{SC}, \tag{6.16}$$

assuming a path loss exponent of 2.7 between BANs[5]. $dist_{ij}$ represents the distance between players i and j, and the reference distance $dist_0 = 5m$ corresponds to a channel attenuation A_t of 54 dB. We consider the average case where body shadowing contributes approximately $A_{BS} = 45$ dB attenuation and adopt a Jakes' model with Doppler spread of 1.1 Hz as the Rayleigh distribution for the small scale fading A_{SC} between BANs.

[4]Please note the 6×6 m^2 square area is only used as a bounded area for the choice of players' initial positions. When the movement simulation starts, no border is considered, e.g., even when the distance between subjects becomes sufficient large, so that the inter-BAN interference is negligible, the distance is still accounted for.

[5]Although other common path loss exponents ≥ 2 for the environments in which BANs are co-located are equally applicable.

6.5 Numerical Analysis

In order to evaluate the proposed non-cooperative power control game, we implement our simulation in Matlab platform to extensively repeat the coexistence game. One individual repeated game consists of 100 repeated game-playing stages. The number of stages is chosen based on the observation in our later simulation that the proposed non-cooperative game converges sufficiently within 30 stages. We extend the observation window to 100 which allows us to investigate the impact of dynamic coexistence on various schemes compared in this chapter. 20 sets of channels are generated based on the description in Section 6.2. Because of the random moving velocity, the walking pattern varies between different channel model sets. With each set, the same 100-stage game is played on 50 occasions, using different segments of the data. Therefore, a total of 1000 games, each with 100 stages, are conducted. Here, a maximum of 8 BAN networks locating in the vicinity is simulated, i.e. $M = 8$ in (6.4). At any time during the simulation, a various number of BANs are active with the others idle. The actual number of networks transmitting concurrently follows the probability distribution P_m described in (6.4). The case of $m = 0$ is neglected as the case of no network transmitting is irrelevant. In terms of inter-BAN TDMA scheme, we assume 4 orthogonal channels ($N_c = 4$) are used. In addition, to investigate the effect of a given number of coexisting BANs on the performance of the proposed algorithm, constant numbers of BANs coexisting are also simulated, with the number coexisting from 2 to 8 each run on 1000 occasions. The exponents in the utility function v_i and w_i are set to be 4 and 1 respectively, $\forall i$, and the weighting factor in the utility function $d_i = 0.1\ \forall i$, which give the optimal outcomes for the game.

Based on the same configuration and channel models, we compare the proposed game with some other schemes commonly applied in BAN. The comparison is based on two criteria – (i) percentage of BANs reaching the target PDR; and (ii) transmission power at each stage. Here, we use (i) as a performance metric, instead of average PDR achieved across all coexisting BAN, is because the reliability improvements in a global point of view are more concerned. Comparing average PDR neglects the difference between BANs with extremely good PDR performance and BANs with bad PDR performance. In contrast, more BANs reaching the target PDR indicates a better and more robust coexistence. The result is averaged across all 1000 games. Complying to Astrin et al. [2012], the target PDR is set to be 0.9. The rest of the schemes are **Sample-and-Hold** (Smith et al. [2011b]), **SINR-Balancing** (Foschini and Miljanic [1993]; Lee and Lin [1996]) and constant transmission power at **0/−5/−10 dBm**. Here in **Sample-and-Hold** current SINR is used for each BAN to set its' next transmission power. In other words, instead of adjusting with respect to channel gain as shown in previous chapter, **Sample-and-Hold** adjusts the transmission power based on the latest packet's SINR to attempt to achieve the target SINR for the next packet.

All power control methods are applied and plotted in Fig.6.6 and 6.7, using BPSK and DPSK modulations respectively for the case where number of concurrently transmitting BANs follows the probability distribution P_m (6.4). From Fig.6.6(a), it is shown that using the proposed game-based power control method, approximately 93% of the BANs are able to achieve the target PDR of 0.9 while this number is only 80% and 77% for Sample-and-Hold and SINR-balancing methods. Constant transmission at different power level shows similar performance to each other with about 87% achieving target PDR. In terms of the time taken to converge to the steady-state minimised transmit power, the proposed method and Sample-and-hold achieve this 16 time slots ahead of SINR-balancing. For the power control game and sample-and-hold scheme, the number of iteration till settling is approximately 10 time slots, which is equivalent to 0.2 seconds with a sampling frequency $T_s = 20ms$. The short convergence time of the first two algorithms ensures that they can quickly respond to time-variations in the target channel and also interference, which is typical for BAN operation. In terms of the output transmit power shown in Fig.6.6(b), the game has an average of −25 dBm while sample-and-hold is about −23 dBm. SINR-balancing has 2 dB less in average transmission power compared with our proposed method. However, with its poor performance in percentage of BANs reaching the target and slow response time, it is not a suitable choice for enabling BANs' coexistence. Further the game has at least 15 dB less average transmit power than the constant power transmission. Similar output transmit powers can be observed in Fig.6.7(a) when

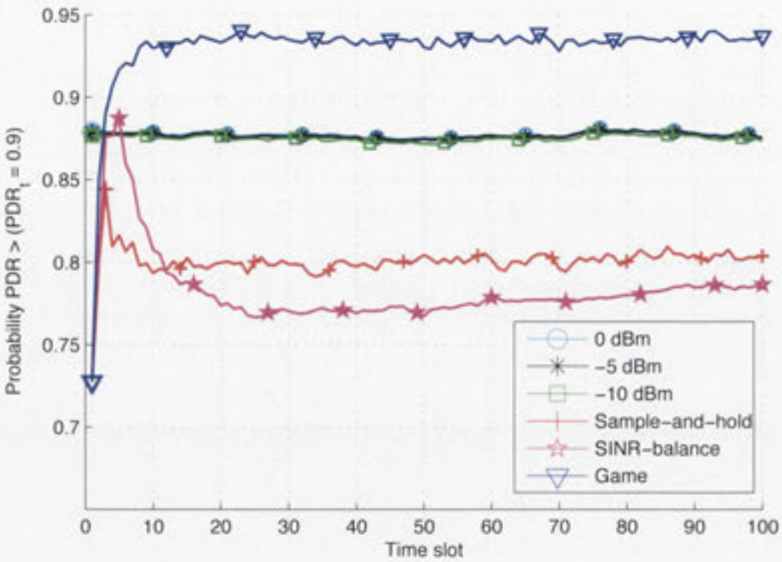

(a) BPSK PDR

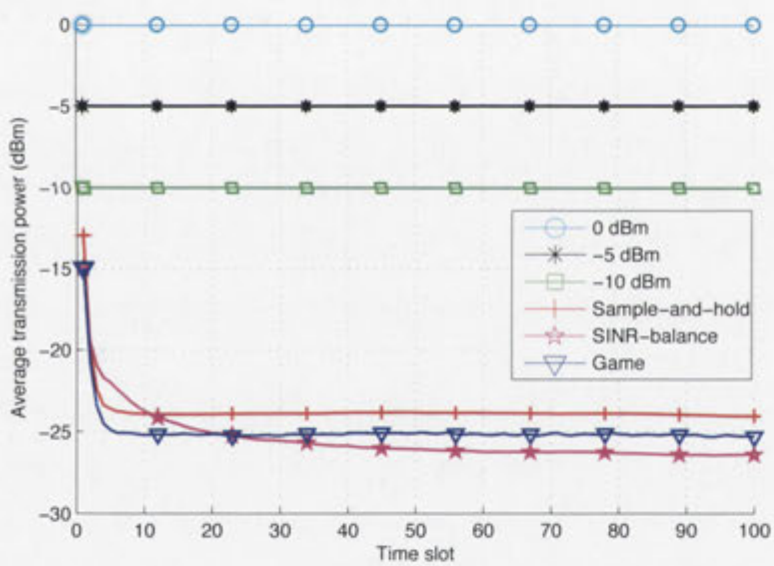

(b) BPSK power

Figure 6.6: BPSK Simulation results

DPSK is employed. In this case, the percentage of BANs reaching the target PDR is 92%, 85%, 76% and 74% for the proposed algorithm, constant power transmission, Sample-and-Hold and SINR-balancing respectively. Since all the calculations for optimal transmit power are performed at the hub, which has significantly less power

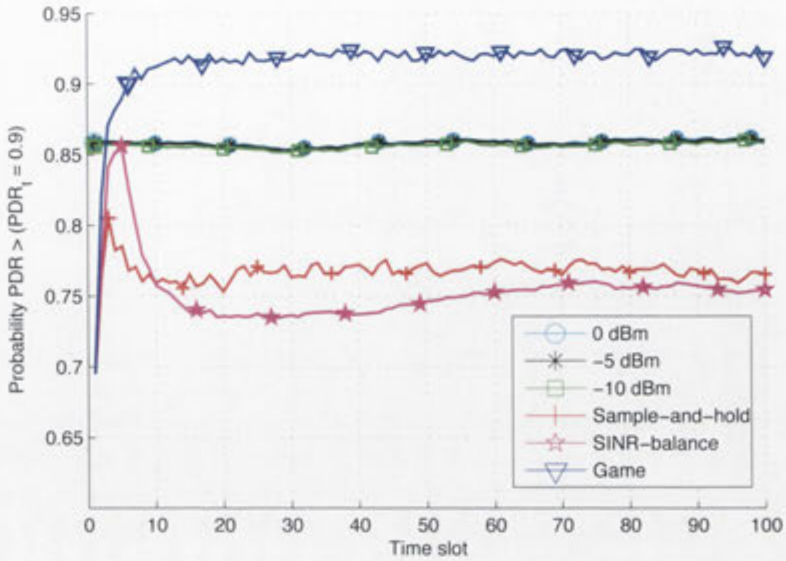

(a) DPSK PDR

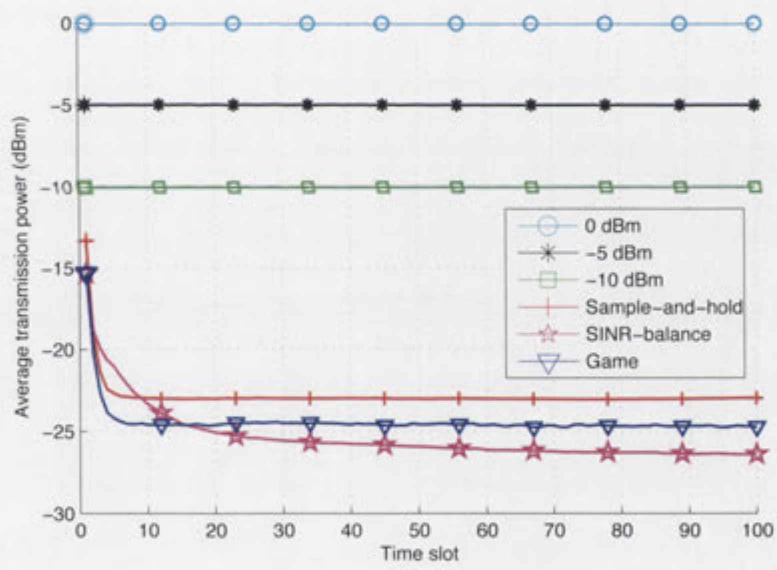

(b) DPSK power

Figure 6.7: DPSK Simulation results

constraints than the sensors, sensors adjust their transmit power as directed by the hub. Therefore, the added power control game to the BAN system does not introduce additional power consumption. Furthermore, most of the energy used by a sensor is during the Tx mode (Shakir et al. [2007]). Thus, reducing transmit power improves

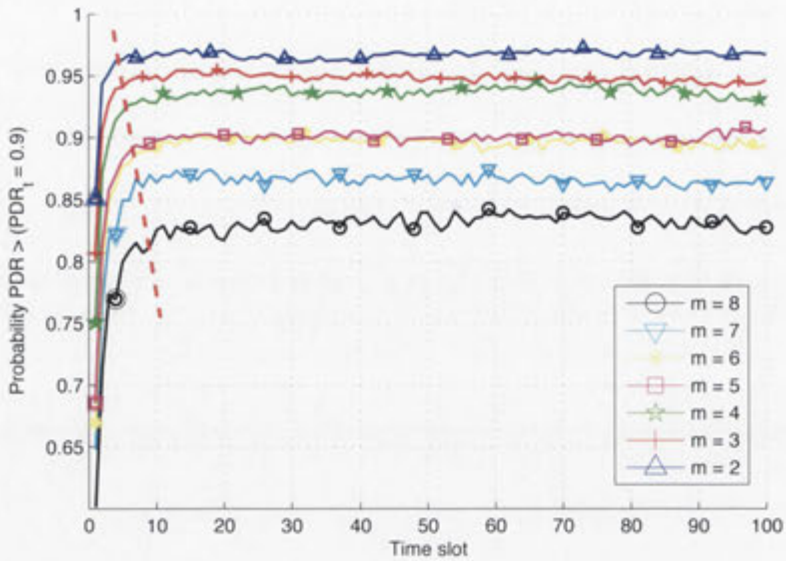

(a) Percentage of BANs reaching target PDR

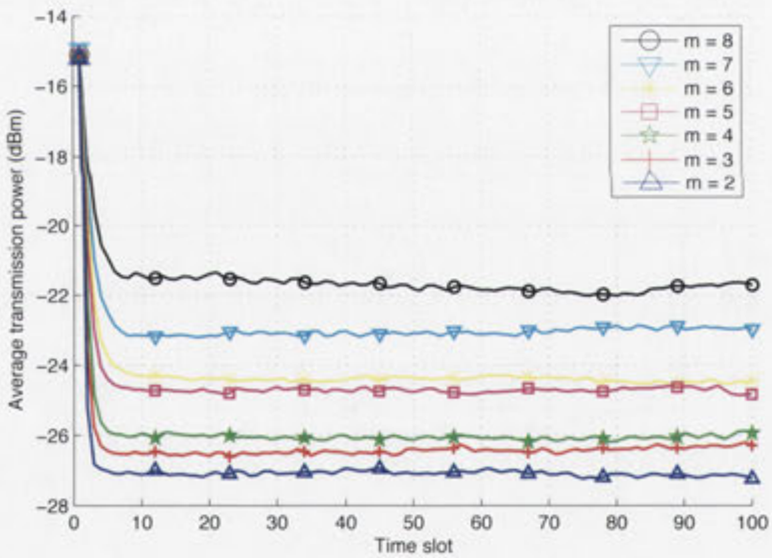

(b) Average transmission power of BANs

Figure 6.8: Different number of BANs coexisting scenarios

the lifetime of the sensor radio.

Next we show the effect of changing the number of players on the performance of the proposed power control game. Fig.6.8 shows the comparison when the number m of coexisting BANs is fixed, $m \in [2, 8]$, with respect to the previous criteria. The same simulation parameters (exponents $v = 4$ and $w = 1$, weighting factor calculation d_i) are used for different values of m. It is observed that the average percentage of BANs reaching the target PDR of 0.9 decreases with increasing m, from 97% to 83%. In Fig.6.8(a), the intercept point of the red broken line and each solid line indicates the approximate time slot for game convergence, which shows that the more players that join the game the longer it takes for the game to converge. In Fig.6.8(b), we can see that transmit power rises from -27 dBm to -21 dBm as m increases from 2 to 8. Note that the performance of the proposed algorithm for different values of m always outperforms any of the previously described schemes described previously in the case of the average percentage of BANs reaching the target. Although SINR balancing uses slightly smaller transmit power it sacrifices a lot in terms of reliability.

6.6 Conclusion

Global coordination for multiple coexisting BANs is difficult, since their highly mobile nature leads to significant inter-BAN coexistence dynamics. Since the non-cooperative coexistence represents the worst coexisting case, we propose effective schemes for this scenario in this chapter. However, one can imagine that by allowing limited cooperation among coexisting BANs, our proposed power control method can be improved by exchanging information amongst each other to some extent. Therefore, the concept of non-cooperative game theory has been adopted to model the coexistence scenario for BANs here. In this game each BAN as a self-interested player chooses its transmit power independently to tradeoff reliability and penalties for the chosen power level. This process was achieved with a novel utility function implemented locally at each BAN. The reliability was represented by the instantaneous PDR. As the information about other coexisting BANs' decisions, particularly their transmit powers, is unknown at one's hub except the SINR. Therefore, PDR was expressed as a compressed exponential function of inverse SINR, which is essentially an implicit impact of others' transmit power on itself. The proposed utility function also constrained output transmit power for each player. It has been shown that unique Nash Equilibrium and also sub-game equilibrium were obtained.

Based on extensive simulation over different instantiations of a realistic channel model, significantly more coexisting BANs reached the target PDR at the lowest possible average transmit power, when employing the game-based power control scheme when compared with other possible methods. In addition, the coexisting system converged to to a stable Nash equilibrium very quickly in a small number of game repetitions. This is particularly beneficial to BAN's response to the dynamic variations in its' operation environment. More importantly, the outcome of the proposed non-cooperative game was shown to be socially optimal across all coexisting BANs. The postulate of social optimality was demonstrated by comparing all the potential action profiles in this game. All the results above held for varying number of coexisting BANs, with the performance only degraded by a small amount, but still outperforming other feasible methods.

Chapter 7

Conclusion and Future Works

7.1 Summary

BANs, the latest generation of personal area networks, is being pervasively used in many areas. Because of its promising advantages and compatibility, it still has a large potential to be developed for many other applications, which could lead to a dramatic growth in the number of active BAN units. However, this trend raises the issue of co-channel interference, as the possibility of multiple BANs coexisting increases. A BAN is sensitive to this interference because: 1) sensors, with small-form factor and limited power supply, are required to consume ultra-low power; 2) BAN-related channels are wide sense non-stationary; 3) the coordination among coexisting BANs is difficult due to networks' mobility. Thus effective algorithms, which improve the reliability, particularly where non-cooperative BANs are coexisting, are urgently needed to meet the requirements specified in the IEEE 802.15.6 BAN standard.

With this as a motivation, the advantages, of cooperative communications and transmit power control, have been demonstrated with respect to the enabling of co-existence and interference mitigation. Although both technologies have been studied for other types of network and communication systems, this thesis emphasised their performance when employed in BAN which is fundamentally different from the other types of networks . For the work presented in this thesis, we have modeled the sensors' transmissions within a BAN using a TDMA implementation at the MAC (i.e., link) layer, where in practice this can be implemented using the contention free period of the CSMA/CA protocol listed as an option in IEEE 802.15 Task Group 6 [2012]. More importantly, the coexistence among multiple BANs is also scheduled using TDMA but each BAN determines the starting time of a superframe transmission independently from others' decision Zhang et al. [2010]. In addition, empirical on-body and inter-body BAN channel measurements at 2.4 GHz Smith et al. [2012b] have been extensively used, together with some realistic inter-body channel models, for the simulation of BAN coexistence. This ensures that the unique and critical factors related to BAN are well captured when studying the effectiveness, in interference mitigation, for cooperative communications and power control.

7.2 Conclusion

Here, some conclusions and answers to the questions raised in the thesis statement of contribution (Sec. 1.2) are provided. For readers' convenience, these questions are re-listed in this section with their corresponding answers and discussions following directly below.

Statement 1. *What is the improvement for a BAN employing two-hop cooperative communications using relays? Does it provide any benefits in inter-BAN interference management when coexisting with other BANs?*

In Chapter 3, a two-hop relay-assisted cooperative communication scheme has been presented for BAN, with the employment of empirical on-body channel data. It was assumed that the BAN used a [31,19] BCH-coded GFSK modulation, which corresponds to the IEEE 802.15 Task Group 6 [2012], and its sensors' transmission were scheduled in a round-robin fashion. The performance of the proposed relay scheme was shown under two scenarios, where the BAN-of-interest is isolated from or coexisting with other non-coordinated BANs. Observing the first scenario, its reliability is significantly improved by increasing the average BER at the hub. When coexisting, a suitable TDMA was implemented as the inter-network access scheme. The BAN-of-interest obtains higher SINR threshold value at the same outage probability when relays are enabled. In addition, inter-body shadowing effect improves the advantage of spatial diversity when relays are in active, and thus assists BANs coexistence. As a result, BANs are encouraged to employ cooperative communications scheme with relays under various circumstances.

Chapter 4 adopts an opportunistic relaying scheme for multiple BANs' coexistence, as it is observed that using an optimal relay is equivalent to the use of all possible relays. By employing opportunistic relaying, only the predicted best relay will be chosen to actively forward the packets. A three-branch opportunistic relaying scheme was simulated for the BANs coexisting scenario. Similar configurations as used in Chapter 3 were inherited, but actual inter-body channel measurements were used, which enables the simulation of a more practical working environment for a typical BAN. By using opportunistic relaying, the glsSINR outage probability is significantly improved as well as the LCR. The scheme works particularly better when channel coherence time is smaller. These benefits found in the simulation were consistent with the observation from an experiment conducted. Several MICAz motes running modified TKN 15.4 MAC protocol were employed to form a three-branch relaying network. It showed significant improvements in outage probability, LCR and average non-fading duration under both isolated-BAN and coexisting BAN scenarios. When inter-BAN interference is present, there is even greater benefits to using relays.

Statement 2. *What is the impact of relay(s)/hub placement, or diversity combining schemes, on the performance of the two-hop cooperative communications?*

In Chapter 3, three different hub locations, chest, left/right hips at where the gateway devices are most commonly placed, were investigated for BAN. They corresponds to the locations of transceivers used when capturing the empirical channel measurements, which are available in Smith et al. [2012b]. Comparing between two-hop and single-hop schemes with the same hub location, the improvements are consistent across all three locations. However, there is a better outage SINR performance when the hub is at chest than when the hub is placed at the left/right hips. It is also found that there may be some advantages to use two relays over one relay if the added complexity is permissible. The relays locations needs to be well considered when using just one relay for the same hub location. With the use of empirical channel measurements, it is shown that no real performance gain is earned for using cooperative maximum ratio combining over selection combining, which is consistent to what was observed in Sharma et al. [2011].

Statement 3. *Is it worthwhile to jointly use simple prediction-based power control with the relays?*

In Chapter 5, a joint relay selection and transmit power control method was proposed for use in the multiple BANs coexisting scenario. A prediction-based power control scheme was introduced to be used in conjunction with the opportunistic relaying, which was presented in Chapter 4. Distributed transmit power control was performed at the active relay and hub with respect to the receiver sensitivity of the destination node and the channel quality of the corresponding source-and-destination link. It was found that the distribution of SINR values can be well described by a lognormal distribution. Theoretical outage probability, LCR and average outage duration match the empirical results well. The joint scheme was demonstrated to significantly prolong sensor battery lifetime and mitigate interference when the BAN-of-interest coexisted with others. Its effectiveness in power saving is even more significant than when no radio interference is present.

Statement 4. *Can the scenario of multiple BANs coexisting be accurately modeled as a repeated non-cooperative game?*

With high BAN mobility, and difficulty in global coordinating amongst multiple BANs, non-cooperative game theory, which has been applied to diverse disciplines, is employed to model the scenario for coexistence. It follows the concept that self-interested players make decisions on their actions independently of trading off their benefits and penalties for chosen actions. In the context of BANs, an individual BAN is treated as a self-interested player who pursues higher reliability. However, the improvements on reliability, i.e. PDR, requires the BAN to increase its transmit power to obtain a higher SINR. This selfish behaviour of all coexisting BANs result in massive co-channel interference that degrades both individual and aggregate performance. By introducing the idea of non-cooperative game theory, BAN is self-constrained by being penalised more for using higher transmit power.

Statement 5. *Does a game-based power control scheme outperform the SINR-balancing or constant-power transmission for BANs coexisting?*

For better interference management, a non-cooperative power control game has been proposed in Chapter 6. In this game, a novel utility function, which constrains output transmit power, is applied for each player. It provides a unique Nash Equilibrium, which is also a Pareto optimal solution. Extensive simulation shows that the coexistence of up-to 10 BANs is much improved, with the proposed non-cooperative power control game, over other methods, in terms of more BANs reaching target PDR at the lowest possible transmit power. In addition, this approach adapts fast to changes in the network environment, which is very beneficial to BAN that typically operate in a dynamic environment.

7.3 Future Work

Prior to discuss the potential research directions, the work presented in Chapter 3 could be further consolidated by deriving analytical results for the complement probability distribution of SINR assuming known channel probability density functions are employed. The theoretical analysis can then be compared with the simulated numerical results. In addition, another important extension of the work presented in this thesis is with respect to the non-cooperative game model for the coexistence of multiple uncoordinated BANs. The postulate of social optimality for the proposed game needs to be mathematically proved.

In Chapter 6, the BANs employing the non-cooperative game all have the single-hop star topology. Only their choices of transmit power is treated as the action profile of the game. Considering the benefits of using cooperative communications in BAN (Chapter 3 and 4), relay selection could be added to the non-cooperative game. One approach is to treat the choice of relay(s) and the transmit power as a joint action, which is then used as an input for a proper designed utility function.

$$U(p_i, r_i) = g(f_1(p_i) + f_2(r_i)) - c(p_i, r_i), \tag{7.1}$$

where $f_1(\cdot)$ and $f_2(\cdot)$ are functions mapping transmit power actions and relay selection actions to the desired utility; $g(\cdot)$ and $c(\cdot)$ are the gain and cost functions

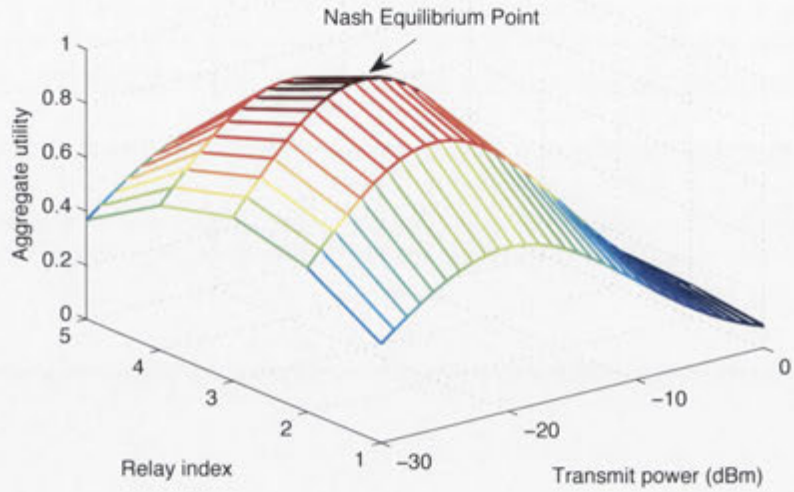

Figure 7.1: An example of a convex utility function for two-dimensional non-cooperative game, involving transmit power control and relay selection, for coexisting BANs.

with respect to a BAN's transmit power and relay choice. However, the results of the game highly depends on a proper design of the utility function implemented at individual BAN. It is important that the proposed utility function is convex to ensure the existence of a unique Nash Equilibrium with two-dimensional action profiles, as shown in Fig.7.1, which might be a difficulty. Another approach is to model non-cooperative relay selection and power control as a two-level non-cooperative game similarly to the one mentioned in Han and Liu. A general idea of the two-level game is to adaptively select the optimal relay first. The term "optimal" is defined in terms of the balance amongst channel quality, interference experienced from and interference created to the neighbouring BANs. Then non-cooperative power control game can be conducted on the optimal relay branch.

The work presented in this thesis considers that all BANs have the same performance requirements. However, as has been addressed in various literature such as Malik and Singh [2013]; Kahsay et al. [2013]; Yang et al. [2015], the ability of adapting to various user priorities in BAN is important. Many existing works focussed on effective MAC protocols supporting differentiated services for various types of traffic

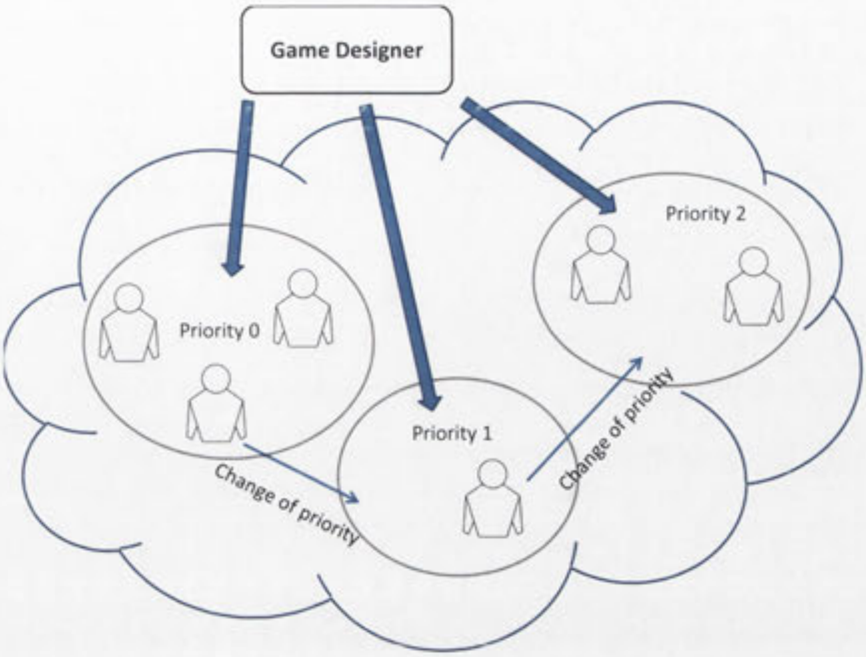

Figure 7.2: Non-cooperative coexistence of BANs with various priority levels. The grouping of BANs doesn't not correspond to their actual physical location, but only priority levels.

generated by sensors within a BAN Bradai et al. [2013]; Kong et al. [2013]. This idea could be generalised to the BAN-level as demonstrated in Fig.7.2, in which case, co-existing BANs could be prioritised depending on factors such as subjects' condition, system status, purpose of BAN usage, etc. The requirements on reliability and power usage can vary with different priorities. Therefore, as the second potential extension to the work, the change of priority for coexisting BANs could be incorporated into our non-cooperative game by introducing an extra priority factor that adaptively alters the weights on the utility function. The existence of social optimality in this case needs to be evaluated.

The last potential approach is to evaluate the energy efficiency of all the proposed schemes. The performance evaluation was more reliability-oriented. One of the assumptions for the work on cooperative communications is that relays and hub are less energy constrained than sensors. The implementation of cooperative communications adds little complexity to the sensor nodes. Therefore, the additional complexity and thus resultant power consumption increase in relays and hub is ignored. For the study of power control schemes, the energy efficiency was investigated in terms of the circuit power consumption in Tx mode. Thus, a thorough study on energy efficiency could be conducted for the whole system incorporating both Tx and Rx mode, which would incorporate all sensors, relay(s) and the hub for any BAN.

Bibliography

2006. Micaz datasheet.

Abbasi, U.; Awang, A.; and Hamid, N., 2013. Performance investigation of opportunistic routing using log-normal and ieee 802.15.6 cm 3a path loss models in wbans. In *Communications (MICC), 2013 IEEE Malaysia International Conference on*, 325–329. doi:10.1109/MICC.2013.6805848.

ABIresearch, 2011. Body Area Networks for Sports and Healthcare. [Online] https://www.telematicsresearch.net/research/product/1005246-body-area-networks-for-sports-and-healthca/.

Akhoondzadeh-Asl, L.; Nechayev, Y.; and Hall, P., 2010. Surface and creeping waves excitation by body-worn antennas. In *Antennas and Propagation Conference (LAPC), 2010 Loughborough*, 48–51. doi:10.1109/LAPC.2010.5666805.

Alomainy, A.; Hao, Y.; Owadally, A.; Parini, C.; Nechayev, Y.; Constantinou, C.; and Hall, P., 2007. Statistical analysis and performance evaluation for on-body radio propagation with microstrip patch antennas. *Antennas and Propagation, IEEE Transactions on*, 55, 1 (Jan 2007), 245–248. doi:10.1109/TAP.2006.888462.

Alpcan, T.; Basar, T.; and Dey, S., 2004. A power control game based on outage probabilities for multicell wireless data networks. In *American Control Conference, 2004. Proceedings of the 2004*, vol. 2, 1661 –1666 vol.2.

Annavajjala, R. and Zhang, J., 2010. Level crossing rates and average outage durations of sinr with multiple co-channel interferers. In *MILITARY COMMUNICATIONS CONFERENCE, 2010 - MILCOM 2010*, 1233 –1238. doi:10.1109/MILCOM.2010.5680111.

Archasantisuk, S. and Aoyagi, T., 2015. The human movement identification using the radio signal strength in wban. In *Medical Information and Communication Technology (ISMICT), 2015 9th International Symposium on*, 59–63. doi: 10.1109/ISMICT.2015.7107498.

Astrin, A. et al., 2012. IEEE Standard for Local and metropolitan area networks part 15.6: Wireless Body Area Networks: IEEE Std 802.15.6-2012. (Feb. 2012).

Au-Yeung, K. and DiCarlo, L., 2012. Cost comparison of wirelessly vs. directly observed therapy for adherence confirmation in anti-tuberculosis treatment. *The International Journal of Tuberculosis and Lung Disease*, 16, 11 (2012), 1498–1504.

Bemporad, A.; Heemels, M.; and Vejdemo-Johansson, M., 2010. *Networked Control Systems*, vol. 406 of *Lecture Notes in Control and Information Sciences*. Springer Science & Business Media. ISBN 978-0-85729-033-5.

Bletsas, A.; Khisti, A.; Reed, D.; and Lippman, A., 2006. A simple cooperative diversity method based on network path selection. *Selected Areas in Communications, IEEE Journal on*, 24, 3 (March 2006), 659–672. doi:10.1109/JSAC.2005.862417.

Bletsas, A.; Shin, H.; and Win, M., 2007. Cooperative communications with outage-optimal opportunistic relaying. *Wireless Communications, IEEE Transactions on*, 6, 9 (september 2007), 3450 –3460. doi:10.1109/TWC.2007.06020050.

Boulis, A.; Smith, D.; Miniutti, D.; Libman, L.; and Tselishchev, Y., 2012. Challenges in body area networks for healthcare: the mac. *Communications Magazine, IEEE*, 50, 5 (May 2012), 100–106. doi:10.1109/MCOM.2012.6194389.

Bradai, N.; Fourati, L. C.; Boudjit, S.; and Kamoun, L., 2013. New priority mac protocol for wireless body area networks. In *Proceedings of the 3rd ACM MobiHoc Workshop on Pervasive Wireless Healthcare*, MobileHealth '13 (Bangalore, India, 2013), 1–6. ACM, New York, NY, USA. doi:10.1145/2491148.2491149. http://doi.acm.org/10.1145/2491148.2491149.

Bulatao, R. A.; Bongaarts, J.; et al., 2000. *Beyond Six Billion:: Forecasting the World's Population*. National Academies Press. ISBN 978-0-309-06990-8.

CAI, X.; YUAN, J.; YUAN, X.; ZHU, W.; LI, J.; LI, C.; AND ULLAH, S., 2013. Energy-efficient relay mac with dynamic power control in wireless body area networks. *KSII Transactions on Internet and Information Systems (TIIS)*, 7, 7 (2013), 1547–1568.

CANDOGAN, U.; MENACHE, I.; OZDAGLAR, A.; AND PARRILO, P., 2010. Near-optimal power control in wireless networks: A potential game approach. In *INFOCOM, 2010 Proceedings IEEE*, 1–9. doi:10.1109/INFCOM.2010.5462017.

CHANDRA, R. AND JOHANSSON, A. J., 2013. An analytical link-loss model for on-body propagation around the body based on elliptical approximation of the torso with arms' influence included. *Antennas and Wireless Propagation Letters, IEEE*, 12 (2013), 528–531.

CHEN, Y.; TEO, J.; LAI, J.; GUNAWAN, E.; LOW, K. S.; SOH, C. B.; AND RAPAJIC, P., 2009. Cooperative communications in ultra-wideband wireless body area networks: Channel modeling and system diversity analysis. *Selected Areas in Communications, IEEE Journal on*, 27, 1 (January 2009), 5–16. doi:10.1109/JSAC.2009.090102.

CHIWEWE, T. AND HANCKE, G., 2012. A distributed topology control technique for low interference and energy efficiency in wireless sensor networks. *Industrial Informatics, IEEE Transactions on*, 8, 1 (Feb 2012), 11–19. doi:10.1109/TII.2011.2166778.

CHU, S.; WANG, X.; AND YANG, Y., 2013. Exploiting cooperative relay for high performance communications in mimo ad hoc networks. *Computers, IEEE Transactions on*, 62, 4 (April 2013), 716–729. doi:10.1109/TC.2012.23.

CONWAY, G. AND SCANLON, W., 2009. Antennas for over-body-surface communication at 2.45 ghz. *Antennas and Propagation, IEEE Transactions on*, 57, 4 (April 2009), 844–855. doi:10.1109/TAP.2009.2014525.

COTTON, S.; MCKERNAN, A.; ALI, A.; AND SCANLON, W., 2011. An experimental study on the impact of human body shadowing in off-body communications channels at 2.45 ghz. In *Antennas and Propagation (EUCAP), Proceedings of the 5th European Conference on*, 3133–3137.

Cotton, S. and Scanlon, W., 2006. A statistical analysis of indoor multipath fading for a narrowband wireless body area network. In *Personal, Indoor and Mobile Radio Communications, 2006 IEEE 17th International Symposium on*, 1–5. doi: 10.1109/PIMRC.2006.254266.

Cotton, S. and Scanlon, W., 2007. Higher-order statistics for κ-μ distribution. *Electronics Letters*, 43, 22 (Oct 2007). doi:10.1049/el:20072372.

Cotton, S. and Scanlon, W., 2009. Channel characterization for single- and multiple-antenna wearable systems used for indoor body-to-body communications. *Antennas and Propagation, IEEE Transactions on*, 57, 4 (April 2009), 980–990. doi:10.1109/TAP.2009.2014576.

Cotton, S.; Scanlon, W.; and Guy, J., 2008. The $\kappa - \mu$ distribution applied to the analysis of fading in body to body communication channels for fire and rescue personnel. *Antennas and Wireless Propagation Letters, IEEE*, 7 (2008), 66–69. doi: 10.1109/LAWP.2008.915807.

Cotton, S. L.; D'Errico, R.; and Oestges, C., 2014. A review of radio channel models for body centric communications. *Radio Science*, 49, 6 (2014), 371–388. doi: 10.1002/2013RS005319. http://dx.doi.org/10.1002/2013RS005319.

Cui, S.; Haimovich, A.; Somekh, O.; and Poor, H., 2009. Opportunistic relaying in wireless networks. *Information Theory, IEEE Transactions on*, 55, 11 (Nov 2009), 5121–5137. doi:10.1109/TIT.2009.2030435.

Davenport, D.; Ross, F.; and Deb, B., 2009. Wireless propagation and coexistence of medical body sensor networks for ambulatory patient monitoring. In *Wearable and Implantable Body Sensor Networks, 2009. BSN 2009. Sixth International Workshop on*, 41–45. doi:10.1109/BSN.2009.8.

Davenport, D. et al. Medwin physical layer proposal. *IEEE P802. 15-09-0328-01*, 6.

de Silva, B.; Natarajan, A.; and Motani, M., 2009. Inter-user interference in body sensor networks: Preliminary investigation and an infrastructure-based solution.

In *Wearable and Implantable Body Sensor Networks, 2009. BSN 2009. Sixth International Workshop on*, 35–40. doi:10.1109/BSN.2009.36.

Deepak, K. and Babu, A., 2015. Improving energy efficiency of incremental relay based cooperative communications in wireless body area networks. *International Journal of Communication Systems*, 28, 1 (2015), 91–111.

D'Errico, R.; Rosini, R.; and Maman, M., 2011. A performance evaluation of cooperative schemes for on-body area networks based on measured time-variant channels. In *Communications (ICC), 2011 IEEE International Conference on*, 1–5. doi:10.1109/icc.2011.5962980.

Deylami, M. and Jovanov, E., 2012. Performance analysis of coexisting ieee 802.15.4-based health monitoring wbans. In *Engineering in Medicine and Biology Society (EMBC), 2012 Annual International Conference of the IEEE*, 2464–2467. doi:10.1109/EMBC.2012.6346463.

Ding, J.; Dutkiewicz, E.; and Huang, X., 2013. Energy efficient cooperative communication for uwb based in-body area networks. In *Proceedings of the 8th International Conference on Body Area Networks*, BodyNets '13 (Boston, Massachusetts, 2013), 29–34. ICST (Institute for Computer Sciences, Social-Informatics and Telecommunications Engineering), ICST, Brussels, Belgium, Belgium. doi:10.4108/icst.bodynets.2013.253567. http://dx.doi.org.virtual.anu.edu.au/10.4108/icst.bodynets.2013.253567.

Dong, J.; Ge, Y.; and Smith, D., 2015a. Two-hop relay-assisted cooperative communication in wireless body area networks: an empirical study. *ACM Transaction on Sensor Networks*, (2015). Manuscript in Preparation, to-be-submitted May-29-2015. Will be available on arXiv.

Dong, J. and Smith, D., 2011. Cooperative receive diversity for coded gfsk body-area communications. *Electronics Letters*, 47, 19 (September 2011), 1098–1100. doi:10.1049/el.2011.1647.

Dong, J. and Smith, D., 2012. Cooperative body-area-communications: Enhancing coexistence without coordination between networks. In *Personal Indoor and Mobile Radio Communications (PIMRC), 2012 IEEE 23rd International Symposium on*, 2269–2274. doi:10.1109/PIMRC.2012.6362733.

Dong, J. and Smith, D., 2013. Opportunistic relaying in wireless body area networks: Coexistence performance. In *Communications (ICC), 2013 IEEE International Conference on*, 5613–5618. doi:10.1109/ICC.2013.6655487.

Dong, J. and Smith, D., 2014. Joint relay selection and transmit power control for wireless body area networks coexistence. In *Communications (ICC), 2014 IEEE International Conference on*, 5676–5681. doi:10.1109/ICC.2014.6884226.

Dong, J. and Smith, D., 2015. Wireless body area networks coexistence: Cooperative communications combining opportunistic relaying and power control. *IEEE Transaction on Communications*, (2015). Manuscript submitted. Available on arXiv.

Dong, J.; Smith, D.; and Hanlen, L., 2015b. Socially optimal coexistence of wireless body area networks enabled by a non-cooperative game. *ACM Transaction on Sensor Networks*, (2015). Major revision will-be-submitted May-26-2015. Will be available on arXiv.

Dotlic, I., 2011. Interference performance of ieee 802.15.6 impulse-radio ultra-wideband physical layer. In *Personal Indoor and Mobile Radio Communications (PIMRC), 2011 IEEE 22nd International Symposium on*, 2148–2152. doi:10.1109/PIMRC.2011.6139895.

Douros, V. G. and Polyzos, G. C., 2011. Review of some fundamental approaches for power control in wireless networks. *Computer Communications*, 34, 13 (2011), 1580–1592.

Douros, V. G.; Toumpis, S.; and Polyzos, G., 2012. Power control under best response dynamics for interference mitigation in a two-tier femtocell network. In *Modeling and Optimization in Mobile, Ad Hoc and Wireless Networks (WiOpt), 2012 10th International Symposium on*, 398–405.

FANG, G.; DUTKIEWICZ, E.; YU, K.; VESILO, R.; AND YU, Y., 2010. Distributed inter-network interference coordination for wireless body area networks. In *Global Telecommunications Conference (GLOBECOM 2010), 2010 IEEE*, 1–5. doi:10.1109/GLOCOM.2010.5683900.

FANG, Y.; ZHOU, W.; LAN, J.; AND YANZAN, S., 2014. Performance evaluation of rake receiver for ultra-wideband wireless body area network communication. In *Signal Processing (ICSP), 2014 12th International Conference on*, 2257–2261. doi:10.1109/ICOSP.2014.7015396.

FELEGYHAZI, M.; HUBAUX, J.-P.; AND BUTTYAN, L., 2005. Cooperative packet forwarding in multi-domain sensor networks. In *Pervasive Computing and Communications Workshops, 2005. PerCom 2005 Workshops. Third IEEE International Conference on*, 345–349. doi:10.1109/PERCOMW.2005.24.

FERRAND, P.; MAMAN, M.; GOURSAUD, C.; GORCE, J.-M.; AND OUVRY, L., 2011. Performance evaluation of direct and cooperative transmissions in body area networks. *Annals of Telecommunications*, 66 (2011), 213–228. http://dx.doi.org/10.1007/s12243-011-0238-y. 10.1007/s12243-011-0238-y.

FOSCHINI, G. AND MILJANIC, Z., 1993. A simple distributed autonomous power control algorithm and its convergence. *Vehicular Technology, IEEE Transactions on*, 42, 4 (Nov 1993), 641–646. doi:10.1109/25.260747.

GE, X.; HUANG, K.; WANG, C.-X.; HONG, X.; AND YANG, X., 2011. Capacity analysis of a multi-cell multi-antenna cooperative cellular network with co-channel interference. *Wireless Communications, IEEE Transactions on*, 10, 10 (October 2011), 3298–3309. doi:10.1109/TWC.2011.11.101551.

GU, D., 2011. A game theory approach to target tracking in sensor networks. *Systems, Man, and Cybernetics, Part B: Cybernetics, IEEE Transactions on*, 41, 1 (Feb 2011), 2–13. doi:10.1109/TSMCB.2010.2040733.

GULATI, K.; CHOPRA, A.; EVANS, B.; AND TINSLEY, K., 2009. Statistical modeling of co-channel interference. In *Global Telecommunications Conference, 2009. GLOBECOM 2009. IEEE*, 1–6. doi:10.1109/GLOCOM.2009.5425480.

Guo, B.; Guan, Q.; Yu, F.; Jiang, S.; and Leung, V., 2014. Energy-efficient topology control with selective diversity in cooperative wireless ad hoc networks. In *Communications (ICC), 2014 IEEE International Conference on*, 197–202. doi:10.1109/ICC.2014.6883318.

Han, Z. and Liu, K. *Resource Allocation for Wireless Networks: Basics, Techniques, and Applications*, chap. 13.Game-Theoretic Approaches for Resource Allocation.

Hanlen, L.; Chaganti, V.; Gilbert, B.; Rodda, D.; Lamahewa, T.; and Smith, D., 2010a. Open-source testbed for body area networks: 200 sample/sec, 12 hrs continuous measurement. In *Personal Indoor and Mobile Radio Communication*. Istanbul, Turkey.

Hanlen, L.; Miniutti, D.; Rodda, D.; and Gilbert, B., 2009. Interference in body area networks: Distance does not dominate. In *Personal, Indoor and Mobile Radio Communications, 2009 IEEE 20th International Symposium on*, 281 –285. doi:10.1109/PIMRC.2009.5450109.

Hanlen, L.; Miniutti, D.; Smith, D.; Rodda, D.; and Gilbert, B., 2010b. Co-channel interference in body area networks with indoor measurements at 2.4ghz: Distance-to-interferer is a poor estimate of received interference power. *International Journal of Wireless Information Networks*, 17, 3-4 (2010), 113–125. doi:10.1007/s10776-010-0123-z. http://dx.doi.org/10.1007/s10776-010-0123-z.

Hauer, J.-H., 2009. Tkn15. 4: An ieee 802.15. 4 mac implementation for tinyos. (2009).

Hayajneh, T.; Almashaqbeh, G.; Ullah, S.; and Vasilakos, A., 2014. A survey of wireless technologies coexistence in wban: analysis and open research issues. *Wireless Networks*, 20, 8 (2014), 2165–2199. doi:10.1007/s11276-014-0736-8. http://dx.doi.org/10.1007/s11276-014-0736-8.

Heikkinen, T., 2006. A potential game approach to distributed power control and scheduling. *Computer Networks*, 50, 13 (2006), 2295 – 2311. doi:10.1016/j.comnet.2005.09.010. http://www.sciencedirect.com/science/article/pii/S1389128605002859.

Hernandez, M. and Miura, R., 2012. Coexistence of uwb systems for body area networks in awgn. In *Medical Information and Communication Technology (ISMICT), 2012 6th International Symposium on*, 1–4. doi:10.1109/ISMICT.2012.6203039.

Huang, Y.; Liang, W.; Yu, H.-b.; and Xiao, Y., 2008. Target tracking based on a distributed particle filter in underwater sensor networks. *Wireless Communications and Mobile Computing*, 8, 8 (2008), 1023–1033. doi:10.1002/wcm.660. http://dx.doi.org/10.1002/wcm.660.

Hwang, K.-S.; chai Ko, Y.; and Alouini, M.-S., 2008. Outage probability of cooperative diversity systems with opportunistic relaying based on decode-and-forward. *Wireless Communications, IEEE Transactions on*, 7, 12 (December 2008), 5100–5107. doi:10.1109/T-WC.2008.071216.

Ileri, O.; Mau, S.-C.; and Mandayam, N., 2004. Pricing for enabling forwarding in self-configuring ad hoc networks. In *Wireless Communications and Networking Conference, 2004. WCNC. 2004 IEEE*, vol. 2, 1034 – 1039 Vol.2. doi:10.1109/WCNC.2004.1311330.

Jakes, W. (Ed.), 1974. *Microwave Mobile Communication*. IEEE Press, New York, USA.

Kahsay, L.; Paso, T.; and Iinatti, J., 2013. Evaluation of ieee 802.15.6 mac user priorities with uwb phy for medical applications. In *Medical Information and Communication Technology (ISMICT), 2013 7th International Symposium on*, 18–22. doi:10.1109/ISMICT.2013.6521691.

Karapistoli, E. and Economides, A., 2014. Defending jamming attacks in wireless sensor networks using stackelberg monitoring strategies. In *Communications in China (ICCC), 2014 IEEE/CIC International Conference on*, 161–165. doi:10.1109/ICCChina.2014.7008264.

Kazemi, R.; Vesilo, R.; and Dutkiewicz, E., 2011a. A novel genetic-fuzzy power controller with feedback for interference mitigation in wireless body area networks. In *Vehicular Technology Conference (VTC Spring), 2011 IEEE 73rd*, 1–5. doi:10.1109/VETECS.2011.5956462.

Kazemi, R.; Vesilo, R.; Dutkiewicz, E.; and Fang, G., 2010. Inter-network interference mitigation in wireless body area networks using power control games. In *Communications and Information Technologies (ISCIT), 2010 International Symposium on*, 81–86. doi:10.1109/ISCIT.2010.5664908.

Kazemi, R.; Vesilo, R.; Dutkiewicz, E.; and Liu, R., 2011b. Dynamic power control in wireless body area networks using reinforcement learning with approximation. In *Personal Indoor and Mobile Radio Communications (PIMRC), 2011 IEEE 22nd International Symposium on*, 2203–2208. doi:10.1109/PIMRC.2011.6139908.

Kazemi, R.; Vesilo, R.; Dutkiewicz, E.; and Liu, R. P., 2012. Reinforcement learning in power control games for internetwork interference mitigation in wireless body area networks. In *Communications and Information Technologies (ISCIT), 2012 International Symposium on*, 256–262. doi:10.1109/ISCIT.2012.6380902.

Khan, M. M.; Abbasi, Q.; Alomainy, A.; and Hao, Y., 2011. Study of line of sight (los) and none line of sight (nlos) ultra wideband off-body radio propagation for body centric wireless communications in indoor. In *Antennas and Propagation (EUCAP), Proceedings of the 5th European Conference on*, 110–114.

Kini, A.; Hosseinian, M.; Sadeghi, P.; and Stern-Berkowitz, J., 2014. A dynamic subframe set power control scheme for interference mitigation in reconfigurable td-lte systems. In *Wireless and Optical Communication Conference (WOCC), 2014 23rd*, 1–6. doi:10.1109/WOCC.2014.6839949.

Kong, R.; Chen, C.; Yu, W.; Yang, B.; and Guan, X., 2013. Data priority based slot allocation for wireless body area networks. In *Wireless Communications Signal Processing (WCSP), 2013 International Conference on*, 1–6. doi:10.1109/WCSP.2013.6677273.

Koskie, S. and Gajic, Z., 2005. A nash game algorithm for sir-based power control in 3g wireless cdma networks. *Networking, IEEE/ACM Transactions on*, 13, 5 (Oct. 2005), 1017 – 1026. doi:10.1109/TNET.2005.857068.

Kumar, N.; Lee, J.-H.; and Rodrigues, J., 2014. Intelligent mobile video surveillance system as a bayesian coalition game in vehicular sensor networks: Learning automata approach. *Intelligent Transportation Systems, IEEE Transactions on*, PP, 99 (2014), 1–14. doi:10.1109/TITS.2014.2354372.

Lee, T.-H. and Lin, J.-C., 1996. A fully distributed power control algorithm for cellular mobile systems. *Selected Areas in Communications, IEEE Journal on*, 14, 4 (May 1996), 692–697. doi:10.1109/49.490420.

Lewis, D., 2008. IEEE 802.15.6 call for applications - summary ID: 802.15-05-0407-05. (July 2008).

Leyton-Brown, K. and Shoham, Y., 2008. *Essentials Of Game Theory: A Concies, Multidisciplinary Introduction*. Morgana and Claypool, Canda and USA, 20008 edition edn.

Li, Q.; Hu, R.; Qian, Y.; and Wu, G., 2012. Cooperative communications for wireless networks: techniques and applications in lte-advanced systems. *Wireless Communications, IEEE*, 19, 2 (April 2012), –. doi:10.1109/MWC.2012.6189409.

Lin, J.; Jung, H.; Chang, Y. J.; Jung, J. W.; and Weitnauer, M. A., 2015. On cooperative transmission range extension in multi-hop wireless ad-hoc and sensor networks: A review. *Ad Hoc Networks*, , 0 (2015), –. doi:http://dx.doi.org/10.1016/j.adhoc.2015.01.018. http://www.sciencedirect.com/science/article/pii/S1570870515000281.

Lin, S.; Zhang, J.; Zhou, G.; Gu, L.; Stankovic, J. A.; and He, T., 2006. Atpc: adaptive transmission power control for wireless sensor networks. In *Proceedings of the 4th international conference on Embedded networked sensor systems*, 223–236. ACM.

Long, C.; Zhang, Q.; Li, B.; Yang, H.; and Guan, X., 2007. Non-cooperative power control for wireless ad hoc networks with repeated games. *Selected Ar-*

eas in Communications, IEEE Journal on, 25, 6 (august 2007), 1101 –1112. doi:10.1109/JSAC.2007.070805.

Madan, R.; Mehta, N.; Molisch, A.; and Zhang, J., 2008. Energy-efficient cooperative relaying over fading channels with simple relay selection. *Wireless Communications, IEEE Transactions on*, 7, 8 (august 2008), 3013 –3025. doi:10.1109/TWC.2008.06090.

Malik, B. and Singh, V., 2013. A survey of research in wban for biomedical and scientific applications. *Health and Technology*, 3, 3 (2013), 227–235. doi:10.1007/s12553-013-0056-5. http://dx.doi.org/10.1007/s12553-013-0056-5.

Martelli, F. and Verdone, R., 2012. Coexistence issues for wireless body area networks at 2.45 ghz. In *European Wireless, 2012. EW. 18th European Wireless Conference*, 1–6.

Australian Bureau of Statistics, 2013. Population Projections Australia 2012 (base) to 2101. No.3222.0.

IEEE 802.15 Task Group 4, 2011. Ieee standard for local and metropolitan area networks-part 15.4: Low-rate wireless personal area networks (lr-wpans). *IEEE Computer Society Approved*, 16 (2011).

IEEE 802.15 Task Group 6, 2012. Ieee standard for local and metropolitan area networks-part 15.6: Wireless body area networks (wbans). *IEEE Standard for Information Technology, IEEE*, 802, 6 (2012), 1–271.

IEEE Standards Association and others, 2005. Ieee standard for telecommunications and information exchange between systems - lan/man - specific requirements - part 15: Wireless medium access control (mac) and physical layer (phy) specifications for wireless personal area networks (wpans). *IEEE Computer Society Approved*, (2005).

Misra, S.; Moulik, S.; and Chao, H., 2015. A cooperative bargaining solution for priority-based data-rate tuning in a wireless body area network. *Wireless Communications, IEEE Transactions on*, PP, 99 (2015), 1–1. doi:10.1109/TWC.2015.2393303.

MISRA, S. AND SARKAR, S., 2014. Priority-based time-slot allocation in wireless body area networks during medical emergency situations: An evolutionary game theoretic perspective. *Biomedical and Health Informatics, IEEE Journal of*, PP, 99 (2014), 1–1. doi:10.1109/JBHI.2014.2313374.

NABI, M.; GEILEN, M.; AND BASTEN, T., 2011. Moban: A configurable mobility model for wireless body area networks. In *Proceedings of the 4th International ICST Conference on Simulation Tools and Techniques*, SIMUTools '11 (Barcelona, Spain, 2011), 168–177. ICST (Institute for Computer Sciences, Social-Informatics and Telecommunications Engineering), ICST, Brussels, Belgium, Belgium. http://dl.acm.org.virtual.anu.edu.au/citation.cfm?id=2151054.2151088.

NECHAYEV, Y.; HU, Z. H.; AND HALL, P., 2010. Fading of the transmission channel between two wireless body area networks in an office at 2.45 ghz and 5.8 ghz. In *Antennas and Propagation Conference (LAPC), 2010 Loughborough*, 489–492. doi:10.1109/LAPC.2010.5666196.

NESSA, A.; YANG, Q.; AND KWAK, K.-S., 2008. Performance analysis of two-hop cooperative mimo transmission with best relay selection in rayleigh fading channel. *matrix*, 10, 1 (2008), 2.

NOSRATINIA, A.; HUNTER, T.; AND HEDAYAT, A., 2004. Cooperative communication in wireless networks. *Communications Magazine, IEEE*, 42, 10 (oct. 2004), 74 – 80. doi:10.1109/MCOM.2004.1341264.

OZEL, O. AND UYSAL-BIYIKOGLU, E., 2009. Distributed power control using non-monotonic reaction curves. In *Game Theory for Networks, 2009. GameNets '09. International Conference on*, 60–67. doi:10.1109/GAMENETS.2009.5137383.

PATEL, M. AND WANG, J., 2010. Applications, challenges, and prospective in emerging body area networking technologies. *Wireless Communications, IEEE*, 17, 1 (February 2010), 80–88. doi:10.1109/MWC.2010.5416354.

PROULX, J.; CLIFFORD, R.; SORENSEN, S.; LEE, D.-J.; AND ARCHIBALD, J., 2006. Development and evaluation of a bluetooth ekg monitoring sensor. In *Computer-Based*

Medical Systems, 2006. CBMS 2006. 19th IEEE International Symposium on, 507–511. doi:10.1109/CBMS.2006.74.

Quwaider, M.; Rao, J.; and Biswas, S., 2010. Body-posture-based dynamic link power control in wearable sensor networks. *Communications Magazine, IEEE*, 48, 7 (July 2010), 134–142. doi:10.1109/MCOM.2010.5496890.

Raicu, I.; Schwiebert, L.; Fowler, S.; and Gupta, S. K., 2005. Local load balancing for globally efficient routing in wireless sensor networks. *International Journal of Distributed Sensor Networks*, 1, 2 (2005), 163–185. doi:10.1080/15501320590966431. http://www.tandfonline.com/doi/abs/10.1080/15501320590966431.

Reusens, E.; Joseph, W.; Vermeeren, G.; Martens, L.; Latre, B.; Moerman, I.; Braem, B.; and Blondia, C., 2007. Path loss models for wireless communication channel along arm and torso: measurements and simulations. In *Antennas and Propagation Society International Symposium, 2007 IEEE*, 345–348. doi:10.1109/APS.2007.4395501.

Roelens, L.; Van den Bulcke, S.; Joseph, W.; Vermeeren, G.; and Martens, L., 2006. Path loss model for wireless narrowband communication above flat phantom. *Electronics Letters*, 42, 1 (Jan 2006), 10–11–. doi:10.1049/el:20063062.

Sadagopan, N.; Singh, M.; and Krishnamachari, B., 2006. Decentralized utility-based sensor network design. *Mobile Networks and Applications*, 11, 3 (2006), 341–350. doi:10.1007/s11036-006-5187-8. http://dx.doi.org/10.1007/s11036-006-5187-8.

Sagan, D., 2009. Ultra-low power medical ban phy proposal. *IEEE802.15.6. 15-09-0351-00-0006-ulp-medical-ban-phy-proposal*, 6 (May 2009).

Saraydar, C.; Mandayam, N.; and Goodman, D., 2002. Efficient power control via pricing in wireless data networks. *Communications, IEEE Transactions on*, 50, 2 (Feb. 2002), 291 –303. doi:10.1109/26.983324.

Selvam, A., 2012. Er overcrowding tied to higher death rate: study.

SENDONARIS, A.; ERKIP, E.; AND AAZHANG, B., 2003. User cooperation diversity. part i. system description. *Communications, IEEE Transactions on*, 51, 11 (nov. 2003), 1927 – 1938. doi:10.1109/TCOMM.2003.818096.

SENEVIRATNE, C. AND LEUNG, H., 2011. A game theoretic approach for resource allocation in cognitive wireless sensor networks. In *Systems, Man, and Cybernetics (SMC), 2011 IEEE International Conference on*, 1992–1997. doi:10.1109/ICSMC.2011.6083964.

SHABAN, H. AND ABOU EL-NASR, M., 2013. Amplify-and-forward cooperative diversity for green uwb-based wbsns. *The Scientific World Journal*, 2013 (2013).

SHAKIR, M.; AHMED, I.; PENG, M.; AND WANG, W., 2007. Optimum transmit power for maximal connectivity and increased network lifetime in wsns. In *Wireless Communications, Networking and Mobile Computing, 2007. WiCom 2007. International Conference on*, 2401–2404. doi:10.1109/WICOM.2007.598.

SHALMASHI, S. AND BEN SLIMANE, S., 2014. Cooperative device-to-device communications in the downlink of cellular networks. In *Wireless Communications and Networking Conference (WCNC), 2014 IEEE*, 2265–2270. doi:10.1109/WCNC.2014.6952682.

SHARMA, S.; SHI, Y.; HOU, Y. T.; AND KOMPELLA, S., 2011. An optimal algorithm for relay node assignment in cooperative ad hoc networks. *IEEE/ACM Trans. Netw.*, 19, 3 (Jun. 2011), 879–892. doi:10.1109/TNET.2010.2091148. http://dx.doi.org.virtual.anu.edu.au/10.1109/TNET.2010.2091148.

SHIN, S.; WEIDONG, S.; AND CHO, J., 2012. A game theory model to support qos in overlapped wban environment. In *Proceedings of the 6th International Conference on Ubiquitous Information Management and Communication*, ICUIMC '12 (Kuala Lumpur, Malaysia, 2012), 47:1–47:4. ACM, New York, NY, USA. doi:10.1145/2184751.2184809. http://doi.acm.org/10.1145/2184751.2184809.

SMITH, D., 2012. Cooperative switched combining for wireless body area networks. In *Personal Indoor and Mobile Radio Communications (PIMRC), 2012 IEEE 23rd International Symposium on*, 2275–2280. doi:10.1109/PIMRC.2012.6362735.

Smith, D., 2014. Improved switched combining with cooperative diversity for wireless body area networks: Empirical analysis and theory. In *Communications (ICC), 2014 IEEE International Conference on*, 5682–5687. doi:10.1109/ICC.2014.6884227.

Smith, D. and Hanlen, L., 2015. Channel modeling for wireless body area networks. In *Ultra-Low Power Short-Range Radios*.

Smith, D.; Hanlen, L.; and Miniutti, D., 2012a. Transmit power control for wireless body area networks using novel channel prediction. In *IEEE Wireless Communications and Networking Conference (WCNC*. Paris/France.

Smith, D.; Hanlen, L.; Rodda, D.; Gilbert, B.; Dong, J.; and Chaganti, V., 2012b. Body Area Network Radio Channel Measurement Set. [Online] http://opennicta.com/datasets.

Smith, D.; Hanlen, L.; Zhang, J.; Miniutti, D.; Rodda, D.; and Gilbert, B., 2011a. First- and second-order statistical characterizations of the dynamic body area propagation channel of various bandwidths. *Annals of Telecommunications*, 66 (2011), 187–203. http://dx.doi.org/10.1007/s12243-010-0233-8. 10.1007/s12243-010-0233-8.

Smith, D.; Lamahewa, T.; Hanlen, L.; and Miniutti, D., 2011b. Simple prediction-based power control for the on-body area communications channel. In *Communications (ICC), 2011 IEEE International Conference on*, 1–5. doi:10.1109/icc.2011.5963355.

Smith, D. and Miniutti, D., 2012. Cooperative body-area-communications: First and second-order statistics with decode-and-forward. In *IEEE Wireless Communications and Networking Conference (WCNC)*. Paris, France.

Smith, D.; Miniutti, D.; Lamahewa, T.; and Hanlen, L., 2013a. Propagation models for body-area networks: A survey and new outlook. *Antennas and Propagation Magazine, IEEE*, 55, 5 (Oct 2013), 97–117. doi:10.1109/MAP.2013.6735479.

Smith, D.; Miniutti, D.; Lamahewa, T.; and Hanlen, L., 2013b. Propagation models for body-area networks: A survey and new outlook. *Antennas and Propagation Magazine, IEEE*, 55, 5 (Oct 2013), 97–117. doi:10.1109/MAP.2013.6735479.

Smith, D.; Portmann, M.; Tan, W. L.; and Tushar, W., 2014. Multi source-destination distributed wireless networks: Pareto-efficient dynamic power control game with rapid convergence. *Vehicular Technology, IEEE Transactions on*, 63, 6 (July 2014), 2744–2754. doi:10.1109/TVT.2013.2294019.

Smith, D.; Zhang, J.; Hanlen, L.; Miniutti, D.; Rodda, D.; and Gilbert, B., 2009. Temporal correlation of dynamic on-body area radio channel. *Electronics Letters*, 45, 24 (Nov. 2009), 1212 –1213. doi:10.1049/el.2009.2057.

Smith, D. et al., 2008. Statistical characterization of the dynamic narrowband body area channel. *Applied Sciences on Biomedical and Communication Technologies, 2008. ISABEL '08. First International Symposium on*, (Oct. 2008), 1–5. doi:10.1109/ISABEL.2008.4712618.

Smith, D. B.; Miniutti, D.; and Hanlen, L. W., 2011c. Characterization of the body-area propagation channel for monitoring a subject sleeping. *Antennas and Propagation, IEEE Transactions on*, 59, 11 (2011), 4388–4392.

Soomro, A. and Cavalcanti, D., 2007. Opportunities and challenges in using wpan and wlan technologies in medical environments [accepted from open call]. *Communications Magazine, IEEE*, 45, 2 (Feb 2007), 114–122. doi:10.1109/MCOM.2007.313404.

Stamatiou, K.; Chiarotto, D.; Librino, F.; and Zorzi, M., 2012. Performance analysis of an opportunistic relay selection protocol for multi-hop networks. *Communications Letters, IEEE*, 16, 11 (November 2012), 1752–1755. doi:10.1109/LCOMM.2012.092112.121221.

Sun, D.; Huang, X.; Liu, Y.; and Zhong, H., 2013. Predictable energy aware routing based on dynamic game theory in wireless sensor networks. *Computers & Electrical Engineering*, 39, 6 (2013), 1601 – 1608. doi:http://dx.doi.org/10.1016/j.compeleceng.2012.05.007. http://www.sciencedirect.com/science/article/pii/S0045790612001012. Special Issue on Wireless Systems: Modeling, Monitoring, Transmission, Performance Evaluation and Optimization.

SUN, Q.; ZENG, X.; CHEN, N.; KE, Z.; AND UR RASOOL, R., 2008. A non-cooperative power control algorithm for wireless ad hoc and sensor networks. In *Genetic and Evolutionary Computing, 2008. WGEC '08. Second International Conference on*, 181 – 184. doi:10.1109/WGEC.2008.95.

SUN, W.; GE, Y.; AND WONG, W.-C., 2012. Inter-user interference in body sensor networks: A case study in moderate-scale deployment in hospital environment. In *e-Health Networking, Applications and Services (Healthcom), 2012 IEEE 14th International Conference on*, 447–450. doi:10.1109/HealthCom.2012.6379458.

TAKIZAWA, K.; LI, H.-B.; HAMAGUCHI, K.; AND KOHNO, R., 2007. Wireless patient monitoring using ieee802.15.4a wpan. In *Ultra-Wideband, 2007. ICUWB 2007. IEEE International Conference on*, 235–240. doi:10.1109/ICUWB.2007.4380948.

TUSHAR, W.; SMITH, D.; LAMAHEWA, T.; AND ZHANG, J., 2012. Non-cooperative power control game in a multi-source wireless sensor network. In *Communications Theory Workshop (AusCTW), 2012 Australian*, 43 –48. doi:10.1109/AusCTW.2012.6164904.

VALENTIN, S.; LICHTE, H. S.; KARL, H.; AAD, I.; LOYOLA, L.; AND WIDMER, J., 2008a. Opportunistic relaying vs. selective cooperation: analyzing the occurrence-conditioned outage capacity. In *Proceedings of the 11th international symposium on Modeling, analysis and simulation of wireless and mobile systems*, MSWiM '08 (Vancouver, British Columbia, Canada, 2008), 193–202. ACM, New York, NY, USA. doi:10.1145/1454503.1454539. http://doi.acm.org/10.1145/1454503.1454539.

VALENTIN, S.; LICHTE, H. S.; KARL, H.; AAD, I.; LOYOLA, L.; AND WIDMER, J., 2008b. Opportunistic relaying vs. selective cooperation: Analyzing the occurrence-conditioned outage capacity. In *Proceedings of the 11th international symposium on Modeling, analysis and simulation of wireless and mobile systems*, 193–202. ACM.

WANG, Y. AND WANG, Q., 2011. Evaluating the ieee 802.15. 6 2.4 ghz wban proposal on medical multi-parameter monitoring under wifi/bluetooth interference. (2011).

WIN, M.; PINTO, P.; AND SHEPP, L., 2009. A mathematical theory of network interference and its applications. *Proceedings of the IEEE*, 97, 2 (Feb 2009), 205–230. doi:10.1109/JPROC.2008.2008764.

Wu, G.; Ren, J.; Xia, F.; Yao, L.; and Xu, Z., 2010. Disg: Decentralized inter-user interference suppression in body sensor networks with non-cooperative game. In *Ubiquitous Intelligence Computing and 7th International Conference on Autonomic Trusted Computing (UIC/ATC), 2010 7th International Conference on*, 256–261. doi: 10.1109/UIC-ATC.2010.6.

Wu, Q., 1999. Performance of optimum transmitter power control in cdma cellular mobile systems. *Vehicular Technology, IEEE Transactions on*, 48, 2 (Mar 1999), 571–575. doi:10.1109/25.752582.

Yang, L.; Li, C.; Song, Y.; Yuan, X.; and Lei, Y., 2015. Performance evaluation of ieee 802.15.6 mac with user priorities for medical applications. In *Ubiquitous Computing Application and Wireless Sensor* (Eds. J. J. J. H. Park; Y. Pan; H.-C. Chao; and G. Yi), vol. 331 of *Lecture Notes in Electrical Engineering*, 23–30. Springer Netherlands. ISBN 978-94-017-9617-0. doi:10.1007/978-94-017-9618-7_3. http://dx.doi.org/10.1007/978-94-017-9618-7_3.

Yang, X. and Petropulu, A., 2003. Co-channel interference modeling and analysis in a poisson field of interferers in wireless communications. *Signal Processing, IEEE Transactions on*, 51, 1 (Jan 2003), 64–76. doi:10.1109/TSP.2002.806591.

Yazdandoost, K. and Sayrafian-Pour, K., 2010. TG6 channel model ID: 802.15-08-0780-12-0006. (IEEE submission, Nov. 2010).

Yuan, J. and Yu, W., 2006. Wsn11-1: Distributed cross-layer optimization of wireless sensor networks: A game theoretic approach. In *Global Telecommunications Conference, 2006. GLOBECOM '06. IEEE*, 1–5. doi:10.1109/GLOCOM.2006.952.

Zander, J., 1992a. Distributed cochannel interference control in cellular radio systems. *Vehicular Technology, IEEE Transactions on*, 41, 3 (Aug 1992), 305–311. doi:10.1109/25.155977.

Zander, J., 1992b. Performance of optimum transmitter power control in cellular radio systems. *Vehicular Technology, IEEE Transactions on*, 41, 1 (Feb 1992), 57–62. doi:10.1109/25.120145.

Zhang, A.; Smith, D.; Miniutti, D.; Hanlen, L.; Rodda, D.; and Gilbert, B., 2010. Performance of piconet co-existence schemes in wireless body area networks. In *Wireless Communications and Networking Conference (WCNC), 2010 IEEE*, 1 –6. Sydney, Australia. doi:10.1109/WCNC.2010.5506746.

Zhang, J.; Smith, D.; Hanlen, L.; Miniutti, D.; Rodda, D.; and Gilbert, B., 2009. Stability of narrowband dynamic body area channel. *Antennas and Wireless Propagation Letters, IEEE*, 8 (2009), 53–56. doi:10.1109/LAWP.2008.2011505.

Zhen, B.; Patel, M.; Lee, S.; and Won, E., 2008a. Body Area Network (BAN) Technical Requirements. (July 2008). IEEE802.15.6 technical contribution, document ID:15-08-0037-01-0006-ieee-802-15-6-technical-requirements-document-v-4-0.

Zhen, B.; Patel, M.; Lee, S.; Won, E.; and Astrin, A., 2008b. TG6 technical requirements document (TRD) ID: 802.15-08-0644. IEEE submission.

Zheng, G.; Liu, S.; and Qi, X., 2012. Clustering routing algorithm of wireless sensor networks based on bayesian game. *Systems Engineering and Electronics, Journal of*, 23, 1 (Feb 2012), 154–159. doi:10.1109/JSEE.2012.00019.

Zhu, C.; Zheng, C.; Shu, L.; and Han, G., 2012. A survey on coverage and connectivity issues in wireless sensor networks. *Journal of Network and Computer Applications*, 35, 2 (2012), 619 – 632. doi:http://dx.doi.org/10.1016/j.jnca.2011.11.016. http://www.sciencedirect.com/science/article/pii/S1084804511002323. Simulation and Testbeds.